

ELECTRON DENSITY AND PAIR CORRELATION FUNCTIONS  
IN METALS

Thesis submitted  
for the  
Degree of Doctor of Philosophy  
of the University of London  
and for the  
Diploma of Imperial College  
by  
STEPHEN ANTHONY CUSACK

Solid State Theory Group  
Physics Department  
Imperial College of Science and Technology  
July 1976

ABSTRACT

The first four chapters of this thesis are concerned with a calculation of valence electron correlation functions in nearly-free electron metals. Using a functional derivative technique, expressions exact to second-order in a weak electron-ion interaction are derived for the electron-electron and electron-ion correlation functions (and their Fourier transforms, the structure factors  $S_{ee}(k)$  and  $S_{ie}(k)$ ). Although equally applicable to solid metals, attention is focused on applying the results to liquid metals within the framework of the two component theory of liquid metals.

Using the adiabatic approximation, simplified expressions for  $S_{ee}(k)$  and  $S_{ie}(k)$  are obtained for liquid metals. Both contain terms which are explicitly shown to give the correct charge neutrality limit as  $k \rightarrow 0$ . An additional second-order term in the case of  $S_{ee}(k)$  involves a four-body response function of jellium. Two approximations to this response function are constructed, both of which rely on knowledge of the corresponding response function for non-interacting jellium. As the latter has not been evaluated fully, this contribution to  $S_{ee}(k)$  cannot be explicitly calculated although it is expected to be small compared to the charge neutrality term.

Calculations of the dominant terms in  $S_{ee}(k)$  and  $S_{ie}(k)$  are presented for liquid sodium and aluminium. These show that electron-ion interaction effects on the electronic correlation functions in these liquid metals are very small. It is concluded that (a) the recent proposal to extract  $S_{ee}(k)$  from a combination of X ray, neutron and electron diffraction data on liquid metals will, at least in the case of sodium, provide an experimental measure of the structure factor of jellium; (b) existing theories are unable to explain the observed differences between X ray and neutron structure factor data on liquid metals.

In chapters 5 and 6, two problems involving charge density in random

binary alloys are discussed. Firstly, the Friedel model of localised screening in dilute alloys is extended to a simple calculation of momentum density in such systems. The possibility of observing the screening charge by means of Compton scattering is then raised. Secondly, using density functional arguments, it is proposed that a set of energy-dependent or  $\beta$ -dependent ( $\beta = 1/kT$ ) periodic potentials can be used to calculate respectively the integrated local density of states and the generalized partition function of disordered binary alloys.

A final chapter is devoted to the problem of correlated bond percolation on the Bethe lattice. A non-linear integral equation is derived for the percolation probability, analysis of which yields exact results for the critical percolation probability and the behaviour in the critical region.

## ACKNOWLEDGEMENTS

This thesis is the culmination of three years work carried out at Imperial College under the supervision of Professor N.H. March and with the financial support of the Science Research Council.

My deepest thanks go to Professor March for suggesting the subject of this research and for frequent illuminating discussions about it. His unfailing enthusiasm and encouragement, and sympathetic understanding of my personal problems have been especially important to me during the course of this work.

I am also pleased to acknowledge much invaluable assistance from Professor M.P. Tosi and Dr. M. Parrinello (particularly with regard to the contents of chapter 2) during their prolonged stays at Imperial College.

I would also like to thank Dr. N. Rivier, for continually being at hand to give advice on a number of problems; Dr. A. Coniglio, for a fruitful discussion on percolation; and Professors K.S. Singwi, P.M. Platzman, J.E. Enderby, D. Jovic and S. Tamaki, as well as my father, N.E. Cusack, all of whom have sent me useful information and comments relating to my work.

Most of my time at Imperial College has been spent in the close company of my fellow research students, with whom I have had innumerable discussions about physics (as well as wider issues). I thank them individually for helping to create a friendly and stimulating atmosphere.

I am indebted to Miss D. Eastwood for her speedy typing of this thesis.

Finally, I am grateful, as ever, for the moral support of my mother and father.

CONTENTS

	page
<u>ABSTRACT</u>	1
<u>ACKNOWLEDGEMENTS</u>	3
<u>INTRODUCTION</u>	7
<u>CHAPTER 1 : PAIR CORRELATION FUNCTIONS AND STATIC STRUCTURE FACTORS IN LIQUID METALS</u>	13
1.1 : Hamiltonian for a two component liquid metal	13
1.2 : Pair correlation functions and static structure factors	14
1.3 : The long wavelength limit of $S_{ab}(k)$	15
1.4 : Density response functions	17
1.5 : Experimental determination of the structure factors $S_{ab}(k)$	20
<u>CHAPTER 2 : SECOND ORDER PERTURBATION THEORY FOR THE ELECTRONIC STRUCTURE FACTORS</u>	24
2.1 : Introduction	24
2.2 : The unperturbed system	25
2.3 : Perturbation expansion for the electron-electron density fluctuation propagator	26
2.4 : A theorem for functional derivatives	27
2.5 : Evaluation of the functional derivatives	28
2.6 : Rigid solids	31
2.7 : Liquid metals	32
2.8 : Use of the adiabatic approximation	33
2.9 : The electron-ion structure factor in liquid metals	34
2.10: Conclusion	37
<u>CHAPTER 3 : TWO APPROXIMATIONS TO THE FOUR-BODY ELECTRON RESPONSE FUNCTION <math>\chi_4</math></u>	38
3.1 : Introduction	38
3.2 : Electron-electron correlation function as a functional of the density	39
3.3 : Diagrammatic analysis of $\chi_4$	44
3.4 : Conclusion	47

	page
<u>CHAPTER 4 :</u> <u>CALCULATIONS AND DISCUSSION OF THE ELECTRON- ELECTRON AND ELECTRON-ION STRUCTURE FACTORS IN LIQUID METALS</u>	49
4.1 : Introduction	49
4.2 : Data used in the calculations	50
4.3 : Results for liquid sodium	53
4.4 : Results for liquid aluminium	56
4.5 : Discussion of the results	57
4.6 : Comparison of X ray and neutron structure factor data for liquid aluminium	61
4.7 : Further discussion	64
4.8 : Final conclusions	70
<u>CHAPTER 5 :</u> <u>A SIMPLE MODEL OF MOMENTUM DENSITY IN DILUTE BINARY ALLOYS</u>	74
5.1 : Introduction	74
5.2 : The Friedel model of primary solid solutions	75
5.3 : Momentum density in the Friedel model	78
5.4 : Compton profile	82
5.5 : Difficulties in observing high momentum components	84
5.6 : Conclusion	85
<u>CHAPTER 6 :</u> <u>PERIODIC POTENTIALS FOR RANDOM BINARY ALLOYS</u>	87
6.1 : Introduction	87
6.2 : Energy dependent periodic potentials for random alloys	89
6.3 : $\beta$ -dependent periodic potentials for random alloys	91
6.4 : Two approximate forms for the $\beta$ -dependent potentials	92
6.5 : Conclusions	96
<u>CHAPTER 7 :</u> <u>CORRELATED BOND PERCOLATION ON THE BETHE LATTICE</u>	97
7.1 : Introduction to percolation theory	97
7.2 : The correlated bond percolation problem	104
7.3 : Percolation probability for the correlated bond model on the Bethe lattice	106
7.4 : Conclusion	110

	page
<u>APPENDIX A</u> : <u>EVALUATION OF THE FREE-PARTICLE FOUR-BODY RESPONSE FUNCTION</u> $\chi_4^0$	114
<u>APPENDIX B</u> : <u>SOME EXACT LONG WAVELENGTH LIMITS OF THE RESPONSE FUNCTIONS</u> $\chi_2^0, \chi_3^0, \chi_4^0, H_4^0$	121
<u>APPENDIX C</u> : <u>SUMMARY OF DENSITY FUNCTIONAL THEORY</u>	125
<u>REFERENCES</u>	129

## INTRODUCTION

In studying liquid metals the physicist is faced with the challenging problem of understanding how the metallic properties associated with the existence of conduction electrons are modified, when, instead of moving in a vibrating ionic lattice possessing long-range order as in crystalline metals, the electrons move in a translationally dynamic and disordered ionic array characteristic of a liquid. The depth of the problem can be appreciated by recognizing the fundamental difficulties that arise in trying to solve the Schrödinger equation for the electronic states in even rigid, disordered systems (as in crystalline alloys and amorphous solids; see Chapter 5, § 5.1), as well as the fact that the liquid state is still the least well understood of the three traditional states of matter. However, much progress has been made in elucidating the structure, dynamics and transport properties of liquid metals and alloys by a synthesis of the theory of classical, non-conducting liquids and the theory of metals<sup>(1)</sup>.

The structure of simple, non-conducting liquids (the prototype being liquid argon) is usually investigated by assuming that the liquid is composed of identical particles interacting in pairs by a temperature and density independent pair potential  $\phi(r)$  (e.g. of the Lennard-Jones type) and then applying the methods of classical statistical mechanics. An important equation used in such an approach is the so called 'force equation' which may be derived from the classical partition function. This exact equation relates the pair correlation function  $g(r)$  of the liquid (see Chapter 1, § 1.2) to the pair potential  $\phi(r)$  by means of the triplet correlation function. To use the equation it is necessary to make an approximation for the triplet function (usually by decoupling it in terms of pair correlation functions). Then one can either assume a form for  $g(r)$  (or use experimental determinations of it from neutron or X-ray scattering experiments) and infer  $\phi(r)$  or vice versa. Various



approximate procedures for doing this are known as the Born-Green, Percus-Yevick and hypernetted chain theories<sup>(2)</sup>.

This treatment of simple liquids relies on the fact that they are one component systems. Liquid metals, on the other hand, are essentially two component systems, consisting of a degenerate electron gas interacting with an array of positive ions (although the division into valence electrons and ionic core electrons may be difficult in some cases). The electron gas, by screening the ions, plays a crucial role in determining the indirect interactions between the ions and hence their dynamics. But it is not obvious that these electronic effects can be adequately accounted for by means of a pairwise-additive effective ion-ion potential of the form described above. Certainly such a potential would be density-dependent by virtue of the sensitivity of electron gas properties to density. However, in 1963 Johnson and March<sup>(3)</sup>, with some theoretical justification based on second-order perturbation theory<sup>(4)</sup>, first suggested that the concept of an effective pair potentials should be useful in liquid metals. Since then much effort has been devoted to the extraction of effective pair potentials from experimental data using the methods mentioned above<sup>(5)</sup>. This procedure is fraught with uncertainties arising from the inaccuracy of experimental data, the need to numerically Fourier transform this data in order to obtain  $g(r)$  and the approximations involved in the solution of the force equation. Consequently results are far from consistent in detail and do not necessarily give temperature-independent results. Even so there is evidence in many liquid metals to support the theoretical expectation that the pair potential, in addition to a hard core, should exhibit damped oscillations (unlike in simple liquids), this being a manifestation of the Friedel oscillations that arise when a point charge is screened by an electron gas.

The concept of an effective ion potential in liquid metals has proved useful,

but the controversy that still remains over its determination and interpretation has prompted several authors, notably Watabe and Hasegawa<sup>(6)</sup>, Chihara<sup>(7)</sup> and March and Tosi<sup>(8)</sup>, to attempt to construct a full two component theory of liquid metals. In such a theory electrons and ions are treated on the same footing, although of course differences arise from the fact that the electrons must be treated as degenerate quantal particles, while the ions because of their much larger mass behave more like classical particles (for instance with translational kinetic energy per particle of  $\frac{3}{2}k_B T$ ). For this reason, the natural formalism for the two component theory is the temperature Green's function formalism which can give zero-temperature or classical limits as appropriate. At the outset, only a knowledge of the bare ion-ion, electron-ion and electron-electron interactions is assumed. The latter is quite simply taken as the Coulomb repulsion between like point charges. The other interactions are less obvious because of the finite size and core structure of the ions, although they must again be Coulombic at large distances. In simple, nearly-free electron metals (i.e. non transition metals) a reasonable model would be to assume a pseudo-potential for the electron-ion potential and a charged hard sphere interaction between the ions. The aim of the theory is then to discuss liquid metal properties from a unified viewpoint which transcends the one component theory (Tosi, Parrinello and March<sup>(9)</sup> have pointed out where this is necessary for a full understanding of electronic effects on ion dynamics), but which hopefully will also show when use of effective ion potentials is valid.

In single component liquids there is only one pair correlation function  $g(r)$ , whereas the two component theory of liquid metals naturally contains three. These are the ion-ion, ion-electron and electron-electron pair correlation functions  $g_{ii}(r)$ ,  $g_{ie}(r)$  and  $g_{ee}(r)$ , and they have to be calculated self consistently. The pair functions are related by Fourier transform to the corresponding static structure

factors  $S_{ii}(k)$ ,  $S_{ie}(k)$  and  $S_{ee}(k)$ . The first four chapters of this thesis are concerned with a calculation of  $S_{ee}(k)$  and  $S_{ie}(k)$  in nearly-free electron metals i.e. where the electron-ion interaction is weak.

Chapter 1 introduces the three correlation functions and their corresponding structure factors and briefly surveys their known properties. In particular, it is shown from charge neutrality considerations that in the long wavelength limit (i.e. as  $k \rightarrow 0$ ),  $S_{ii}(k)$ ,  $S_{ie}(k)$  and  $S_{ee}(k)$  are all proportional to the same quantity which is related to the isothermal compressibility of the system. The aim is to generalise this relationship between the structure factors to all  $k$  in a way that preserves the correct  $k \rightarrow 0$  limit. Also in chapter 1, the suggestion by Egelstaff, March and McGill<sup>(10)</sup> that  $S_{ii}(k)$ ,  $S_{ie}(k)$  and  $S_{ee}(k)$  can be individually determined by combining the results of accurate X ray, neutron and electron diffraction experiments, is outlined.

In Chapter 2, a functional derivative technique is used to derive expressions, correct to second order in the electron-ion interaction, for the time ordered electron-electron and electron-ion density response functions (from which the pair correlation functions can be easily obtained). The formalism is applicable to both solid and liquid nearly-free electron metals and involves treating the electron-ion potential as an external potential which couples to the product of the ionic and electron density fluctuations. Two special cases are then considered, rigid solids and liquid metals. In the latter case, simplification of the general expressions is possible by use of the adiabatic approximation which relies on the large ionic to electronic mass ratio. Furthermore, ensemble averaging over the ionic configurations of the liquid explicitly introduces the ion-ion structure factor into the calculation. Finally, expressions to second order in the electron-ion potential are obtained for the change in  $S_{ee}(k)$  and  $S_{ie}(k)$  from their jellium values (i.e. when the electron-ion

interaction in zero). Specific terms in each case are shown to give the correct long wavelength limits.

In the case of  $S_{ee}(k)$  there is an additional second order term involving a four-body electronic response function of jellium. Chapter 3 discusses two approximations to this response function, one based on density functional theory and the other based on diagrammatic analysis. Both approaches rely on knowledge of the corresponding response function for non-interacting jellium and Appendix A is concerned with the evaluation of this function. In Appendix B some long wavelength sum-rules relating to the various response functions that have been introduced are derived.

Calculations of the dominant terms in  $S_{ee}(k)$  and  $S_{ie}(k)$  for liquid sodium and aluminium are presented in chapter 4, use being made of experimental neutron data for  $S_{ii}(k)$ . The results show that electron-ion corrections to  $S_{ie}(k)$  and  $S_{ee}(k)$  are generally small. One conclusion is that the proposal of Egelstaff et al to extract  $S_{ee}(k)$  from a combination of scattering data will, at least in the case of sodium, provide a measure of the structure factor of jellium at the density of liquid sodium. On the other hand, it is shown that the large discrepancies between existing X ray and neutron structure factor data cannot be explained by the theory of this thesis, perhaps indicating that the experiments are not yet accurate enough to justify carrying out the proposal of Egelstaff et al.

Chapters 5 and 6 are concerned with two problems relating to electron density in random binary alloys, and the problems are introduced at the beginning of each chapter. Similarly, chapter 7 starts with a general introduction to percolation theory before going on to give the solution to the correlated bond percolation problem on the Bethe lattice. Finally, Appendix C gives a summary of the main results of density functional theory to which appeal is made at several places during this thesis.

Much of the work presented in this thesis has already been published in the following papers:

- (a) S. Cusack, N.H. March, M. Parrinello and M.P. Tosi, Electron-electron pair correlation function in solid and molten nearly-free electron metals, J. Phys. F6, 749, (1976).
- (b) S. Cusack and N.H. March, Charge and momentum density in metals and alloys, Int. J. Quantum Chem. 9, 481, (1975).
- (c) S. Cusack, Correlated bond percolation on the Bethe lattice, J. Phys. A9, L55, (1976).

## CHAPTER 1

PAIR CORRELATION FUNCTIONS AND STATIC STRUCTURE FACTORS IN LIQUIDMETALS§ 1.1 Hamiltonian for a two component liquid metal

In the introduction it has been argued that in simple liquid metals, where a more or less clear distinction can be made between valence and core electrons, a model which treats the liquid metal explicitly as an interacting two component assembly of valence electrons and ions is appropriate. If the bare electron-electron, electron-ion and ion-ion interactions are denoted respectively by  $V_{ee}$ ,  $V_{ie}$  and  $V_{ii}$ , then the Hamiltonian for such an assembly can be written

$$H = \sum_i \frac{p_i^2}{2m} + \sum_j \frac{P_j^2}{2M} + \frac{1}{2} \sum_{i \neq i'} V_{ee}(\underline{r}_i - \underline{r}_{i'}) + \frac{1}{2} \sum_{j \neq j'} V_{ii}(\underline{R}_j - \underline{R}_{j'}) + \sum_{ij} V_{ie}(\underline{r}_i - \underline{R}_j) \quad (1.1)$$

Here  $\underline{p}_i$  and  $\underline{r}_i$  are the momentum and position of the  $i$  th electron (mass  $m$ );  $\underline{P}_j$  and  $\underline{R}_j$  are the momentum and position of the  $j$  th ion (mass  $M$ ). (1.1) can be written in second quantised form by introducing density fluctuation operators  $\rho_{\underline{k}}(t)$  for each component. These are defined in terms of the local number densities  $\rho_e(\underline{r}, t)$  and  $\rho_i(\underline{r}, t)$  of electrons and ions by the relations

$$\rho_e(\underline{r}, t) = \sum_i \delta(\underline{r} - \underline{r}_i(t)) = \sum_{\underline{k}} \rho_{\underline{k}}(t) e^{i\underline{k} \cdot \underline{r}} \quad (1.2)$$

$$\rho_i(\underline{r}, t) = \sum_j \delta(\underline{r} - \underline{R}_j(t)) = \sum_{\underline{k}} \rho_{i\underline{k}}(t) e^{i\underline{k} \cdot \underline{r}} \quad (1.3)$$

which on inversion give

$$\rho_{\underline{k}}(t) = \frac{1}{V} \sum_i e^{-i\underline{k} \cdot \underline{r}_i(t)} ; \rho_{i\underline{k}}(t) = \frac{1}{V} \sum_j e^{-i\underline{k} \cdot \underline{R}_j(t)} \quad (1.4)$$

where  $V$  is the volume of the liquid metal (conveniently taken as unity). The

Hamiltonian now becomes

$$H = \sum_i \frac{p_i^2}{2m} + \sum_j \frac{P_j^2}{2M} + \frac{1}{2} \sum_{\underline{k}} V_{ee}(\underline{k}) (\rho_{-\underline{k}} \rho_{\underline{k}} - n_e) + \frac{1}{2} \sum_{\underline{k}} V_{ii}(\underline{k}) (\rho_{i-\underline{k}} \rho_{i\underline{k}} - n_i) + \sum_{\underline{k}} V_{ie}(\underline{k}) \rho_{e-\underline{k}} \rho_{i\underline{k}} \quad (1.5)$$

where the mean electron and ionic densities  $n_e$  and  $n_i$  are related by  $n_e = Z n_i$ ,  $Z$  being the valency.

### § 1.2 Pair correlation functions and static structure factors

In the two component theory of liquid metals one must work with three pair correlation functions, the electron-electron  $g_{ee}(r)$ , the electron-ion  $g_{ei}(r)$  and the ion-ion  $g_{ii}(r)$  pair correlation functions. In general these will be denoted by  $g_{ab}(r)$  where  $a$  and  $b$  can be either  $e$  and  $i$  and  $\bar{a} = e$  if  $a = i$  (and vice versa). This notation will also be used for other functions entering the two component theory. The  $g_{ab}(r)$  are defined in terms of the two particle distribution functions  $P_{ab}(r)$  as follows

$$\begin{aligned} P_{ab}(r) &= \langle \rho_a(\underline{r}) \rho_b(\underline{r} + \underline{r}) \rangle \\ &= \left\langle \sum_{i_a} \delta(\underline{r} - \underline{r}_{i_a}) \sum_{i_b} \delta(\underline{r} + \underline{r} - \underline{r}_{i_b}) \right\rangle \\ &= \delta_{ab} \delta(r) n_a + n_a n_b g_{ab}(r) \end{aligned} \quad (1.6)$$

$$g_{ab}(r) = \left\langle \sum_{i_a \neq i_b} \delta(\underline{r} - \underline{r}_{i_a}) \delta(\underline{r} + \underline{r} - \underline{r}_{i_b}) \right\rangle \quad (1.7)$$

Here  $\langle \rangle$  indicates an average taken in the grand canonical ensemble. As a result,  $P_{ab}(r)$  and  $g_{ab}(r)$  will be configurationally averaged properties of the liquid metal and will thus be isotropic. A physical interpretation of  $g_{ab}(r)$  is that the quantity  $\int_{4\pi r} r^2 g_{ab}(r) dr$  gives the probability of finding a particle of type  $b$  within the spherical shell of width  $dr$  at distance  $r$  from an  $a$  type particle at the origin. Note that the total energy density  $U$  of the liquid metal can be written in terms of the  $g_{ab}(r)$ ,

$$\begin{aligned} U &= \frac{3}{2} n_i k_B T + t_e \\ &\quad + \int d\underline{r} \frac{1}{2} \left[ n_e^2 g_{ee}(r) v_{ee}(r) + n_i^2 g_{ii}(r) v_{ii}(r) + 2 n_i n_e g_{ie}(r) v_{ie}(r) \right] \end{aligned} \quad (1.8)$$

the first two terms being the kinetic energy density of the ions (classical) and electrons and the other terms being the potential energy density.

We now introduce the static structure factors  $S_{ab}(k)$  defined by

$$\begin{aligned} S_{ab}(k) &= \frac{1}{(n_a n_b)^{\frac{1}{2}}} \int e^{i\mathbf{k}\cdot\mathbf{r}} (P_{ab}(r) - n_a n_b) d\mathbf{r} \\ &= S_{ab} + (n_a n_b)^{\frac{1}{2}} \int e^{i\mathbf{k}\cdot\mathbf{r}} (g_{ab}(r) - 1) d\mathbf{r} \end{aligned} \quad (1.9)$$

The Fourier inverse of (1.9) gives

$$g_{ab}(r) = 1 + \frac{1}{(n_a n_b)^{\frac{1}{2}}} \int e^{-i\mathbf{k}\cdot\mathbf{r}} (S_{ab}(k) - S_{ab}) \frac{d\mathbf{k}}{(2\pi)^3} \quad (1.10)$$

(1.9) and (1.10) are generalisations of the familiar radial distribution function  $g(r)$  and structure factor  $S(k)$  of a one component liquid. In such a system  $S(k)$  is interpreted physically as the measured intensity when a monochromatic plane wave disturbance (e.g. electron, neutron or X ray) is transmitted through the system. The experimental determination of the  $S_{ab}(k)$  will be discussed in § 1.5.

### § 1.3 The long wavelength limit of the $S_{ab}(k)$

We now derive the interesting 'charge neutrality' condition which relates the three structure factors  $S_{ab}(k)$  in the long wavelength limit, i.e. as  $k \rightarrow 0$ . We follow the simple, direct argument of March and Tosi<sup>(8)</sup>, although the result was first derived in references (6) and (7).

The strong electrostatic forces between the charged components of a liquid metal ensure that the system must be electrically neutral overall. In other words the long wavelength fluctuations of each component must be neutralised by the other component. In particular, the total charge surrounding an electron at the origin must be +1 i.e.

$$\int Z n_i g_{ie}(r) d\mathbf{r} - \int n_e g_{ee}(r) d\mathbf{r} = 1 \quad (1.11)$$

while that around an ion at the origin must be  $-Z$ , i.e.

$$\int Z n_i g_{ii}(r) d\mathbf{r} - \int n_e g_{ie}(r) d\mathbf{r} = -Z \quad (1.12)$$

Using the fact that  $n_e = Z n_i$  it follows from (1.11) that

$$\int Z n_i (g_{ie}(r) - 1) d\mathbf{r} - \int n_e (g_{ee}(r) - 1) d\mathbf{r} = 1$$



which using (1.9) gives

$$\sum^{\frac{1}{2}} S_{ie}(0) = S_{ee}(0)$$

Similarly (1.12) leads to

$$\sum S_{ii}(0) = \sum^{\frac{1}{2}} S_{ie}(0)$$

Thus we have the final result that for a liquid metal

$$S_{ii}(0) = \frac{i}{\sum^{\frac{1}{2}}} S_{ie}(0) = \frac{1}{\sum} S_{ee}(0) \quad (1.13)$$

Furthermore,  $S_{ii}(0)$  may be related to the isothermal compressibility  $K_T$  of the system by the usual result of thermodynamic fluctuation theory extended to multi-component systems<sup>(11), (12)</sup>.

$$S_{ii}(0) = \frac{n_i K_T}{\rho} \quad (1.14)$$

where  $\beta = (k_B T)^{-1}$ .

In liquid metals therefore,  $S_{ee}(0)$  is non zero, although still very small as  $S_{ii}(0) \sim 0.01 - 0.03$  for most liquid metals at their melting points<sup>(1a)</sup>. This is to be compared with the long wavelength limit of the electron structure factor  $S(k)$  in the jellium model. In this model, interacting electrons move against a uniform, positive, neutralising background and it can be rigorously established that for small  $k$

$$S(k) = \frac{\hbar k^2}{2m\omega_p} + O(k^4) \quad (1.15)$$

where  $\omega_p = (4\pi n_e e^2/m)^{\frac{1}{2}}$  is the electronic plasma frequency. In chapter 2 where  $\Delta S_{ee}(k) = S_{ee}(k) - S(k)$  is calculated it will therefore be necessary to show that  $\Delta S_{ee}(0) = \sum S_{ii}(0)$ .

Note that the arguments leading to (1.13) have been generalised in two directions:

(a) to relate the long wavelength limits of electronic triplet correlations functions to thermodynamic quantities<sup>(13)</sup>; and (b) to relate the  $k \rightarrow 0$  limits of the structure factors

in binary liquid alloys which are three component systems<sup>(14)</sup>. Also, Tosi and March<sup>(15)</sup> have discussed the terms of order  $k^2$  in the structure factors  $S_{ab}(k)$ .

Assuming that in the long wavelength limit the dominant excitations in a liquid metal are collective modes, these authors conclude on the basis of a simple plasmon-phonon model, that a term of the form (1.15) is still important in  $S_{ee}(k)$  (although modified to contain the reduced plasma frequency given by  $\omega_p = \left[ 4\pi n_e e^2 (M+Zm)/Mm \right]^{\frac{1}{2}}$ ) but the corresponding terms in  $S_{ii}(k)$  and  $S_{ie}(k)$  are extremely small because of the large ionic mass. This latter point is borne out by the characteristic flatness of measured  $S_{ii}(k)$ 's in the low  $k$  region.

### § 1.4 Density response functions

An alternative means of defining the  $S_{ab}(k)$  is via the linear density response functions  $\chi_{ab}(k, \omega)$  of the two component liquid metal. These are defined by

$$\delta \rho_a(k, \omega) = \sum_b \chi_{ab}(k, \omega) V_b^{\text{ext}}(k, \omega) \quad (1.16)$$

Thus  $\chi_{ab}(k, \omega)$  gives the response of the density of component  $a$  to a weak external potential  $V_b^{\text{ext}}(k, \omega)$  of wavenumber  $k$  and frequency  $\omega$  applied to component

$b$ . The  $\chi_{ab}(k, \omega)$ 's are properties of the unperturbed liquid metal and are given in terms of the density fluctuations (1.4) by the Kubo formulae

$$\chi_{ab}(k, \omega) = i/\hbar \int_0^\infty dt e^{i\omega t} \langle [ \rho_{ak}(t), \rho_{b-k}(0) ] \rangle \quad (1.17)$$

where again the notation implies a thermal average. The dynamic structure factors

$S_{ab}(k, \omega)$  may now be defined via the Fluctuation-Dissipation theorem

$$S_{ab}(k, \omega) = -\frac{\hbar}{\pi} \frac{1}{1 - e^{-\beta \hbar \omega}} \text{Im} \chi_{ab}(k, \omega) \quad (1.18)$$

and thence the static structure factors  $S_{ab}(k)$  by

$$S_{ab}(k) = \left( \frac{1}{n_a n_b} \right)^{\frac{1}{2}} \int_{-\infty}^{\infty} d\omega S_{ab}(k, \omega) \quad (1.19a)$$

$$= \left( \frac{1}{n_a n_b} \right)^{\frac{1}{2}} \langle \rho_{ak} \rho_{b-k} \rangle \quad (1.19b)$$

Tosi, Parrinello and March (TPM)<sup>(9)</sup> have shown how the  $\chi_{ab}(k\omega)$ 's and their generalisations to mass and charge density response functions may be used to discuss a wide variety of liquid metal properties such as electrical resistivity, sound attenuation, viscosity and elastic neutron scattering. They are particularly concerned to point out how electronic effects enter the dynamics of the ions. For the present purpose it is interesting to briefly follow their analysis of  $\chi_{ab}(k\omega)$  (which closely resembles that of Watabe and Hasegawa<sup>(6)</sup>) to obtain information about  $S_{ab}(k)$ .

We introduce the Hartree potentials  $V_a^H(k\omega)$  for each component, defined by

$$V_a^H(k\omega) = V_a^{\text{ext}}(k\omega) + \sum_r V_{ar}(k) \rho_r(k\omega) \quad (1.20)$$

where  $V_{ab}(k)$  are the bare interparticle potentials. Proper (irreducible) density response functions  $\Pi_{ab}(k\omega)$  are then defined by

$$\delta \rho_a(k\omega) = \sum_r \Pi_{ar}(k\omega) V_r^H(k\omega) \quad (1.21)$$

From (1.16) and (1.21) it follows that

$$\chi_{ab}(k\omega) = \Pi_{ab}(k\omega) + \sum_c \sum_d \Pi_{ac}(k\omega) V_{cd}(k) \chi_{db}(k\omega) \quad (1.22a)$$

or equivalently

$$\underline{\chi} = \underline{\Pi} + \underline{\Pi} \underline{V} \underline{\chi} \quad (1.22b)$$

in an obvious matrix notation. (1.22) may be readily solved for the  $\chi_{ab}(k\omega)$ 's

in the form

$$\begin{aligned} \chi_{ab} &= \sum_c (\underline{1} - \underline{\Pi} \underline{V})_{ac}^{-1} \Pi_{cb} \\ &= \frac{1}{\Delta} \sum_c |\underline{1} - \underline{\Pi} \underline{V}|_{ac} \Pi_{cb} \end{aligned} \quad (1.23)$$

where  $|\underline{1} - \underline{\Pi} \underline{V}|_{ac}$  is the cofactor matrix and  $\Delta$  is the determinant of  $\underline{1} - \underline{\Pi} \underline{V}$

Explicitly

$$\begin{aligned} \Delta &= [1 - (\Pi_{ii} V_{ii} + \Pi_{ie} V_{ie})][1 - (\Pi_{ei} V_{ie} + \Pi_{ee} V_{ee})] \\ &\quad - (\Pi_{ii} V_{ie} + \Pi_{ie} V_{ee})(\Pi_{ei} V_{ii} + \Pi_{ee} V_{ei}) \end{aligned} \quad (1.24)$$

where the  $\underline{k}\omega$  arguments have been omitted for simplicity.

These equations can be expressed in diagrammatic form. However TPM proceed to obtain exact expressions for the  $\chi_{ab}$ 's and  $\Pi_{ab}$ 's by formally solving the linearised equation of motion for the particle densities in the presence of an external potential. The results (which are rather complicated) contain three particle correlation functions of the unperturbed liquid metal. By this means compressibility sum-rules (c.f. (1.13) and (1.14)) are obtained of the form

$$\lim_{k \rightarrow 0} \left\{ \chi_{ab}(k, 0) = -\beta (n_a n_b)^{\frac{1}{2}} S_{ab}(k) \right\} = -n_a n_b \quad (1.25)$$

with  $K_T$  being expressed in terms of explicit microscopic quantities. (1.25) contains the result  $\lim_{k \rightarrow 0} [\chi_{ii}(k, 0) = -n_i \beta \rho_{ii}(k)]$  which follows from the classical limit of the Fluctuation-Dissipation theorem (1.18) and the Kramers-Kronig relations between the real and imaginary parts of  $\chi_{ii}(k, \omega)$  and is therefore to be expected for the ions. However (1.25) shows that the long wavelength charge neutrality requirements also impose classical behaviour of the electrons in this limit.

Simple results for the  $\chi_{ab}$ 's are obtained if it is assumed that in simple metals, where the bare electron-ion interaction is weak, the indirect proper polarisations  $\Pi_{a\bar{a}}$  can be neglected and the  $\Pi_{aa}$ 's can be approximated by their free particle values  $\Pi_a^0$  (in appropriate classical and zero-temperature limits for the ions and electrons). This random-phase approximation (RPA) gives<sup>(6), (9)</sup>

$$\chi_{aa}^{RPA}(k, \omega) = \frac{\Pi_a^0(k, \omega)}{(1 - \Pi_a^0(k, \omega) V_{aa}^{eff}(k, \omega))} \quad (1.26)$$

$$\chi_{a\bar{a}}^{RPA}(k, \omega) = \chi_a^{RPA}(k, \omega) V_{a\bar{a}}(k) \chi_{\bar{a}\bar{a}}^{RPA}(k, \omega) \quad (1.27)$$

where  $\chi_a^{RPA} = \Pi_a^0 / (1 - V_{aa} \Pi_a^0)$  is the usual RPA density response function for a single component system and the frequency dependent effective potentials for each component are given by

$$V_{aa}^{eff}(k, \omega) = V_{aa}(k) + V_{a\bar{a}}(k) \chi_{\bar{a}\bar{a}}^{RPA}(k, \omega) V_{\bar{a}a}(k) \quad (1.28)$$

Although the RPA is not a good approximation for real metallic systems, these expressions afford a physical interpretation which TPM have shown to be general. According to (1.26), each component responds to a direct perturbation as if it were a single component with an interparticle potential modified as a result of screening by the other component. (1.27) shows that the indirect response is that of a single component responding to the polarisation potential of the other component as if it were an external potential. Note however, that the effective potentials are in general more complicated and the electron-ion interaction is also modified.

Very recently Trigger<sup>(23)</sup> has improved on the RPA approximation (although he still puts  $\overline{\Pi}_{ei}(\underline{k}, \omega) \sim 0$ ) and using the Fluctuation-Dissipation theorem and adiabatic approximation has derived the dominant terms which relate  $S_{ie}(k)$  and  $S_{ee}(k)$  to  $S_{ii}(k)$  in the case of weak electron-ion coupling. These terms are easily shown to satisfy the correct charge neutrality conditions (1.13). Cusack, March, Parrinello and Tosi<sup>(22)</sup> have independently obtained the same results by a different method (see Chapter 2) which does not put  $\overline{\Pi}_{ei}(\underline{k}, \omega) \sim 0$  but does rely on the adiabatic approximation (see § 2.8). Consequently, additional terms arise which are second order in  $V_{ie}(k)$  and involve higher order correlation functions, although they are expected to be small.

### § 1.5 Experimental determination of the structure factors $S_{ab}(k)$

In 1973 Egelstaff, March and McGill (EMM)<sup>(10)</sup> suggested that in principle each of the three liquid metal structure factors could be empirically determined by suitably combining the results of X ray, neutron and electron diffraction experiments. The possibility arises from the fact that these three probes are each scattered by different elements of the liquid metal.

X rays are scattered by the electrons of the system, that is both core and valence electrons. Scattering by the nuclei can be neglected as it gives

contributions to the cross section that are a factor of  $(m/M)^2$  less. First order time dependent perturbation theory gives for the differential cross section for X rays<sup>(16)</sup>

$$\frac{\partial^2 \sigma_x}{\partial \Omega \partial \omega} = \left(\frac{e^2}{m}\right)^2 (\underline{e}_1 \cdot \underline{e}_2) \frac{\omega_2}{\omega_1} S_x(\underline{k}, \omega) \quad (1.29)$$

Here an incident photon of frequency  $\omega_1$ , wave vector  $\underline{k}_1$  and polarisation  $\underline{e}_1$  is scattered into a photon with corresponding parameters  $\omega_2, \underline{k}_2, \underline{e}_2$  and  $\omega = \omega_1 - \omega_2, \underline{k} = \underline{k}_1 - \underline{k}_2$ .  $S_x(\underline{k}, \omega)$  is a dynamic structure factor given by

$$S_x(\underline{k}, \omega) = \frac{1}{2\pi} \int_{-\infty}^{\infty} e^{i\omega t} \langle \rho_{\underline{k}}(t) \rho_{-\underline{k}}(0) \rangle dt \quad (1.30)$$

$\rho_{\underline{k}}$  being the total (core and valence) electron density fluctuations. As in X ray experiments  $\omega_2/\omega_1 \sim 1$  integration over energy transfer gives (c.f. (1.19) )

$$\frac{d\sigma_x}{d\Omega} \propto S_x(k) ; S_x(k) = \frac{1}{n_i} \langle \rho_{\underline{k}} \rho_{-\underline{k}} \rangle \quad (1.31)$$

Neutrons are essentially scattered by the ionic nuclei (if magnetic scattering by the electrons is neglected) and the coherent cross section is given by<sup>(17)</sup>

$$\frac{\partial^2 \sigma_N^{coh}}{\partial \Omega \partial \omega} = N \langle b \rangle^2 \frac{|\underline{k}_2|}{|\underline{k}_1|} S_N^{coh}(\underline{k}, \omega) \quad (1.32)$$

where  $\langle b \rangle$  is the mean scattering length of the N nuclei. Again making the static approximation that  $|\underline{k}_2| \sim |\underline{k}_1|$  (see §4.7 for a mention of corrections that have to be made in analysing actual neutron data) and integrating over  $\omega$  gives

$$\frac{d\sigma_N^{coh}}{d\Omega} \propto S_N(k) ; S_N(k) = \frac{1}{n_i} \langle \rho_{i\underline{k}} \rho_{i-\underline{k}} \rangle \quad (1.33)$$

Electrons are scattered by all charges present and one finds

$$\frac{d\sigma_E}{d\Omega} \propto \frac{1}{k^4} S_E(k) ; S_E(k) = \frac{1}{n_i} \langle \rho_{\underline{k}} \rho_{-\underline{k}} \rangle \quad (1.34)$$

where  $\rho_{\underline{k}} = Q\rho_{i\underline{k}} - \rho_{\underline{k}}$ ,  $Q$  being the total nuclear charge.

Consistent with the assumptions of the two component theory of simple liquid metals, we now divide the total electronic density into two parts, one due to the  $Z$  valence electrons and one due to  $Z_c = Q - Z$  core electrons. The core electrons are assumed to be rigidly attached to the nucleus and their density to be adequately described by the free ion form factor  $f_c(\underline{k})$  which is available from wave function calculations<sup>(18)</sup>. Thus any environmental effects which might redistribute the core charge density are neglected. Under these assumptions  $\rho_{\underline{k}} = \rho_{e\underline{k}} + \rho_{i\underline{k}}f_c(\underline{k})$

Using (1.19) and (1.31), (1.33), (1.34) we now find that

$$S_x(k) = Z S_{ee}(k) + 2Z \frac{1}{2} f_c(k) S_{ie}(k) + f_c^2(k) S_{ii}(k) \quad (1.35a)$$

$$S_N(k) = S_{ii}(k) \quad (1.35b)$$

$$S_E(k) = Q^2 S_{ii}(k) - 2Q(Z \frac{1}{2} f_c(k) + f_c(k) S_{ii}(k)) + S_x(k) \quad (1.35c)$$

Neutron scattering, as expected, gives a direct measure of  $S_{ii}(k)$ . Solving for

$S_{ie}(k)$  and  $S_{ee}(k)$  we obtain

$$Z \frac{1}{2} S_{ie}(k) = \frac{1}{2Q} [S_x(k) - S_E(k) + Q(Q - 2f_c(k)) S_N(k)] \quad (1.36a)$$

$$Z S_{ee}(k) = \frac{1}{Q} [(Q - f_c(k)) S_x(k) + f_c(k) S_E(k) - Q f_c(k) (Q - f_c(k)) S_N(k)] \quad (1.36b)$$

It is therefore in principle possible to determine  $S_{ie}(k)$  and  $S_{ee}(k)$  from experiment, although in order to do this reliably, the scattering data needs to

be highly accurate as only small differences are involved. For instance, in

(1.35a) the ratio of the three terms contributing to  $S_x(k)$  as  $k \rightarrow 0$  is

$Z^2 : 2Z(Q - Z) : (Q - Z)^2$  (where the charge neutrality limits have been used for

the  $S_{ab}(k)$  and also  $f_c(0) = Q - Z$ ). Thus only for lighter elements ( $Q$  small) will

the valence electron correlation effects be detectable (unless they are particularly strong).

In the absence of reliable electron scattering data EMM proceeded to analyse the available X ray and neutron data on liquid metals on the basis of the above equations. In particular, they draw attention to systematic differences between the heights of the first (principal) peak at  $k = k_0$  as given by neutron structure factor data and normalised X ray data. (X ray structure factor data is conventionally presented as  $S_X(k)/f_a^2(k)$  where  $f_a(k)$  is the calculated free atom form factor). A summary of their results is shown in table 1.1.

Liquid group	$\frac{S_N(k_0)}{S_X(k_0)/f_a^2(k_0)}$
Liquefied rare gases	0.98 $\pm$ 0.03
Molecular fluids	1.12 $\pm$ 0.04
Monovalent metals	0.87 $\pm$ 0.04
Polyvalent metals	0.92 $\pm$ 0.03

Table 1.1 Intensity ratios at the principal peak for various liquid groups.

EMM conclude from these observations that, if systematic errors in the data are discounted, the consistently greater X ray peak heights in liquid metals are indicative of longer range instantaneous correlations between the valence electrons than between the ions. In other words the conduction electrons in a liquid metal form an electron liquid rather than electron gas. According to (1.35a) and (1.35b) the difference,  $\Delta(k)$ , between normalised X ray and neutron structure factor measurements is given by

$$\Delta(k) = \frac{S_X(k)}{f_a^2(k)} - S_N(k) = \frac{Z}{f_a^2(k)} S_{ee}(k) + \frac{2Z^{\frac{1}{2}} f_c(k) S_{ie}(k)}{f_a^2(k)} + S_{ii}(k) \left[ \frac{f_c^2(k)}{f_a^2(k)} - 1 \right] \quad (1.37)$$

It was part of the purpose of this thesis to see if a theoretical calculation of  $S_{ee}(k)$  and  $S_{ie}(k)$  could be used in conjunction with (1.37) to help explain the discrepancies between experimental X ray and neutron data (see § 4.6 ).



## CHAPTER 2

### SECOND-ORDER PERTURBATION THEORY FOR THE ELECTRONIC STRUCTURE

#### FACTORS

##### § 2.1 Introduction

In this chapter a second-order perturbation theory is developed for the electronic structure factors  $S_{ee}(k)$  and  $S_{ie}(k)$  in the presence of weak electron-ion interactions.

The theory is applicable to both liquid and solid nearly-free electron metals but calculations have only been carried out in the liquid metal case (see chapter 4). One reason for this is that, as described in chapter 1,  $S_{ee}(k)$  and  $S_{ie}(k)$  naturally enter the two component theory of liquid metals. Also, the work of EMM<sup>(10)</sup> provides motivation for calculating these functions in liquid metals for comparison with the results of scattering experiments when they become available\* and more immediately, to clarify the observed difference between X ray and neutron structure factor data.

As will become apparent, the fact that the ensemble averaged liquid metal correlation functions are isotropic and the density a constant, leads to considerable simplifications in the following theory. However, to be able also to describe correlation functions in crystalline metals, where the electron density varies periodically, we have to consider the full two particle correlation function, or more conveniently its cluster part defined in the electron-electron case by (c.f.(1.9) )

$$P_{ee}^c(\underline{r}_1, \underline{r}_2) = \langle \rho_e(\underline{r}_1) \rho_e(\underline{r}_2) \rangle_c = \langle \rho_e(\underline{r}_1) \rho_e(\underline{r}_2) \rangle - \langle \rho_e(\underline{r}_1) \rangle \langle \rho_e(\underline{r}_2) \rangle \quad (2.1)$$

---

\* Dr. P. Dobson and Dr. B. Unvala of Imperial College, London, are currently engaged in a research programme to study the structure of various liquid metals by electron diffraction.

and with Fourier transform (c.f. (1.10) )

$$S_{ee}(\underline{k}, \underline{G}-\underline{k}) = \iint e^{i\underline{k} \cdot (\underline{r}_1 - \underline{r}_2)} e^{i\underline{G} \cdot \underline{r}_2} \rho_{ee}^c(\underline{r}_1, \underline{r}_2) d\underline{r}_1 d\underline{r}_2 \quad (2.2)$$

In (2.1) and elsewhere the notation  $\langle \rangle_c$  indicates the cluster (or cumulant) part and in (2.2),  $\underline{G}$  is a reciprocal lattice vector. Thus complete information about the correlation functions in periodic solids will require knowledge of the non-diagonal ( $\underline{G} \neq 0$ ) elements of the response functions that enter the theory, whereas for liquid metals, the diagonal ( $\underline{G} = 0$ ) elements will be sufficient.

### § 2.2 The unperturbed system

The principle of the perturbation theory is to switch on a weak electron-ion interaction  $V_{ie}(\underline{r})$  to an unperturbed system consisting of a jellium of interacting electrons superimposed on (but not interacting with) a jellium of ions. Using a functional derivative technique, the linear and quadratic response functions which determine the first- and second-order changes in the electronic correlation functions from their unperturbed values are then calculated.

The Hamiltonian for the unperturbed system,  $H_0$ , is given by (c.f. (1.5) )

$$\begin{aligned} H_0 &= H_e + H_i \\ &= \sum_i p_i^2 / 2m + \frac{1}{2} \sum_{\underline{k}}' V_{ee}(\underline{k}) (\rho_{e\underline{k}} \rho_{e-\underline{k}} - \rho_e) \\ &\quad + \sum_j p_j^2 / 2M + \frac{1}{2} \sum_{\underline{k}}' V_{ii}(\underline{k}) (\rho_{i\underline{k}} \rho_{i-\underline{k}} - \rho_i) \end{aligned} \quad (2.3)$$

where the  $\sum_{\underline{k}}'$  indicates that the  $\underline{k} = 0$  term is excluded from the summation to take account of the uniform neutralising background of jellium<sup>(19a)</sup>. In the unperturbed system, the electrons may be treated as fully degenerate (i.e. at  $T=0$ ) while the ions behave classically. The unperturbed electron-ion structure factor is clearly zero, and the unperturbed electron-electron structure factor is that of

jellium and denoted by  $S(k)$  (c.f. (1.15)).

The electron-ion interaction  $V_{ie}(r)$  will be treated as a time dependent perturbation  $H_{ie}(t)$  which couples the electron and ion densities and is given by

$$H_{ie}(t) = \iint V_{ie}(\underline{x}-\underline{y}) \rho_e(\underline{x}, t) \rho_i(\underline{y}, t) d\underline{x} d\underline{y} \quad (2.4)$$

### § 2.3 Perturbation expansion for the electron-electron density fluctuation propagator

To allow for the greatest generality we now generate a perturbation expansion for the electron-electron density fluctuation propagator. (For the electron-ion case, see § 2.9). This propagator,  $D_{ee}(X_1, X_2)$ , is defined by

$$D_{ee}(X_1, X_2) = \langle T [\rho_e(X_1) \rho_e(X_2)] \rangle_c \quad (2.5)$$

where  $X_1 \equiv \underline{r}_1 t_1$  and  $T$  is the Wick time-ordering operator. We can obtain

$P_{ee}^c(r_1, r_2)$  (equation (2.1)) simply by putting  $t_1 = t_2^+$  in (2.5) and hence the

structure factor  $S_{ee}$  by Fourier transform. Furthermore in the unperturbed system,

$D_{ee}(X_1 - X_2)$  is closely related to  $\chi(X_1 - X_2)$  the causal, linear density response function for interacting electrons in the jellium model<sup>(19b)</sup>. In the static limit

( $\omega = 0$ ), which will be required later,  $\chi(\underline{k}, 0) = -i/\hbar D_{ee}(\underline{k}, 0)$  where  $\chi(\underline{k}, \omega)$

and  $D_{ee}(\underline{k}, \omega)$  are the Fourier transforms of  $\chi(X_1 - X_2)$  and  $D_{ee}(X_1 - X_2)$ .

The first- and second-order terms in the perturbation expansion for the change in  $D_{ee}(X_1, X_2)$  due to weak electron-ion interactions may now be formally written

in terms of functional derivatives as

$$\delta D_{ee}(X_1, X_2) = \int \frac{\delta D_{ee}(X_1, X_2)}{\delta V_{ie}(X_3)} V_{ie}(X_3) dX_3 + \frac{1}{2} \iint \frac{\delta^2 D_{ee}(X_1, X_2)}{\delta V_{ie}(X_3) \delta V_{ie}(X_4)} V_{ie}(X_3) V_{ie}(X_4) dX_3 dX_4 \quad (2.6)$$

where  $V_{ie}(X_3) = V_{ie}(\underline{r}_3)$ . The response functions, expressed here as functional

derivatives, have to be evaluated in the unperturbed system and this may be done

using the following theorem, proved for instance by Hedin and Lundqvist<sup>(20)</sup>  
(see also Kadanoff and Baym<sup>(21)</sup>).

### § 2.4 A theorem for functional derivatives

The theorem states the following. For a system described by the Hamiltonian

$$H(t) = H_0 + \int \rho(\underline{r}, t) V^{\text{ext}}(\underline{r}, t) d\underline{r} \quad (2.7)$$

where the second term describes the coupling of the density to an external potential, the functional derivative with respect to the external potential of the interacting ground state expectation value of a time ordered product of operators

$\langle T[O_1(t_1)O_2(t_2)\dots O_n(t_n)] \rangle$  is given by

$$\frac{\delta \langle T[O_1(t_1)O_2(t_2)\dots O_n(t_n)] \rangle}{\delta V^{\text{ext}}(\underline{r}, t)} = -i/\hbar \langle T[\tilde{\rho}(\underline{r}, t)O_1(t_1)\dots O_n(t_n)] \rangle \quad (2.8)$$

where  $\tilde{\rho}(\underline{r}, t) = \rho(\underline{r}, t) - \langle \rho(\underline{r}, t) \rangle$ .

This theorem is proved by using the methods of time dependent perturbation theory<sup>(19)</sup> i.e. by transforming from the Heisenberg representation (in which the above expectation values are expressed) into the interaction representation. In this representation,

$$\langle T[O_1(t_1)O_2(t_2)\dots O_n(t_n)] \rangle = \frac{\langle 0|T[S O_1^{\text{I}}(t_1)O_2^{\text{I}}(t_2)\dots O_n^{\text{I}}(t_n)]|0 \rangle}{\langle 0|S|0 \rangle} \quad (2.9)$$

where the interaction picture operators  $O^{\text{I}}(t)$  are related to the Heisenberg operators  $O(t)$  by

$$O(t) = e^{iHt/\hbar} e^{-iH_0 t/\hbar} O^{\text{I}}(t) e^{iH_0 t/\hbar} e^{-iHt/\hbar} \quad (2.10)$$

$|0\rangle$  is the non-interacting ground state and all the effects of the external potential are contained in the S-matrix which is given by

$$S = T \left[ e^{-i/\hbar \int_{-\infty}^{\infty} dt \int d\underline{r} \rho^{\text{I}}(\underline{r}, t) V^{\text{ext}}(\underline{r}, t)} \right] \quad (2.11)$$

From (2.11) we find

$$\frac{\delta S}{\delta V^{\text{ext}}(\underline{r}t)} = -i/k S e^{\mathcal{I}}(\underline{r}t) \quad (2.15)$$

Now taking the functional derivative of (2.9) gives

$$\begin{aligned} \frac{\delta \langle T[O_1(t_1)O_2(t_2)\dots O_n(t_n)] \rangle}{\delta V^{\text{ext}}(\underline{r}t)} &= \frac{\langle 0|T[\frac{\delta S}{\delta V^{\text{ext}}(\underline{r}t)} O_1^{\mathcal{I}}(t_1)O_2^{\mathcal{I}}(t_2)\dots O_n^{\mathcal{I}}(t_n)]|0 \rangle}{\langle 0|S|0 \rangle} \\ &= -\frac{1}{\langle 0|S|0 \rangle^2} \langle 0|T[\frac{\delta S}{\delta V^{\text{ext}}(\underline{r}t)}]|0 \rangle \langle 0|T[SO_1^{\mathcal{I}}(t_1)\dots O_n^{\mathcal{I}}(t_n)]|0 \rangle \end{aligned} \quad (2.16)$$

from which we obtain on returning to the Heisenberg picture

$$\frac{\delta \langle T[O_1(t_1)O_2(t_2)\dots O_n(t_n)] \rangle}{\delta V^{\text{ext}}(\underline{r}t)} = -i/k \langle T[(\rho(\underline{r}t) - \langle \rho(\underline{r}t) \rangle) O_1(t_1)\dots O_n(t_n)] \rangle \quad (2.17)$$

This is the same as (2.8).

### § 2.5 Evaluation of the functional derivatives

The above theorem is applicable to the problem in hand if it is recognised that the time dependent perturbation  $H_{ie}(t)$  given by (2.4) can be thought of as being due to a non-local external potential coupling to the combined density operator  $\overline{\rho_e(\underline{x}t)\rho_i(\underline{y}t)}$ . It is then found from (2.6) and (2.8) that

$$\begin{aligned} \delta D_{ee}(X_1, X_2) &= \int \Gamma_1(X_1, X_2; \underline{x}, \underline{y}) V_{ie}(\underline{x}-\underline{y}) d\underline{x} d\underline{y} \\ &+ \frac{1}{2} \iint \Gamma_2(X_1, X_2; \underline{x}, \underline{y}, \underline{x}', \underline{y}') V_{ie}(\underline{x}-\underline{y}) V_{ie}(\underline{x}'-\underline{y}') \\ &\quad \cdot d\underline{x} d\underline{x}' d\underline{y} d\underline{y}' \end{aligned} \quad (2.18)$$

with the linear and quadratic response functions  $\Gamma_1$  and  $\Gamma_2$  given by

$$\Gamma_1(X_1, X_2; \underline{x}, \underline{y}) = -i/k \int_{-\infty}^{\infty} dt \langle T[\overline{\rho_e(\underline{x}t)\rho_i(\underline{y}t)} \rho_e(X_1)\rho_e(X_2)] \rangle_c \quad (2.19)$$

$$\begin{aligned} \Gamma_2(X_1, X_2; \underline{x}, \underline{y}, \underline{x}', \underline{y}') & \\ &= (-i/k)^2 \int_{-\infty}^{\infty} dt \int_{-\infty}^{\infty} dt' \langle T[\overline{\rho_e(\underline{x}'t')\rho_i(\underline{y}'t')} \overline{\rho_e(\underline{x}t)\rho_i(\underline{y}t)} \rho_e(X_1)\rho_e(X_2)] \rangle_c \end{aligned} \quad (2.20)$$

Note that in (2.19) and (2.20) the time integrations arise because  $V_{ie}$  is time independent (see after (2.6) ) and the  $\tilde{\rho}(\underline{x}t)$  appearing in (2.8) are accounted for by the fact that cluster parts are taken.

For the purposes of a perturbation expansion, the response functions  $\Gamma_1$  and  $\Gamma_2$  have to be evaluated in the unperturbed system whose wave function is simply a product of electronic and ionic wave functions. This allows a decoupling of the electronic and ionic densities that occur in (2.18) and (2.19) in the following way,

$$\Gamma_1(X_1, X_2; \underline{x}, \underline{y}) = -i\hbar \int_{-\infty}^{\infty} \langle T \rho_e(\underline{x}t) \rho_e(X_1) \rho_e(X_2) \rangle_c \langle \rho_i(\underline{y}t) \rangle dt \quad (2.21)$$

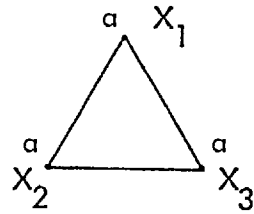
$$\begin{aligned} \Gamma_2(X_1, X_2; \underline{x}, \underline{y}, \underline{x}', \underline{y}') & \quad (2.22) \\ &= (-i\hbar)^2 \int_{-\infty}^{\infty} dt \int_{-\infty}^{\infty} dt' \left\{ \langle T \rho_e(\underline{x}'t') \rho_e(\underline{x}t) \rho_e(X_1) \rho_e(X_2) \rangle_c \langle T \rho_i(\underline{y}'t') \rho_i(\underline{y}t) \rangle_c \quad (a) \right. \\ &+ \langle T \rho_e(\underline{x}'t') \rho_e(\underline{x}t) \rho_e(X_1) \rho_e(X_2) \rangle_c \langle \rho_i(\underline{y}'t') \rangle \langle \rho_i(\underline{y}t) \rangle \quad (b) \\ &+ 2 \langle T \rho_e(\underline{x}t) \rho_e(X_1) \rho_e(X_2) \rangle_c \langle T \rho_i(\underline{y}'t') \rho_i(\underline{y}t) \rangle_c \langle \rho_e(\underline{x}'t') \rangle \quad (c) \\ &\left. + 2 \langle T \rho_e(\underline{x}'t') \rho_e(X_1) \rangle_c \langle T \rho_i(\underline{y}'t') \rho_i(\underline{y}t) \rangle_c \langle T \rho_e(\underline{x}t) \rho_e(X_2) \rangle_c \right\} \quad (d) \end{aligned}$$

The factors of 2 appearing in the third and fourth terms in (2.22) arise because there are two distinct ways of writing these terms, corresponding to interchange of  $\rho_e(\underline{x}t)$  and  $\rho_e(\underline{x}'t')$ .

A physical understanding of these decouplings is assisted by a diagrammatic representation, although this will not be done rigorously. We introduce the symbols (with  $a = e, i$ )

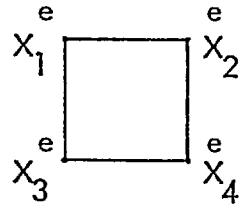
$$\begin{aligned} V_{ie}(X_1 - X_2) & \quad \begin{array}{c} i \\ \diagup \quad \diagdown \\ X_1 \quad \quad X_2 \end{array} \\ \langle \rho_a(X_1) \rangle & \quad \begin{array}{c} a \\ \circ \\ X_1 \end{array} \\ \langle T[\rho_a(X_1) \rho_a(X_2)] \rangle_c & \quad \begin{array}{c} a \quad a \\ \text{---} \\ X_1 \quad X_2 \end{array} \end{aligned} \quad (2.23)$$

$$\langle T [ p_a(x_1) p_a(x_2) p_a(x_3) ] \rangle_c$$

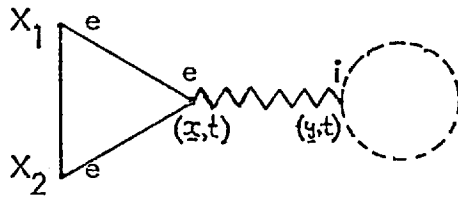


(2.23)

$$\langle T [ p_e(x_1) p_e(x_2) p_e(x_3) p_e(x_4) ] \rangle_c$$

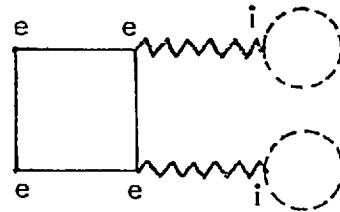
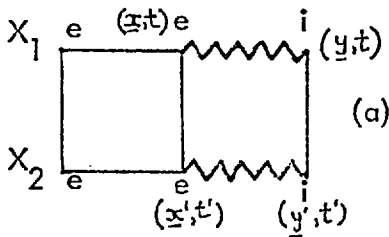


From (2.18) and (2.21), the first-order change in  $D_{ee}$  is now represented by



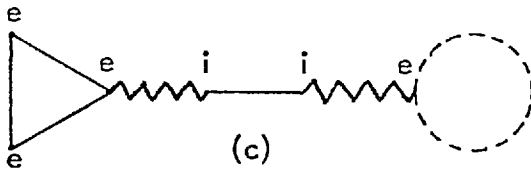
(2.24)

and the four second-order contributions are using (2.18) and (2.22)

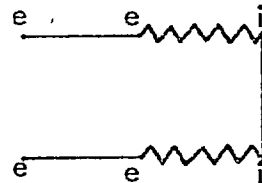


(b)

(2.25)



(c)



(d)

These diagrams represent the possible ways electron-ion interactions influence the (time-ordered) correlations between the two electrons at  $X_1$  and  $X_2$  (the two on the left in each case). For instance in (2.25d) the correlations between the electrons are indirect and mediated by ionic correlations, whereas in (2.25a) there are additional direct correlations via the four-body electronic response function. It is easy to see that these diagrams are the only possible fully connected diagrams, this being a necessary property as we are dealing with cluster-type functions.

The three and four-body electronic response functions entering these expressions are properties of interacting jellium and thus it is not possible to calculate them

exactly. In the next chapter two approximations to the four body function will be discussed. It is to be expected however that terms involving this function will be very small, as being a cluster-type function it will only be significant when all four electrons are close together which is not favoured energetically or by the exclusion principle.

The most general system to which the expansion (2.18) applies is a non-rigid (i.e. vibrating) solid in which case all the diagrams contribute. It will now be shown that in two cases of interest, rigid solids and liquid metals, considerable simplification arises from the dropping out of some of the terms.

### § 2.6 Rigid solids

A rigid solid is characterised by an ionic density of the form

$$\langle \rho_i(\underline{r}t) \rangle = \sum_l \delta(\underline{r} - \underline{R}_l) \quad (2.26)$$

where  $\underline{R}_l$  are the frozen ion sites (or lattice sites in the case of a crystal). As

there can be no fluctuations in the ionic density, the cluster function  $\langle T[\rho_i(\underline{y}t)\rho_i(\underline{y}'t')] \rangle_c$

is identically zero and consequently only the first order term (2.24) and the second

order term (2.25b) contribute. Thus we have

$$\delta D_{ee}(X_1, X_2) = -i/k \iint \langle T \rho_e(\underline{x}t) \rho_e(X_1) \rho_e(X_2) \rangle_c U(\underline{x}) d\underline{x} dt \quad (2.27)$$

$$+ \frac{1}{2} (i/k)^2 \iiint \langle T \rho_e(\underline{x}t') \rho_e(\underline{x}t) \rho_e(X_1) \rho_e(X_2) \rangle_c U(\underline{x}) U(\underline{x}) d\underline{x} dt' d\underline{x} dt$$

where  $U(\underline{x}) = \sum_l V_{ie}(\underline{x} - \underline{R}_l)$ . If we now put  $t_1 = t_2^+$  we find for the change

in the electron-electron correlation function

$$\begin{aligned} \delta P_{ee}^c(\underline{r}_1, \underline{r}_2) &= \int \chi_3(\underline{r}_1, \underline{r}_2; \underline{r}_3) U(\underline{r}_3) d\underline{r}_3 \\ &+ \frac{1}{2} \iint \chi_4(\underline{r}_1, \underline{r}_2; \underline{r}_3, \underline{r}_4) U(\underline{r}_3) U(\underline{r}_4) d\underline{r}_3 d\underline{r}_4 \end{aligned} \quad (2.28)$$

where the static three- and four-body electron response functions are defined by

$$\chi_3(\underline{r}_1, \underline{r}_2; \underline{r}_3) = -i/k \int_{-\infty}^{\infty} \langle T \rho_e(\underline{r}_3 t) \rho_e(\underline{r}_1 0^+) \rho_e(\underline{r}_2 0) \rangle_c dt \quad (2.29)$$




$$N_{k_4}(\underline{r}_1, \underline{r}_2; \underline{r}_3, \underline{r}_4) = (-i/\hbar)^2 \int_{-\infty}^{\infty} dt \int_{-\infty}^{\infty} dt' \langle T \rho_e(\underline{r}_1 t') \rho_e(\underline{r}_2 t) \rho_e(\underline{r}_3 0^+) \rho_e(\underline{r}_4 0) \rangle_c \quad (2.30)$$

### § 2.7 Liquid metals

To apply the results of § 2.5 to liquid metals it is necessary to ensemble average over the possible ionic positions. The ensemble averaged electron and ion densities are constants and given by

$$\langle \rho_e(\underline{x}t) \rangle = n_e = Z n_i = \langle \rho_i(\underline{y}t) \rangle \quad (2.31)$$

where  $Z$  is the valency. As a result, the three terms (2.21), (2.22b) and (2.22c) (corresponding to diagrams (2.24), (2.25b) and (2.25c), i.e. those with density

bubbles  a) all contain factors

$$\int V_{ie}(\underline{x}-\underline{y}) d\underline{x} = V_{ie}(k=0) \quad (2.32)$$

This factor can be taken as identically zero by suitable choice of energy zero. This is because in introducing the electron-ion interaction as a perturbation, we should also include the direct Coulomb interactions between the electrons and the negative background of the ionic jellium, between the ions and the positive background of the electron jellium and between the two backgrounds. The net result is effectively to remove the long wavelength ( $k=0$ ) part of the electron-ion interaction, this being also Coulombic in this limit.

Thus for a liquid metal we are left with only the two second-order terms (2.25a) and (2.25d) which may be written as

$$\begin{aligned} S D_{ee}(X_1, X_2) = & \frac{1}{2} (-i/\hbar)^2 \left\{ \langle T \rho_e(\underline{x}t') \rho_e(\underline{x}t) \rho_e(\underline{x}_1) \rho_e(\underline{x}_2) \rangle_c \langle \rho_i(\underline{y}t') \rho_i(\underline{y}t) \rangle_c \right. \\ & \left. + 2 \langle T [\rho_e(\underline{x}t') \rho_e(\underline{x}_1)] \rangle_c \langle T \rho_e(\underline{x}t) \rho_e(\underline{x}_2) \rangle_c \langle \rho_i(\underline{y}t') \rho_i(\underline{y}t) \rangle_c \right\} \\ & \times V_{ie}(\underline{x}-\underline{y}) V_{ie}(\underline{x}-\underline{y}') d\underline{x} d\underline{y} d\underline{x}' d\underline{y}' dt' \quad (2.33) \end{aligned}$$

The time-ordering has been dropped in the ionic terms, as these are now taken to be classical, ensemble averaged dynamic ion correlation functions.

## § 2.8 Use of the adiabatic approximation

The time dependence in (2.33) can be greatly simplified by making use of the so called adiabatic approximation. This is based on the fact that because of the large ionic to electronic mass ratio, ionic motions are measured on a considerably longer time scale than electronic motion or in other words, characteristic ion excitation frequencies are significantly lower than those of the electrons (for instance plasma frequencies are proportional to  $(\text{mass})^{-\frac{1}{2}}$ ). This situation can be approximately handled by putting  $t' = t$  in the ionic correlation functions and keeping  $t' \neq t$  in the electronic response functions. The integrations over  $t$  then give static ( $\omega = 0$ ) limits of the electron response functions, this being in line with the observation above, that the relatively low frequencies at which ionic excitations are significant, are effectively zero as regards the electrons.

The final result for the second-order change  $\delta P_{ee}^c(\underline{\tau}_1 - \underline{\tau}_2)$  in the electron-electron correlation function for liquid metals is (using the adiabatic approximation and putting  $t_1 = t_2^+$  in (2.33) ),

$$\begin{aligned} \delta P_{ee}^c(\underline{\tau}_1 - \underline{\tau}_2) &= \frac{1}{2} \left( \frac{-i}{\hbar} \right)^2 \int \int \left\{ \langle T \rho_e(\underline{x}'t') \rho_e(\underline{x}t) \rho_e(\underline{\tau}_1 0^+) \rho_e(\underline{\tau}_2 0) \rangle_c \langle \rho_i(\underline{y}') \rho_i(\underline{y}) \rangle_c \right. \\ &\quad \left. + 2 \langle T \rho_e(\underline{x}'t') \rho_e(\underline{\tau}_1 0) \rangle_c \langle T \rho_e(\underline{x}t) \rho_e(\underline{\tau}_2 0) \rangle_c \langle \rho_i(\underline{y}') \rho_i(\underline{y}) \rangle_c \right\} \\ &\quad \times V_{ie}(\underline{x} - \underline{y}) V_{ie}(\underline{x}' - \underline{y}') d\underline{x} d\underline{y} dt d\underline{x}' d\underline{y}' dt' \quad (2.34) \end{aligned}$$

which on Fourier transform gives for the change  $\Delta S_{ee}(k)$  of the electron-electron structure factor (using (1.10) )

$$\begin{aligned} \Delta S_{ee}(k) &= \frac{1}{2Z} \int N_{\underline{k}_+}(\underline{k}, -\underline{k}; \underline{q}, -\underline{q}) S_{ii}(\underline{q}) |V_{ie}(\underline{q})|^2 \frac{d\underline{q}}{(2\pi)^3} \\ &\quad + \frac{1}{Z} |N(k) V_{ie}(k)|^2 S_{ii}(k) \quad (2.35) \end{aligned}$$

In (2.35)  $N(k) \equiv N(k, \omega=0)$  is the static density response function of jellium (see comments following (2.5) ) and  $N_{\underline{k}_+}(\underline{k}, -\underline{k}; \underline{q}, -\underline{q})$  is the diagonal ( $\underline{G} = 0$ )

element of the four-body response function of jellium defined in  $\underline{r}$  - space by (2.30) and in Fourier transform by

$$\begin{aligned} \chi_4(\underline{k}, \underline{q}-\underline{k}; \underline{q}-\underline{q}, -\underline{q}) \\ = \int e^{i\underline{k} \cdot (\underline{r}_1 - \underline{r}_2)} e^{i\underline{q} \cdot (\underline{r}_2 - \underline{r}_3)} e^{i\underline{q} \cdot (\underline{r}_3 - \underline{r}_4)} \chi_4(\underline{r}_1, \underline{r}_2; \underline{r}_3, \underline{r}_4) d(\underline{r}_1 - \underline{r}_2) d(\underline{r}_2 - \underline{r}_3) d(\underline{r}_3 - \underline{r}_4) \end{aligned} \quad (2.36)$$

The first term in (2.35) is easily shown to give the correct charge neutrality limit for  $S_{ee}(k)$ . In the long wave-length limit,  $V_{ie}(k) \sim -\frac{4\pi Ze^2}{k^2}$  and  $\chi(k) \sim -\frac{k^2}{4\pi e^2}$  hence

$$\lim_{k \rightarrow 0} \chi(k) V_{ie}(k) = Z \quad (2.37)$$

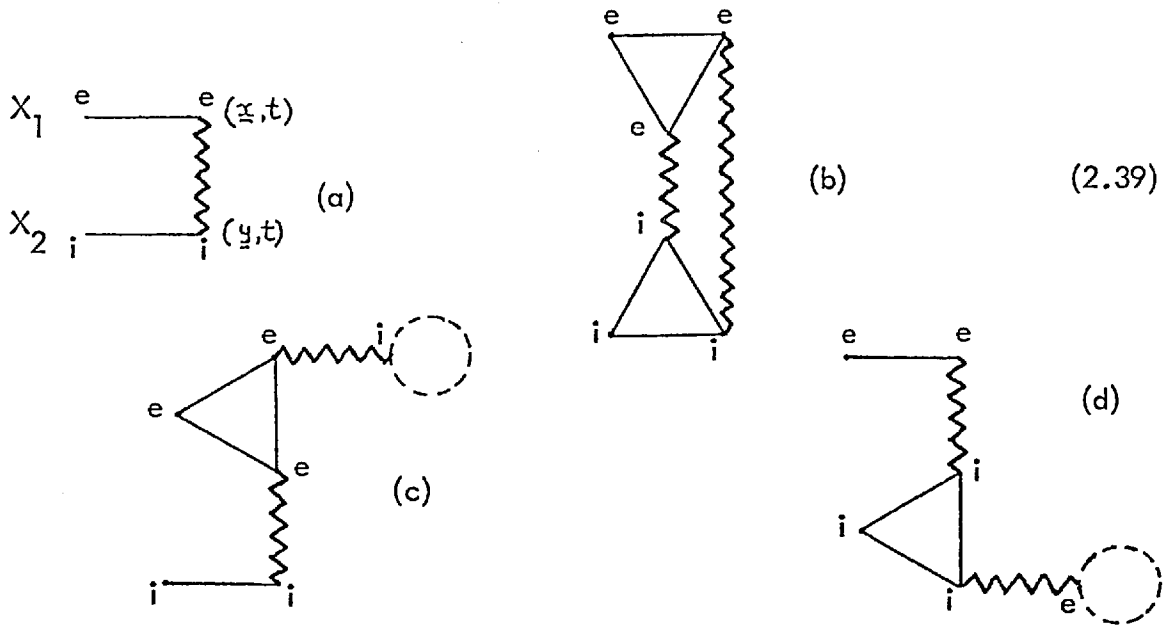
Thus (2.35) gives (c.f. (1.13))

$$\Delta S_{ee}(0) = S_{ee}(0) = Z S_{ii}(0) \quad (2.38)$$

as required, provided the  $\chi_4$  term is zero in this limit. This latter point has not been proved to be the case in general, but the two approximations to  $\chi_4(\underline{k}, \underline{q}-\underline{k}; \underline{q}, -\underline{q})$  discussed in the next chapter both have the necessary property for it to be true of being zero as  $k \rightarrow 0$ . Trigger<sup>(23)</sup> has obtained exactly the same charge neutrality term as in (2.35) but the  $\chi_4$  term is absent in his work for the reason mentioned at the end of § 1.4. Note that in (2.35),  $S_{ii}(k)$  is strictly to be evaluated in the unperturbed system i.e. it is the structure factor of a classical ion jellium. However, in view of the correct charge neutrality result (2.38) it is clear that a partial summation can be effected so that the exact liquid metal ion-ion structure factor is used instead.

## § 2.9 The electron-ion structure factor in liquid metals

Having described in detail the derivation of the perturbation theory for the electron-electron structure factor in a liquid metal it is straightforward to apply the same formalism to a calculation of the electron-ion structure factor. The diagrams that contribute to second-order to the perturbation expansion of the electron-ion propagator  $\langle T[\rho_e(x_1) \rho_i(x_2)] \rangle_c$  are



In (2.39) note the symmetry under the interchange of the electron at  $X_1$  and the ion at  $X_2$ . By the arguments of § 2.7, only the first-order term (2.39a) and the second-order term (2.39b) are non zero in liquid metals and these two terms give the following for the electron-ion correlation function

$$\begin{aligned}
 P_{ie}^c(\underline{r}_1 - \underline{r}_2) &= -i/k \int \langle T \rho_e(\underline{x}t) \rho_e(\underline{r}_1 0) \rangle_c \langle \rho_i(\underline{y}t) \rho_i(\underline{r}_2 0) \rangle_c V_{ie}(\underline{x} - \underline{y}) d\underline{x} d\underline{y} dt \\
 &+ \frac{1}{2} (-i/k)^2 \int \langle T \rho_e(\underline{x}t) \rho_e(\underline{x}t) \rho_e(\underline{r}_1 0) \rangle_c \langle \rho_i(\underline{y}t) \rho_i(\underline{y}t) \rho_i(\underline{r}_2 0) \rangle_c \\
 &\quad \times V_{ie}(\underline{x} - \underline{y}) V_{ie}(\underline{x} - \underline{y}') d\underline{x} d\underline{y} dt d\underline{x}' d\underline{y}' dt' \quad (2.40)
 \end{aligned}$$

Using the adiabatic approximation, by which all the times in the ionic functions are put the same but the electronic times are still integrated over, the final result in Fourier transform is

$$\begin{aligned}
 S_{ie}(k) &= \frac{1}{Z} \chi(k) V_{ie}(k) S_{ii}(k) \\
 &+ \frac{1}{2} \int S_{iii}(k, \underline{q} - k, -\underline{q}) \chi_2(k, \underline{q} - k, -\underline{q}) V_{ie}(\underline{q}) V_{ie}(k - \underline{q}) \frac{d\underline{q}}{(2\pi)^3}
 \end{aligned} \quad (2.41)$$

where  $S_{iii}$  is the ion triplet correlation function and  $\chi_2(k, \underline{q} - k, -\underline{q})$  is the static, quadratic density response function of the interacting electron gas given by

$$\begin{aligned}
 \chi_2(k, \underline{q} - k, -\underline{q}) &= \int e^{i\underline{k} \cdot (\underline{r}_1 - \underline{r}_2)} e^{i\underline{q} \cdot (\underline{r}_2 - \underline{r}_3)} \left[ (-i/k)^2 \int \langle T \rho_e(\underline{r}_1 t_1) \rho_e(\underline{r}_2 t_2) \rho_e(\underline{r}_3 0) \rangle_c dt_1 dt_2 \right] d(\underline{r}_1 - \underline{r}_2) d(\underline{r}_2 - \underline{r}_3) \quad (2.42)
 \end{aligned}$$

Using (2.37) it follows that the first-order term in (2.41) gives the correct charge neutrality limit

$$\rho_{ie}(0) = \sum_i \frac{1}{2} \rho_{ii}(0) \quad (2.43)$$

provided the second-order term is zero in this limit. That this is so follows from the result (see Appendix B, equation (B.19))

$$\lim_{k \rightarrow 0} \chi_2(k, q-k, -q) = \lim_{k \rightarrow 0} \chi(k) \frac{\partial \chi(q)}{\partial n_e} = 0 \quad (2.44)$$

Tosi and March<sup>(15)</sup> have obtained the first-order term by the following simple argument. An external potential  $V_e^{\text{ext}}(\underline{k}, \omega)$  coupled to the electrons in a liquid metal causes polarisations of the electrons and ions according to (c.f. (1.16))

$$\rho_e(\underline{k}, \omega) = \chi_{ee}(\underline{k}, \omega) V_e^{\text{ext}}(\underline{k}, \omega) \quad (2.45)$$

$$\rho_i(\underline{k}, \omega) = \chi_{ie}(\underline{k}, \omega) V_e^{\text{ext}}(\underline{k}, \omega) \quad (2.46)$$

If the electron-ion interaction is weak, the polarisation of the ions can also be written

$$\rho_i(\underline{k}, \omega) = \chi_{ii}(\underline{k}, \omega) V_{ie}(\underline{k}) \rho_e(\underline{k}, \omega) \quad (2.47)$$

from which it follows that

$$\chi_{ie}(\underline{k}, \omega) = \chi_{ii}(\underline{k}, \omega) V_{ie}(\underline{k}) \chi_{ee}(\underline{k}, \omega) \quad (2.48)$$

Using the adiabatic approximation, the static limit ( $\omega = 0$ ) of the electronic response function is taken and then the Fluctuation-Dissipation theorem (1.18) gives the result

$$\rho_{ie}(k) = \frac{1}{2} \chi_{ee}(k) V_{ie}(k) \rho_{ii}(k)$$

(Note that  $\chi_{ee}(k) \sim \chi(k)$  to second-order in  $V_{ie}$ ).

The simplest way to make a calculation of the second-order term in (2.41) would be to use the Kirkwood superposition for the triplet ion function and use an

approximation for  $\chi_2$  of the form (c.f. chapter 3, § 3.3)

$$\chi_2(\underline{k}, \underline{q}-\underline{k}, -\underline{q}) = \frac{\chi_2^0(\underline{k}, \underline{q}-\underline{k}, -\underline{q})}{\epsilon(\underline{k}) \epsilon(\underline{q}-\underline{k}) \epsilon(\underline{q})} \quad (2.49)$$

where  $\chi_2^0$  is the quadratic density response function for free electrons and  $\epsilon(\underline{k})$  is the dielectric function of jellium.

### § 2.10 Conclusion

The achievement of this chapter has been to develop a perturbation theory for the electron-electron and electron-ion correlation functions in a system with weak electron-ion interactions. The general result has been specialised to the case of rigid solids and, with the help of the adiabatic approximation, to liquid metals. In the latter case, specific terms have been shown to give the correct charge neutrality limits for  $S_{ee}(k)$  and  $S_{ie}(k)$  at  $k \rightarrow 0$ . These terms are the same as those obtained by Trigger<sup>(23)</sup>. However it has not been shown that a further second-order term in the expression for  $S_{ee}(k)$  involving a four-body response function of jellium, is zero in this limit. This point will be discussed in the next chapter.

## CHAPTER 3

TWO APPROXIMATIONS TO THE FOUR-BODY ELECTRON RESPONSE FUNCTION§ 3.1 Introduction

Equations (2.35) and (2.41) of the preceding chapter give expressions for the electron-electron and electron-ion structure factors in liquid metals, correct to second-order in the electron-ion interaction (within the adiabatic approximation). In chapter 4, the dominant charge neutrality terms will be evaluated for liquid sodium and liquid aluminium. In this chapter we examine two approximations to the four-body electron response function  $\chi_4(\underline{k}, \underline{k} ; \underline{q}, -\underline{q})$  which occurs in the second-order terms for the electron-electron structure factor in both the liquid and rigid solid cases. This function is defined by (c.f. (2.30) and (2.36)).

$$\chi_4(\underline{k}, \underline{k} ; \underline{q}, -\underline{q}) = \int e^{i\underline{k} \cdot (\underline{r}_1 - \underline{r}_2)} e^{i\underline{q} \cdot (\underline{r}_3 - \underline{r}_4)} \chi_4(\underline{r}_1, \underline{r}_2 ; \underline{r}_3, \underline{r}_4) d(\underline{r}_1 - \underline{r}_2) d(\underline{r}_3 - \underline{r}_4) \quad (3.1a)$$

$$\chi_4(\underline{r}_1, \underline{r}_2 ; \underline{r}_3, \underline{r}_4) = \int_{-\infty}^{\infty} dt \int_{-\infty}^{\infty} dt' \langle T \rho_e(\underline{r}_4 t') \rho_e(\underline{r}_1 t) \rho_e(\underline{r}_3 0^+) \rho_e(\underline{r}_2 0) \rangle_c \quad (3.1b)$$

We shall be particularly concerned to see whether  $\lim_{\underline{k} \rightarrow 0} \chi_4(\underline{k}, -\underline{k} ; \underline{q}, -\underline{q}) = 0$ , this being the necessary and sufficient condition for the exact satisfaction of the charge neutrality limit on  $S_{ee}(\underline{k})$  in liquid metals.

One possible procedure when confronted by complicated multi-body correlation or response functions is to attempt to decouple them in terms of lower order functions. In practice this often means approximating them by function(s) of the two-body function, usually the only function about which much is known. In this spirit is the familiar Kirkwood superposition approximation which expresses the triplet correlation function of a liquid as a symmetrical product of three pair correlation functions<sup>(2)</sup>. However it is often the case that different decouplings

are required in different regimes of application of the multi-body function. For instance Abramo and Tosi<sup>(24)</sup> (see also Feenberg<sup>(25)</sup>), in discussing systematic improvements to the Kirkwood approximation in classical one-component plasmas, have shown that it is not possible to satisfy simultaneously, with the same decoupling, the various sum-rules and limiting properties of the triplet function. Another drawback to decoupling schemes is that singularities peculiar to the higher-order functions will be missed. It is well known that the logarithmic singularity in the linear density response function of interacting electrons shows up as the 'Kohn anomaly' in the phonon spectra of metals<sup>(26)</sup>. In a series of papers, Brovman and Kagan<sup>(27)</sup> have shown that the singularities of the higher-order (three- and four-body) density response functions that enter their more sophisticated theory of phonon spectra, also give rise to visible anomalies.

For these reasons, the two approximations to  $\chi_{4+}$  to be discussed here do not involve decoupling. Instead they rely on knowledge of the corresponding response function for free electrons  $\chi_{4+}^0$ , to which screening is introduced in two different ways: firstly using a density functional theory argument (§ 3.2) and secondly using a simple diagrammatic analysis of  $\chi_{4+}$  (§ 3.3). It is reasonable to suppose that the singularity structure of the interacting  $\chi_{4+}$  will at least resemble that of its non-interacting counterpart  $\chi_{4+}^c$ , even though the discontinuity in electron occupation of momentum space at the Fermi surface (which will be responsible for the singularities) is weakened by interactions. This singularity structure will presumably manifest itself in the electron-electron correlation functions of liquid and solid metals. However it should be admitted that even  $\chi_{4+}^c$  (which is discussed in Appendix A) has proved too complicated to analyse fully.

### § 3.2 Electron-electron correlation function as a functional of the density

The fundamental proposition of density functional theory is that the ground-



state properties of an interacting  $N$  electron system can be expressed as functionals of the exact ground-state electron density of the system. Furthermore, this electron density can be generated by summing the squares of the lowest  $N$  normalised eigenfunctions of the Schrödinger equation solved with the so called Hohenberg-Kohn one-body potential  $V^{\text{HK}}(\mathbf{r})$ . This potential is the sum of the Hartree potential and the exchange and correlation potential which includes the many-body effects. (See Appendix C for an amplification of these statements).

We now return to § 2.1 where the change in the electron-electron correlation function  $P_{ee}^c(\underline{r}, \underline{r}_2)$  due to the frozen-ion potential  $U(\mathbf{r})$  in a rigid solid is given in the form

$$\begin{aligned} \delta P_{ee}^c(\underline{r}, \underline{r}_2) &= \int \chi_3(\underline{r}, \underline{r}_2; \underline{r}_3) U(\underline{r}_3) d\underline{r}_3 \\ &+ \frac{1}{2} \int \chi_4(\underline{r}, \underline{r}_2; \underline{r}_3, \underline{r}_4) U(\underline{r}_3) U(\underline{r}_4) d\underline{r}_3 d\underline{r}_4 \end{aligned} \quad (3.2)$$

The change,  $\delta \rho_e(\underline{r})$ , in the electron density to second order in the perturbation  $U(\mathbf{r})$  is given by

$$\begin{aligned} \delta \rho_e(\underline{r}) &= \int \chi(\underline{r}, \underline{r}_1) U(\underline{r}_1) d\underline{r}_1 \\ &+ \frac{1}{2} \int \chi_2(\underline{r}, \underline{r}_1, \underline{r}_2) U(\underline{r}_1) U(\underline{r}_2) d\underline{r}_1 d\underline{r}_2 \end{aligned} \quad (3.3)$$

where  $\chi$  and  $\chi_2$  are the linear and quadratic density response functions of jellium.

According to density functional theory,  $P_{ee}^c(\underline{r}, \underline{r}_2)$  is a functional of the density  $\rho_e(\underline{r})$ , so we may formally introduce linear and quadratic response functions  $H_3$  and  $H_4$  defined by

$$\begin{aligned} \delta P_{ee}^c(\underline{r}, \underline{r}_2) &= \int H_3(\underline{r}, \underline{r}_2; \underline{r}_3) \delta \rho_e(\underline{r}_3) d\underline{r}_3 \\ &+ \frac{1}{2} \int H_4(\underline{r}, \underline{r}_2; \underline{r}_3, \underline{r}_4) \delta \rho_e(\underline{r}_3) \delta \rho_e(\underline{r}_4) d\underline{r}_3 d\underline{r}_4 \end{aligned} \quad (3.4)$$

Furthermore, the perturbation  $U(\mathbf{r})$  will produce a change  $\Delta V^{\text{HK}}(\mathbf{r})$  in the

Hohenberg-Kohn one-body potential of the system and in terms of this potential we can write equations analogous to (3.2) and (3.3) for  $\delta P_{ee}^c(\underline{r}_1, \underline{r}_2)$  and  $\delta \rho_e(\underline{r})$ ,

$$\begin{aligned} \delta P_{ee}^c(\underline{r}_1, \underline{r}_2) &= \int \chi_3^{HK}(\underline{r}_1, \underline{r}_2; \underline{r}_3) \Delta V^{HK}(\underline{r}_3) d\underline{r}_3 \\ &+ \frac{1}{2} \int \chi_4^{HK}(\underline{r}_1, \underline{r}_2; \underline{r}_3, \underline{r}_4) \Delta V^{HK}(\underline{r}_3) \Delta V^{HK}(\underline{r}_4) \\ &\quad \times d\underline{r}_3 d\underline{r}_4 \end{aligned} \quad (3.5)$$

$$\begin{aligned} \delta \rho_e(\underline{r}) &= \int \chi^o(\underline{r}, \underline{r}_1) \Delta V^{HK}(\underline{r}_1) d\underline{r}_1 \\ &+ \frac{1}{2} \int \chi_2^o(\underline{r}, \underline{r}_1, \underline{r}_2) \Delta V^{HK}(\underline{r}_1) \Delta V^{HK}(\underline{r}_2) d\underline{r}_1 d\underline{r}_2 \end{aligned} \quad (3.6)$$

In (3.6) (but not in (3.5)), as Stoddart, March and Stott<sup>(28)</sup> have shown, it is correct to use the free-electron linear and quadratic density response functions  $\chi^o$  and  $\chi_2^o$ . The reason is that the Hohenberg-Kohn potential reproduces the exact electron density within an independent particle formalism but not the correlation function (which is derived from the second order density matrix<sup>(29)</sup>). Note also that  $\chi^o$  and  $\chi_2^o$  are known analytically (see equations (A29), (A30) in Appendix A).

The procedure now is to relate the  $\chi_3$  and  $\chi_4$  in (3.2) to the analogous Hohenberg-Kohn response functions  $\chi_3^{HK}$  and  $\chi_4^{HK}$  in (3.5) using (3.3), (3.4) and (3.6).  $\chi_3^{HK}$  and  $\chi_4^{HK}$  will then be approximated by their free-electron counterparts.

It is convenient to proceed in Fourier space by introducing the Fourier transforms of general three- and four-body response functions  $G_3$  and  $G_4$  as follows (see next page)

$$\begin{aligned}
 G_3(\underline{k}, \underline{G}-\underline{k}, -\underline{G}) \\
 = \int e^{i\underline{k} \cdot (\underline{r}_1 - \underline{r}_2)} e^{i\underline{G} \cdot (\underline{r}_2 - \underline{r}_3)} G_3(\underline{r}_1, \underline{r}_2, \underline{r}_3) d(\underline{r}_1 - \underline{r}_2) d(\underline{r}_2 - \underline{r}_3) \quad (3.7)
 \end{aligned}$$

$$\begin{aligned}
 G_4(\underline{k}, \underline{G}-\underline{k}, \underline{q}-\underline{k}, -\underline{q}) \\
 = \int e^{i\underline{k} \cdot (\underline{r}_1 - \underline{r}_2)} e^{i\underline{G} \cdot (\underline{r}_2 - \underline{r}_3)} e^{i\underline{q} \cdot (\underline{r}_3 - \underline{r}_4)} G_4(\underline{r}_1, \underline{r}_2, \underline{r}_3, \underline{r}_4) \\
 \times d(\underline{r}_1 - \underline{r}_2) d(\underline{r}_2 - \underline{r}_3) d(\underline{r}_3 - \underline{r}_4) \quad (3.8)
 \end{aligned}$$

where, because we are dealing with response functions of a homogeneous system, the momentum transfers at the vertices sum to zero.

Equation (3.6) may now be inverted to give  $\Delta V^{\text{HK}}(\underline{q})$  in terms of

$$\begin{aligned}
 \Delta V^{\text{HK}}(\underline{q}) &= \frac{\delta \rho_e(\underline{q})}{\chi^{\circ}(\underline{q})} \\
 &- \frac{1}{2} \frac{1}{\chi^{\circ}(\underline{q})} \int \frac{d\underline{q}'}{(2\pi)^3} \chi_2^{\circ}(\underline{q}, \underline{q}' - \underline{q}, -\underline{q}') \frac{\delta \rho_e(\underline{q}')}{\chi^{\circ}(\underline{q}')} \frac{\delta \rho_e(\underline{q} - \underline{q}')}{\chi^{\circ}(\underline{q} - \underline{q}')} \quad (3.9)
 \end{aligned}$$

Substituting (3.9) in (3.5) and comparing with (3.4) we find

$$H_3(\underline{k}, \underline{G}-\underline{k}; -\underline{G}) = \frac{\chi_3^{\text{HK}}(\underline{k}, \underline{G}-\underline{k}; -\underline{G})}{\chi^{\circ}(\underline{G})} \quad (3.10a)$$

$$\begin{aligned}
 H_4(\underline{k}, \underline{G}-\underline{k}; \underline{q}-\underline{k}, -\underline{q}) &= \frac{\chi_4^{\text{HK}}(\underline{k}, \underline{G}-\underline{k}; \underline{q}-\underline{k}, -\underline{q})}{\chi^{\circ}(\underline{q}) \chi^{\circ}(\underline{G}-\underline{q})} \\
 &- \frac{\chi_3^{\text{HK}}(\underline{k}, \underline{G}-\underline{k}; -\underline{G})}{\chi^{\circ}(\underline{G})} \frac{\chi_2^{\circ}(\underline{G}, \underline{q}-\underline{k}, -\underline{q})}{\chi^{\circ}(\underline{q}-\underline{k})} \quad (3.10b)
 \end{aligned}$$

Now substituting (3.3) into (3.4) and comparing with (3.2) we can express  $\chi_3$  and  $\chi_4$  in terms of  $H_3$  and  $H_4$ ,

$$\chi_3(\underline{k}, \underline{G}-\underline{k}; -\underline{G}) = H_3(\underline{k}, \underline{G}-\underline{k}; -\underline{G}) \chi(\underline{G}) \quad (3.11a)$$

$$\begin{aligned} \chi_4(\underline{k}, \underline{G}-\underline{k}; \underline{q}-\underline{G}, -\underline{q}) &= H_3(\underline{k}, \underline{G}-\underline{k}; -\underline{G}) \chi_2(\underline{G}, \underline{q}-\underline{G}, -\underline{q}) \quad (3.11b) \\ &+ H_4(\underline{k}, \underline{G}-\underline{k}; \underline{q}-\underline{G}, -\underline{q}) \chi(\underline{G}-\underline{q}) \chi(\underline{q}) \end{aligned}$$

Finally,  $\chi_3$  and  $\chi_4$  can be related to  $\chi_3^{\text{HK}}$  and  $\chi_4^{\text{HK}}$  by substituting (3.10) into (3.11). This will only be done explicitly for the diagonal ( $\underline{G} = 0$ ) element of  $\chi_4$ , which is required in the liquid metal case,

$$\begin{aligned} \chi_4(\underline{k}, -\underline{k}; \underline{q}, -\underline{q}) & \quad (3.12) \\ &= \left( \frac{\chi(\underline{q})}{\chi^0(\underline{q})} \right)^2 \left\{ \chi_4^{\text{HK}}(\underline{k}, -\underline{k}; \underline{q}, -\underline{q}) - \frac{\chi_3^{\text{HK}}(\underline{k}, -\underline{k}; 0) \chi_2^0(0, \underline{q}, -\underline{q})}{\chi^0(0)} \right\} \end{aligned}$$

In obtaining (3.12) the fact that  $\lim_{\underline{G} \rightarrow 0} \chi_2(\underline{G}, \underline{q}-\underline{G}, -\underline{q}) = 0$  has been used (c.f. (2.44), see also Appendix B). This makes the  $H_3$  term in (3.11b) zero in this limit.

Equation (3.12) is formally exact and in order to make use of it, it is necessary to approximate. The simplest one can do is to replace  $\chi_4^{\text{HK}}$  and  $\chi_3^{\text{HK}}$  by their free-electron counterparts  $\chi_4^0$  and  $\chi_3^0$ . This gives the approximate form

$$\begin{aligned} \chi_4(\underline{k}, -\underline{k}; \underline{q}, -\underline{q}) & \\ &\sim (\chi(\underline{q}))^2 H_4^0(\underline{k}, -\underline{k}; \underline{q}, -\underline{q}) \\ &\sim \left( \frac{\chi(\underline{q})}{\chi^0(\underline{q})} \right)^2 \left\{ \chi_4^0(\underline{k}, -\underline{k}; \underline{q}, -\underline{q}) - \frac{1}{\chi^0(0)} \chi_3^0(\underline{k}, -\underline{k}; 0) \chi_2^0(0, \underline{q}, -\underline{q}) \right\} \quad (3.13) \end{aligned}$$

This approximation corresponds to the assumption that the Hohenberg-Kohn potential fully takes into account all exchange and correlation effects, not only with regard

to the electron density (which is rigorously true as mentioned above), but also with regard to the pair correlation function.

Two properties of the approximation (3.13) should be noted. Firstly, as will be shown in Appendix B (where various sum rules for the response functions introduced in this section will be derived),  $\lim_{\underline{k} \rightarrow 0} H_4^0(\underline{k}, -\underline{k}; \underline{q}, -\underline{q}) = 0$ . Thus (3.13) has the necessary long-wavelength behaviour that ensures that the  $\chi_4$  term in (2.35) gives no contribution as  $k \rightarrow 0$  to  $S_{ee}(k)$  in liquid metals. Consequently the charge neutrality limit on  $S_{ee}(k)$  is exactly satisfied. Secondly, the factor  $(\chi(q)/\chi^0(q))$  in (3.13) can be written in the form

$$\left(\frac{\chi(q)}{\chi^0(q)}\right)^2 = \frac{1}{\epsilon^2(q)} \frac{\Pi^2(q)}{\Pi^{0^2}(q)} \quad (3.14)$$

where  $\epsilon(q) = 1 - 4\pi\Pi(q)/q^2$  is the jellium dielectric function;  $\Pi(q)$  is the irreducible (two-body) polarisability of jellium and  $\Pi^0(q) = \chi^0(q)$  is the corresponding free-electron function. The  $\epsilon^{-2}(q)$  factor in (3.14) clearly has the effect of screening the bare electron-ion potential when (3.13) is substituted in (2.35).

### § 3.3 Diagrammatic analysis of $\chi_4(\underline{k}, \underline{q}-\underline{k}; \underline{q}, -\underline{q})$

The response function  $\chi_4$  can be derived from the most general time-ordered four-body Green's function  $\Gamma_4$ , defined in  $X (= (\underline{x}, t))$  space by

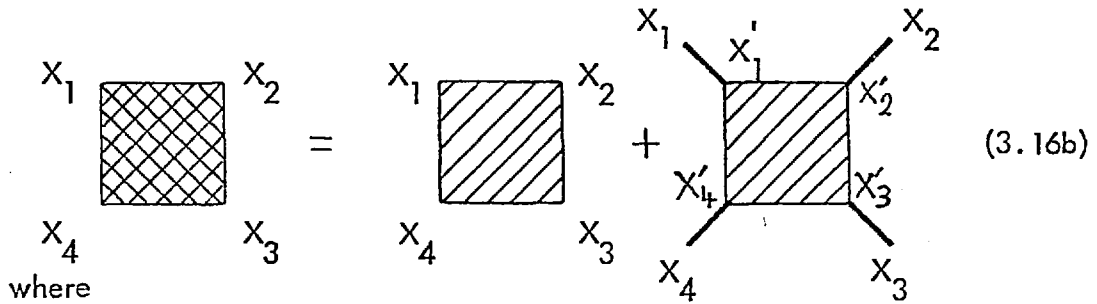
$$\Gamma_4(X_1, X_2, X_3, X_4) = (-i)^4 \langle T[\rho_e(X_1)\rho_e(X_2)\rho_e(X_3)\rho_e(X_4)] \rangle_c \quad (3.15)$$

$\Gamma_4$  is susceptible to Feynman diagram analysis<sup>(19)</sup>, though clearly rather drastic approximations will have to be made in order to obtain useful results. Brovman and Kagan<sup>(27a)</sup> and Pethick<sup>(30)</sup>, in discussing similar multi-body functions, have found it useful to introduce the corresponding irreducible multi-body function.

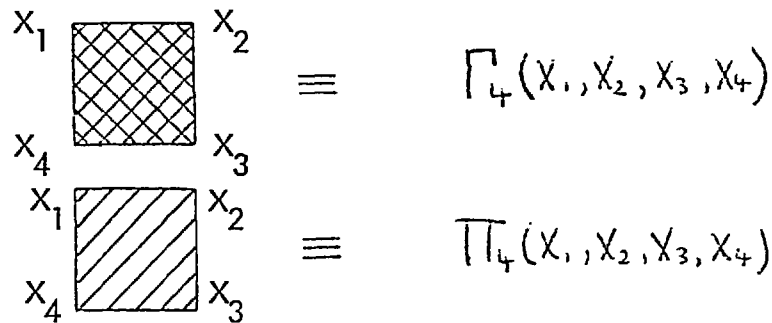
We therefore define an irreducible four-body polarisability,  $\Pi_4$ , by the equation

$$\Gamma_4(X_1, X_2, X_3, X_4) = \int dX'_1 dX'_2 dX'_3 dX'_4 \left\{ \Pi_4(X'_1, X'_2, X'_3, X'_4) \varepsilon^{-1}(X_1 - X'_1) \varepsilon^{-1}(X_2 - X'_2) \times \varepsilon^{-1}(X_3 - X'_3) \varepsilon^{-1}(X_4 - X'_4) \right\} \quad (3.16a)$$

where  $\varepsilon(X - X')$  is the dielectric function.  $\Pi_4$  is irreducible in the sense that it contains no two-body polarisation parts which can be separated from it by cutting a single electron-electron interaction line. This can be seen more readily from the diagrammatic representation of (3.16a),



where



The heavy lines in the second term of the RHS of (3.16b) represent a summation over two-body polarisation parts and may be written

$$X_1 \text{---} X'_1 = X_1 \text{---} \text{---} X'_1 + X_1 \text{---} \text{---} \text{---} X'_1 + X_1 \text{---} \text{---} \text{---} \text{---} X'_1 + \dots \quad (3.17)$$

$$\equiv \Pi V_{ee} + \Pi V_{ee} \Pi V_{ee} + \Pi V_{ee} \Pi V_{ee} \Pi V_{ee} + \dots$$

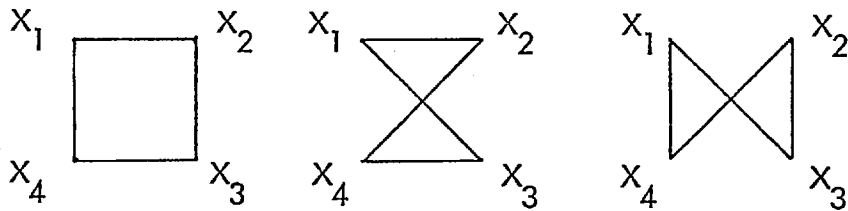
where  $\Pi \equiv \text{---}$  is the two-body irreducible polarisability (introduced at the end of the previous section) and  $V_{ee} \equiv \text{---}$  is the electron-electron interaction. The summation (3.17) ~~which in fact gives the density response function~~ when taken into account with the first term on the RHS of (3.16b) gives back the  $\varepsilon^{-1}$  factors in (3.16a).

Fourier transforming (3.16a) we find the following formally exact expression for  $\chi_4(\underline{k}, \underline{G}-\underline{k}; \underline{q}-\underline{k}, -\underline{q})$

$$\chi_4(\underline{k}, \underline{G}-\underline{k}; \underline{q}-\underline{k}, -\underline{q}) = \int \frac{d\omega}{(2\pi)} e^{i\omega\delta} \frac{\Pi_4(\underline{k}\omega, \underline{G}-\underline{k}-\omega; \underline{q}-\underline{k}, -\underline{q})}{\varepsilon(\underline{k}, \omega) \varepsilon(\underline{G}-\underline{k}, -\omega) \varepsilon(\underline{q}-\underline{k}) \varepsilon(-\underline{q})} \quad (3.18)$$

where the  $e^{i\omega\delta}$  maintains the correct time-ordering as in (3.1b) ( $\delta$  being an infinitesimal). The factors  $\varepsilon(\underline{q}-\underline{k}) \varepsilon(-\underline{q})$  in the denominator of (3.18) are now seen to effect a screening of the electron-ion potential when (3.18) is used to calculate  $S_{ee}(\underline{k})$  as in (2.35).

To proceed further one must now approximate, and the simplest thing to do is to replace  $\Pi_4$  in (3.18) by its value for free particles,  $\Pi_4^0$ . This corresponds to taking the zeroth order terms in the diagrammatic perturbation expansion of  $\Pi_4$ . In Appendix A it will be shown that  $\Pi_4^0(X_1, X_2, X_3, X_4)$  has the following diagrams



where the lines now represent free electron Green's functions. A further simplification will be to neglect dynamic effects in the dielectric functions in (3.18) by replacing them by their static limits. This enables the  $\omega$ -integration to be carried out analytically.

The final form for this approximation to  $\chi_4$  can be written

$$\chi_4(\underline{k}, \underline{G}-\underline{k}; \underline{q}-\underline{k}, -\underline{q}) \sim \frac{\chi_4^0(\underline{k}, \underline{G}-\underline{k}; \underline{q}-\underline{k}, -\underline{q})}{\varepsilon(\underline{k}) \varepsilon(\underline{G}-\underline{k}) \varepsilon(\underline{q}-\underline{k}) \varepsilon(-\underline{q})} \quad (3.19)$$

where we have made the identification,

$$\chi_4^0(\underline{k}, \underline{G}-\underline{k}; \underline{q}-\underline{k}, -\underline{q}) = \int \frac{d\omega}{(2\pi)} e^{i\omega\delta} \Pi_4^0(\underline{k}\omega, \underline{G}-\underline{k}-\omega; \underline{q}-\underline{k}, -\underline{q}) \quad (3.20)$$

From (3.19) it follows that if  $\underline{G} = 0$ ,  $\chi_4$  has a factor  $\varepsilon^{-2}(\underline{k})$ . Since  $\varepsilon(\underline{k}) \sim 1/k^2$

as  $\underline{k} \rightarrow 0$ , it is clear that, in this approximation,  $\chi_4(\underline{k}, -\underline{k}; \underline{q}, -\underline{q})$  goes to zero at least as  $k^4$  in the limit of small  $k$ .

### §3.4 Conclusion

In the preceding two sections, two approximate forms, given by (3.13) and (3.19), have been derived for the four-body response function  $\chi_4$ , (a) by density functional arguments and (b) by diagrammatic analysis. For ease of reference, the diagonal elements ( $\underline{G} = 0$ ) are repeated here.

$$(a) \quad \chi_4(\underline{k}, -\underline{k}; \underline{q}, -\underline{q}) \sim \chi^2(\underline{q}) H_4^0(\underline{k}, -\underline{k}; \underline{q}, -\underline{q}) \quad (3.21a)$$

$$\sim \left( \frac{\chi(\underline{q})}{\chi^0(\underline{q})} \right)^2 \left\{ \begin{array}{l} \chi_4^0(\underline{k}, -\underline{k}; \underline{q}, -\underline{q}) \\ - \frac{\chi_3^0(\underline{k}, -\underline{k}; 0) \chi_2^0(0, \underline{q}, -\underline{q})}{\chi^0(0)} \end{array} \right\} \quad (3.21b)$$

$$(b) \quad \chi_4(\underline{k}, -\underline{k}; \underline{q}, -\underline{q}) \sim \frac{\chi_4^0(\underline{k}, -\underline{k}; \underline{q}, -\underline{q})}{\epsilon^2(\underline{k}) \epsilon^2(\underline{q})} \quad (3.22)$$

In each case it has been demonstrated that (1) the dielectric constant appears in a way that screens the electron-ion interaction and (2)  $\lim_{\underline{k} \rightarrow 0} \chi_4(\underline{k}, -\underline{k}; \underline{q}, -\underline{q}) = 0$ , so that the charge neutrality limit on  $S_{ee}(\underline{k})$  for liquid metals is exactly satisfied to second order.

However it should be pointed out that property (2) comes about by different mechanisms in the two cases. In (a), the result follows from particle number conservation which implies that  $\lim_{\underline{k} \rightarrow 0} H_4^0(\underline{k}, -\underline{k}; \underline{q}, -\underline{q}) = 0$  (see Appendix B, § B1). This result has not been generalised to the exact  $H_4$ . It turns out in fact that

$$\lim_{\underline{k} \rightarrow 0} \chi_4^0(\underline{k}, -\underline{k}; \underline{q}, -\underline{q}) = -\frac{1}{\pi^2 q} \ln \left| \frac{q + 2k_F}{q - 2k_F} \right| \neq 0 \quad (3.23)$$

where  $k_F = (3\pi^2 n_e)^{\frac{1}{3}}$  is the Fermi wave number. The second term in (3.21b)



(which is evaluated explicitly in Appendix B) is needed to exactly cancel (3.23) as  $\underline{k} \rightarrow 0$ , thus leading to the desired result.

On the other hand, in the diagrammatic case (b), the result does not depend on free particle properties but on the existence of the screening factors of  $\tilde{\epsilon}^2(\underline{k})$  in (3.22). But these factors only arise because of the neglect of the frequency dependence of the dielectric function. To treat the  $\underline{k} \rightarrow 0$  limit properly, one should return to (3.18) and attempt to do the  $\omega$  -integration.

The discrepancy between the two approximations has not yet been satisfactorily resolved. Neither has it proved possible to evaluate (3.21) nor (3.22) fully, so that they cannot be compared numerically. However it is to be recalled from the discussion at the end of § 2.5 that the contribution of the  $\chi_{\pm}$  term to  $S_{ee}(\underline{k})$  in liquid metals is expected to be small compared to the charge neutrality term.

## CHAPTER 4

CALCULATIONS AND DISCUSSION OF THE ELECTRON-ELECTRON  
AND ELECTRON-ION STRUCTURE FACTORS IN LIQUID METALS

§ 4.1 Introduction

In this chapter, the dominant charge neutrality terms that appear in expressions (2.35) and (2.41) for  $S_{ee}(k)$  and  $S_{ie}(k)$  are calculated for liquid sodium and aluminium. These terms are given by

$$S_{ee}(k) - S(k) \sim \frac{1}{Z} (V_{ie}(k)\chi(k))^2 \rho_{ii}(k) \quad (4.1)$$

$$S_{ie}(k) \sim \frac{1}{Z^{\frac{1}{2}}} V_{ie}(k)\chi(k) \rho_{ii}(k) \quad (4.2)$$

After some general considerations given immediately below, § 4.2 discusses the input data required for the calculations. In § 4.3 and § 4.4 the results for liquid sodium and aluminium are presented, followed in § 4.5 by a discussion of them. The implications of these results for the differences between X ray and neutron structure factor data are then examined in § 4.6 and § 4.7 using the framework suggested by Egelstaff et al (EMM)<sup>(10)</sup>. Finally in § 4.8 there is a summary of the conclusions of this work.

Liquid sodium and aluminium have been chosen for these calculations because they are both nearly-free electron metals with relatively weak electron-ion interactions and to which the theory developed here should therefore be applicable. Also, tabulated structure factor data has been obtained for these metals, this being preferable to attempting to deduce the data from the diagrams usually presented in the literature. Sodium and aluminium differ, of course, in that monovalent sodium has a relatively lower mean electron density ( $r_s \sim 4$ ) than trivalent aluminium ( $r_s \sim 2$ ). Here  $r_s = \frac{1}{a_0} \left( \frac{3}{4\pi n_e} \right)^{\frac{1}{3}}$  is the usual electron gas parameter which measures the mean separation of the electrons in units of the Bohr radius  $a_0 = 0.53 \text{ \AA}$ . The jellium functions  $S(k)$  and  $\chi(k)$  that appear in (4.1) and (4.2) naturally depend on  $r_s$ , this dependence usually being displayed

through the Fermi wavenumber  $k_F$  defined by

$$k_F = (3\pi^2 n_e)^{\frac{1}{3}} = \left(\frac{9\pi}{4}\right)^{\frac{1}{3}} \frac{1}{a_0 r_s} \quad (4.3)$$

In the theory of liquid metals, the position of  $2k_F$  relative to that of the first (principal) peak in the ion-ion structure factor is of considerable importance. For monovalent metals,  $2k_F$  (which is proportional to  $z^{\frac{1}{3}}$ ) is characteristically just on the low  $k$  side of this peak (c.f. figure 4.1a for sodium); for divalent metals it is just on the high  $k$  side; and for trivalent metals it is in the trough between the first and second peaks of  $S_{ii}^{(1b)}$  (c.f. figure 4.2a for aluminium). Since  $\chi(k)$  becomes small for  $k > 2k_F$  it follows that, other things being equal, the effect of the principal peak in  $S_{ii}(k)$  should be more apparent in  $\Delta S_{ee}(k)$  and  $S_{ie}(k)$  in polyvalent metals than in monovalent metals. However, as will appear in the case of aluminium, the behaviour of the electron-ion potential is also of crucial importance.

It is interesting to note that these same considerations arise in discussion of the resistivity,  $\rho$ , of liquid metals on the basis of the Ziman formula. This formula gives (1c)

$$\rho \propto \int_0^{2k_F} k^3 \left( \frac{V_{ie}(k)}{\epsilon(k)} \right)^2 S_{ii}(k) dk \quad (4.4)$$

The integrand of (4.3) closely resembles (4.1) and one is led to suppose that metals with a high resistivity are likely to have larger electron-ion contributions to their electron-electron structure factors.

## § 4.2 Data used in the calculations

To evaluate (4.1) and (4.2) one requires specific forms for (a) the electron-ion interactions  $V_{ie}(k)$ , (b) the density response function  $\chi(k)$  and (c) the ion-ion structure factor  $S_{ii}(k)$ .

(a) The electron-ion interaction  $V_{ie}(k)$ 

It is now well established that in nearly-free electron metals, the electron-ion interaction is well described by means of a pseudopotential<sup>(31)</sup>. Pseudopotential theory explains the apparent weakness of this interaction by taking into account the need to make the valence electron wave functions orthogonal to those of the core electrons. Rigorous pseudopotentials are non-local and energy dependent, but several simpler, model pseudopotentials have been proposed whose parameters are usually determined by fitting to various observable properties. One such pseudopotential, which will be employed here because of its simple analytic form, is the one-parameter, empty core pseudopotential of Ashcroft<sup>(32)</sup>. In  $r$ -space this has the form

$$V_{ie}(r) = \begin{cases} -Z/r & r > R_c \\ 0 & r < R_c \end{cases} \quad (4.5a)$$

where  $R_c$  is the empty core radius. In Fourier transform this becomes

$$V_{ie}(k) = -\frac{4\pi Z}{k^2} \cos(kR_c) \quad (4.5b)$$

This pseudopotential has a node (zero) when  $kR_c = \pi/2$ . The values of  $R_c$  (see table 4.1 on page 53) have been taken from Cohen and Heine<sup>(31)</sup>, it being assumed that  $R_c$  does not vary significantly from the solid to the liquid state. For further discussion of the use of pseudopotentials specifically in liquid metals see the first chapter of<sup>(1)</sup>.

(b) The density response function of jellium  $\chi(k)$ 

Current theories of interacting jellium usually express the static density response function in the form

$$\chi(k) = \frac{\chi^0(k)}{(1 - \epsilon_{ee}(k)\chi^0(k))} \quad (4.6)$$

where  $\chi^0(k)$  is the free-electron density response function given by

$$\chi^0(k) = -\frac{k_F}{\pi^2} \left[ \frac{1}{2} + \frac{k_F}{2k} \left( 1 - \frac{k^2}{4k_F^2} \right) \ln \left| \frac{k+2k_F}{k-2k_F} \right| \right] \quad (4.7)$$

If  $\phi_{ee}(k)$  is taken as the bare electron-electron interaction  $4\pi/k^2$ , one obtains the familiar RPA form for  $\chi(k)$ . However the more recent generalised RPA (GRPA) theories put

$$\phi_{ee}(k) = \frac{4\pi}{k^2} (1 - G(k)) \quad (4.8)$$

where  $G(k)$  is a local field correction which modifies the Hartree field acting on each electron by taking into account short-range electron correlations. Several forms for  $G(k)$  have been proposed. Here we use the now classic work of Singwi et al (SSTL)<sup>(33)</sup> whose self-consistent determination of  $G(k)$  constituted a major improvement over the RPA. SSTL have found that a useful parameterisation of their  $G(k)$  is given by

$$G(k) = A(r_s) \left[ 1 - e^{-B(r_s)k^2/k_F^2} \right] \quad (4.9)$$

The values of  $A$  and  $B$  appropriate to sodium and aluminium are given in table 4.1.

(c) The ion-ion structure factor  $S_{ii}(k)$

According to the discussion of scattering experiments in § 1.5,  $S_{ii}(k)$  is strictly only determined by neutron scattering. However, there is a surprising lack of recent neutron data on liquid sodium and so the author has had to use the early results of Gringrich and Heaton<sup>(34)</sup>. These are undoubtedly inferior to the highly accurate X ray results of Greenfield et al<sup>(35)</sup>, and so comparison between the two has not been seriously attempted (but see § 4.6). The data of Gringrich and Heaton is particularly inaccurate at small  $k$  and so has been amended to agree with the X ray data in this region. Both sets of data are for liquid sodium at 100°C.

$S_{ii}(k)$  for liquid aluminium was taken from the recent, unpublished neutron experiments of Jović<sup>(36)</sup>. X ray measurements were taken from Waseda<sup>(37)</sup> whose

data appears to be in good agreement with the (unpublished) results of Fessler et al.<sup>(104)</sup>. Both sets of data are for liquid aluminium just above its melting temperature of 666°C.

The mean electron density of each metal at the appropriate temperature is given in table 4.1 below. In this table atomic units ( $\hbar = e = m = 1$ ) are used.

Quantity (atomic units)	Liquid Na	Liquid Al
Temperature	100°C	666°C
Electron density	0.003564 <sup>(38)</sup>	0.02363 <sup>(39)</sup>
$r_s$	4.061	2.162
$k_F$	0.473	0.880
A } see equation (4.9)	0.9959 ( $r_s = 4$ )	0.8994 ( $r_s = 2$ )
B }	0.2612 ( $r_s = 4$ )	0.3401 ( $r_s = 2$ )
Empty core radius $R_c$ <sup>(31)</sup>	1.67	1.12

Table 4.1 Summary of parameters used in the calculations

### § 4.3 Results for liquid sodium

Figures 4.1 a-d show as a function of  $k/k_F$  (a)  $S_{ii}(k)$  for liquid sodium, (b) the form factor  $\chi(k)V_{ie}(k)$ , (c) the change,  $\Delta S_{ee}(k)$ , in the electron-electron structure factor from its jellium value as given by the charge neutrality term (4.1), and (d)  $S_{ie}(k)$  as given by (4.2). Note the variation in vertical scale in each case.

The first thing to notice about  $\Delta S_{ee}(k)$  from figure 4.1c is that it is very small, in fact never being greater than its  $k = 0$  value. For monovalent metals,

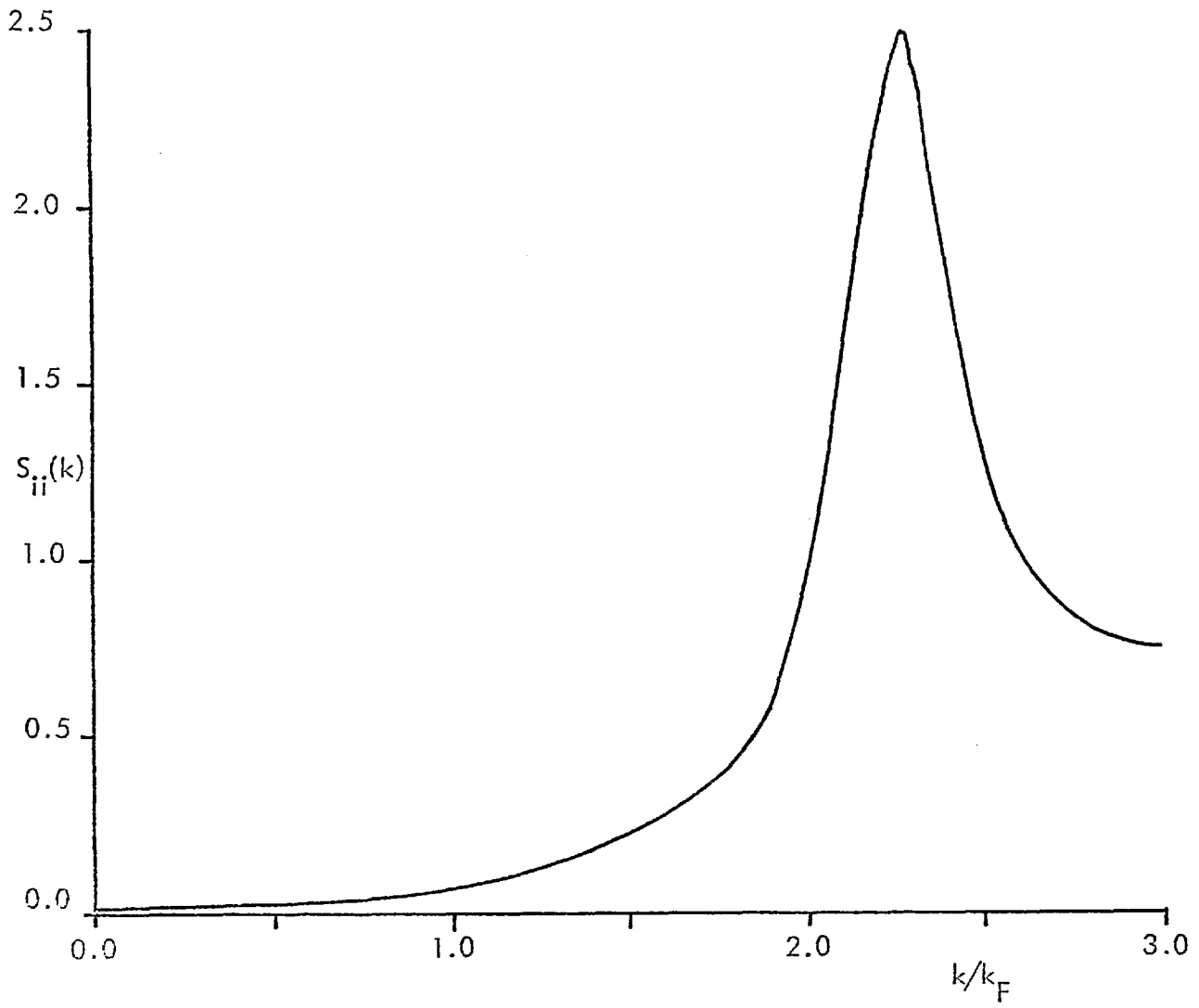


FIGURE 4.1a

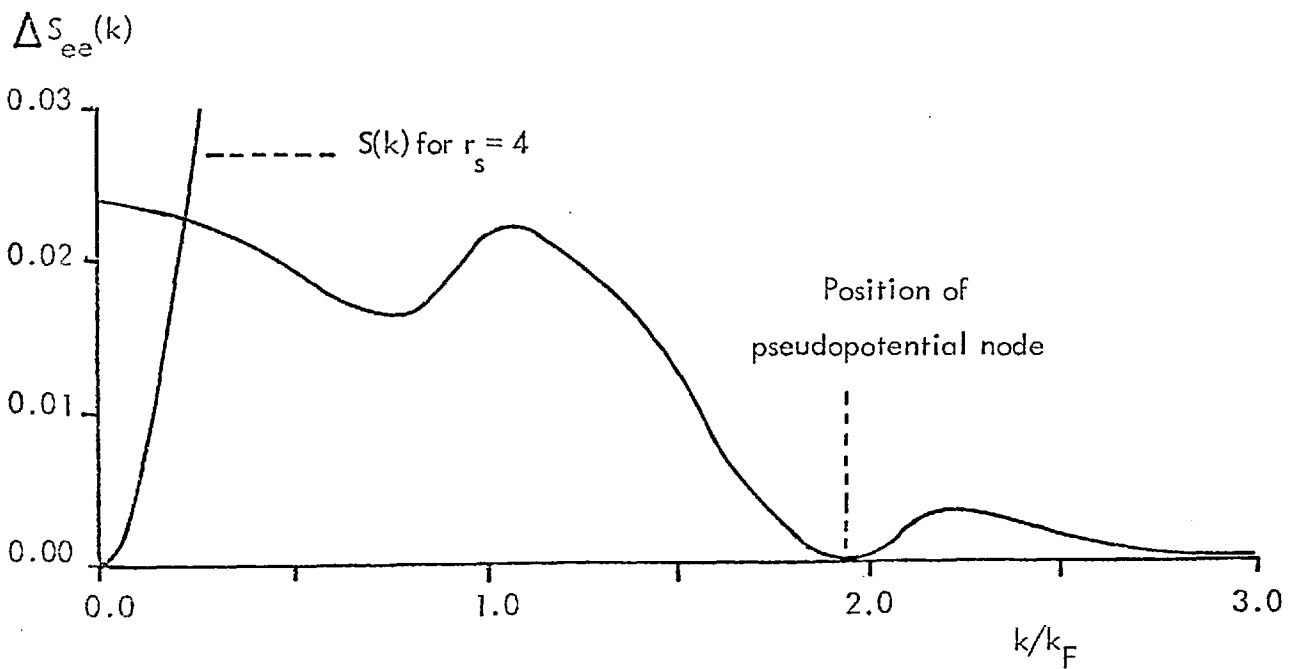


FIGURE 4.1c

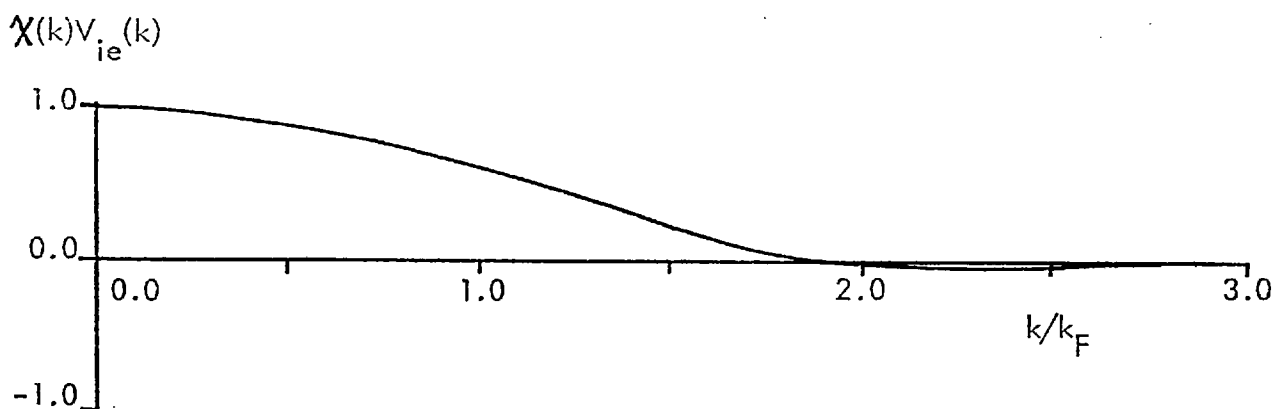


FIGURE 4.1b

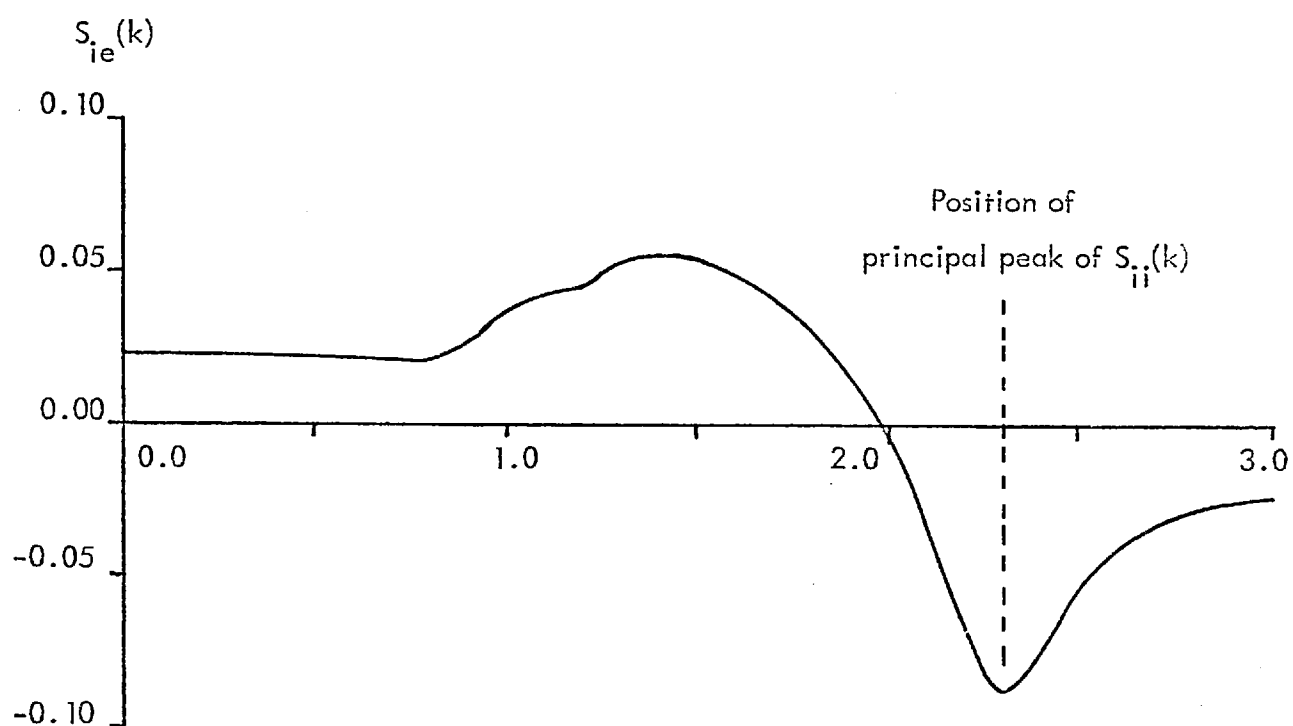


FIGURE 4.1d

FIGURE 4.1a THE ION-ION STRUCTURE FACTOR FOR LIQUID SODIUM<sup>(34)</sup>

FIGURE 4.1b THE FORM FACTOR  $\chi(k)V_{ie}(k)$

FIGURE 4.1c CHANGE IN THE ELECTRON-ELECTRON STRUCTURE FACTOR

FIGURE 4.1d THE ELECTRON-ION STRUCTURE FACTOR



this is the same as  $S_{ii}(0)$  and for sodium equals 0.0240.  $S(k)$ , the jellium contribution to  $S_{ee}(k)$ , rises monotonically from zero at  $k = 0$  (c.f. (1.15)) to  $\sim 1$  for  $k \geq 2k_F$ . It is shown on the left of figure 4.1c, but rapidly goes off scale for  $k/k_F \sim 0.1$ . Thus electron-ion contributions to  $S_{ee}(k)$  are only one or two percent of the jellium contribution except in the charge neutrality limit.

The structure of  $\Delta S_{ee}(k)$  and its smallness is easily explained by reference to the behaviour of  $S_{ii}(k)$  (figure 4.1a) and  $\chi(k)V_{ie}(k)$  (figure 4.1b). For liquid sodium, the node in the pseudopotential is at  $k/k_F \sim 1.95$  and  $\chi(k)V_{ie}(k)$  remains very small beyond  $2k_F$ . Thus the effect of the principal peak of  $S_{ii}$  at  $k/k_F = 2.27$  is almost totally absent from  $\Delta S_{ee}(k)$ . It should be noted that the details of  $\Delta S_{ee}(k)$  for  $k/k_F \sim 1$  (that is where  $S_{ii}(k)$  is beginning to rise towards the first peak, while the form factor is steadily decreasing) are quite sensitive to small changes in  $S_{ii}$ . For instance, if the peak of  $S_{ii}(k)$  were narrower (as is suggested by the X ray data), the bulge in  $\Delta S_{ee}(k)$  at  $k/k_F \sim 1.1$  would be less pronounced. Clearly more accurate neutron data for  $S_{ii}(k)$  is needed in order to better predict the detailed form of  $\Delta S_{ee}(k)$ .

$S_{ie}(k)$  is shown in figure (4.1d). As it is first order in  $V_{ie}$ , it is of greater magnitude than  $\Delta S_{ee}(k)$ , but does not exceed 0.1. The negative values of  $S_{ie}(k)$  are consistent with the relation between  $S_{ie}(k)$  and  $g_{ie}(r)$  (see equation (1.10)) and the fact that  $g_{ie}(0) \sim 0$ . Again the structure of  $S_{ie}(k)$  reflects that of  $\chi(k)V_{ie}(k)$  and  $S_{ii}(k)$ , the most obvious feature being the rapid change of sign as the pseudopotential passes through its node.  $S_{ie}(k)$  reaches its maximum magnitude of -0.09 at the position of the principal peak of  $S_{ii}(k)$ .

#### § 4.4 Results for liquid aluminium

The corresponding curves for (a)  $S_{ii}(k)$ , (b)  $\chi(k)V_{ie}(k)$  (c)  $\Delta S_{ee}(k)$

and (d)  $S_{ie}(k)$  for liquid aluminium are shown in figure 4.2 a-d.

Aluminium might be expected to show greater electron-ion effects on  $S_{ee}(k)$  than sodium, because, being a trivalent metal, its electron-ion interaction is stronger and also, as pointed out in § 4.1,  $k_0$ , the position of the principal peak of  $S_{ii}$  is less than  $2k_F$ . However it turns out that the pseudopotential node at  $k/k_F \approx 1.6$  almost exactly coincides with  $k_0$  so that the effect of the principal peak is virtually annulled.  $\Delta S_{ee}(k)$ , as a result, remains small for all  $k$ , not exceeding its  $k = 0$  value as given by  $z S_{ii}(0) \sim 0.06$ . As with sodium, there is some sensitivity to the neutron diffraction data used. The measurements of Honma and Tamaki<sup>(39)</sup> show a curious bump in  $S_{ii}(k)$  at  $k/k_F \sim 0.7$  not present in the neutron data of Jović or the X ray data of Waseda or Fessler et al. If real, this bump would give a corresponding peak of height  $\sim 0.11$  in  $\Delta S_{ee}(k)$  at this position.

$S_{ie}(k)$  for liquid aluminium is of similar form to that for sodium, with a maximum positive and negative magnitude of  $\sim 0.1$  and a rapid change of sign at the pseudopotential node.

#### § 4.5 Discussion of the results

The results of the preceding two sections strongly suggest that electron-ion interactions make only small modifications to the electronic structure factors of liquid sodium and aluminium. In both these metals the change,  $\Delta S_{ee}(k)$ , in  $S_{ee}(k)$  from its jellium value  $S(k)$  is never more than a few percent of  $S(k)$  except in the charge neutrality limit ( $k \rightarrow 0$ ) when  $\Delta S_{ee}(k)$  constitutes the total contribution. However, as discussed in § 4.1, it is possible that  $\Delta S_{ee}(k)$  could be large in a polyvalent metal in which the node of the pseudopotential does not coincide with the principal peak of the structure factor  $S_{ii}(k)$ .

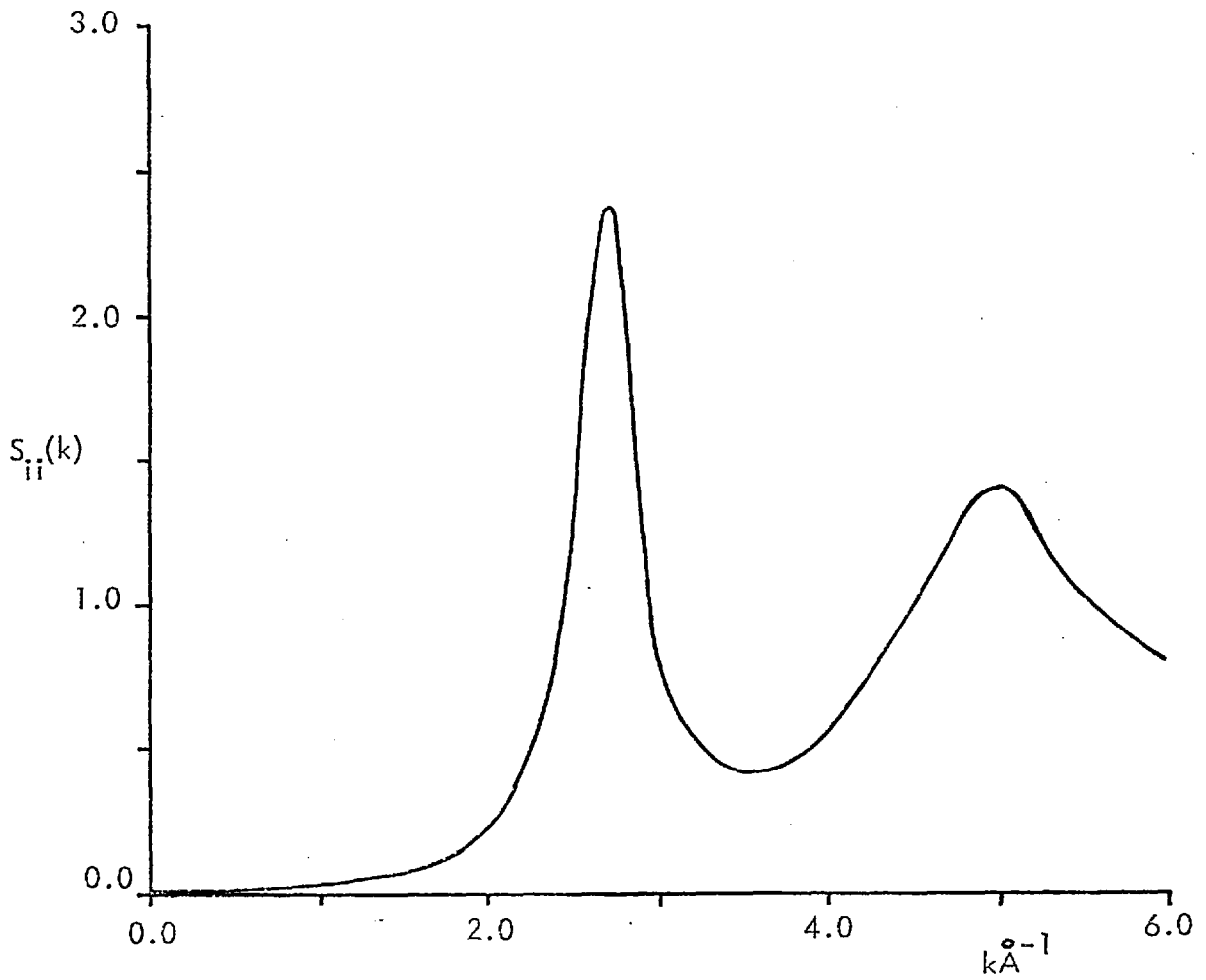


FIGURE 4.2a ION-ION STRUCTURE FACTOR FOR LIQUID ALUMINIUM

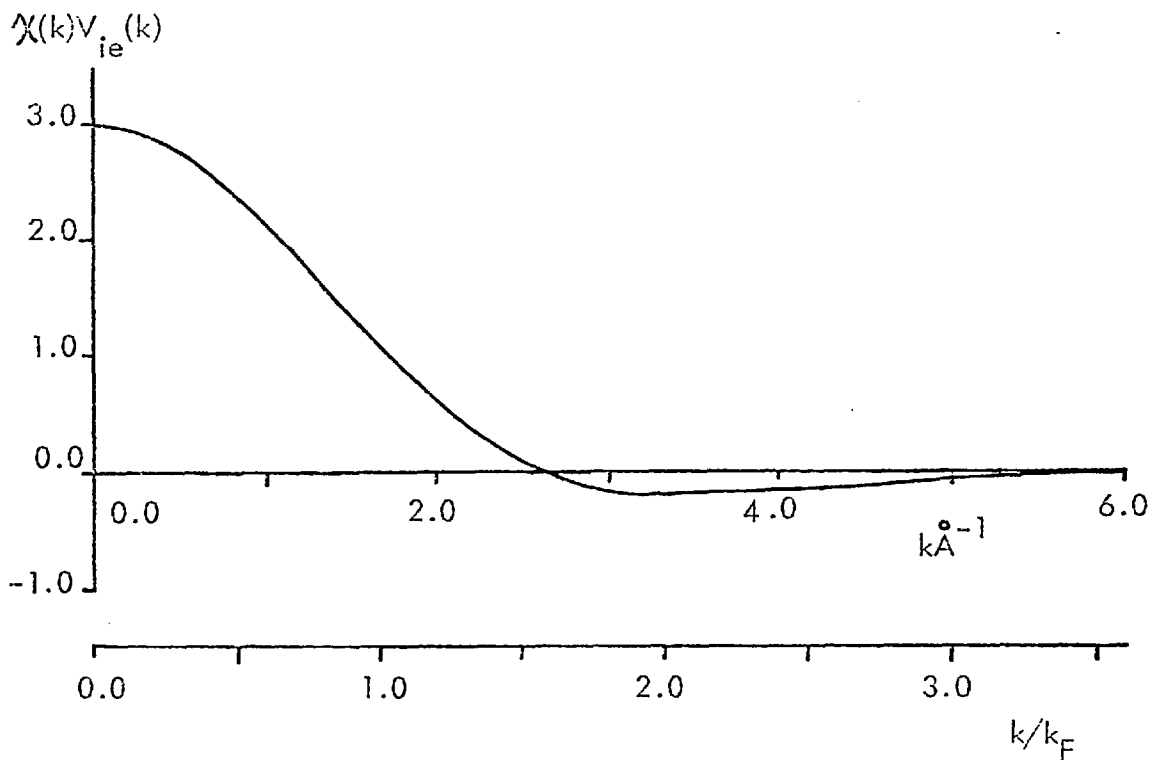


FIGURE 4.2b THE FORM FACTOR  $\chi(k)V_{ie}(k)$

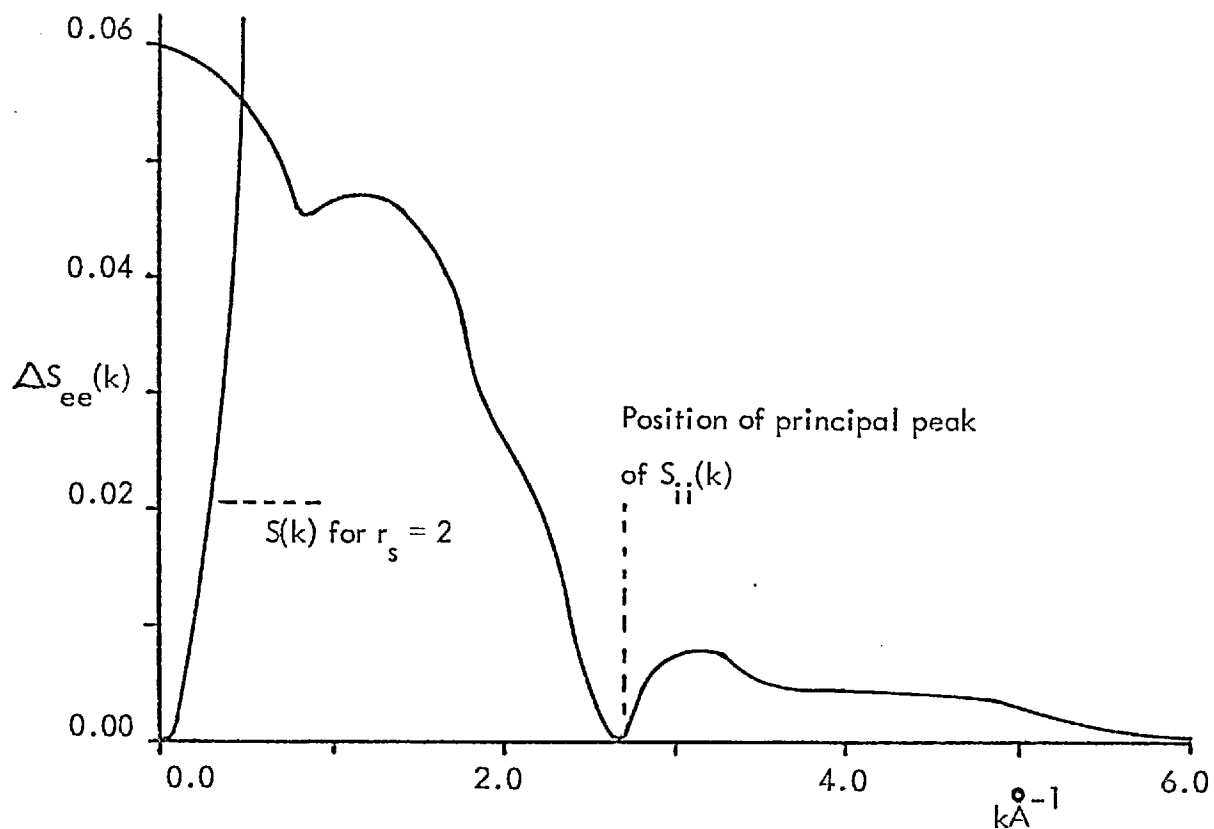


FIGURE 4.2c CHANGE IN THE ELECTRON-ELECTRON STRUCTURE FACTOR

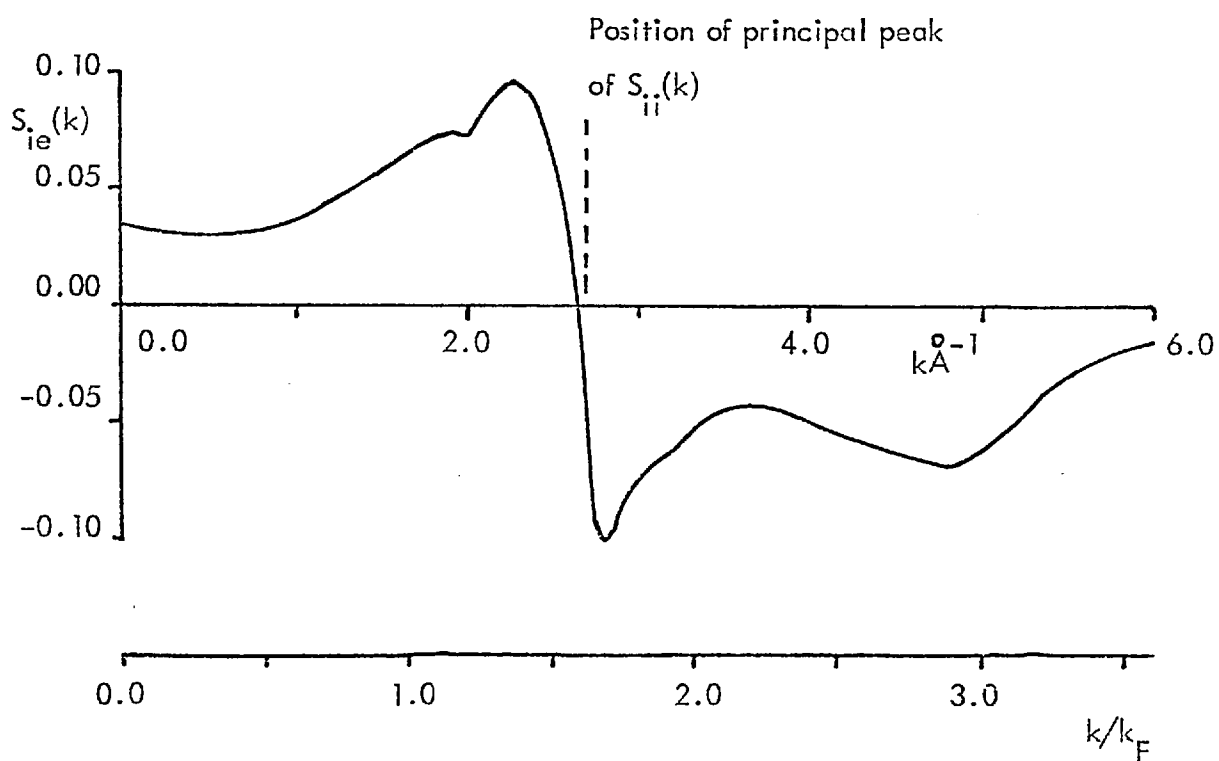


FIGURE 4.2d THE ELECTRON-ION STRUCTURE FACTOR

We recall that the calculations have been simplified by the use of the adiabatic approximation and a simple model pseudopotential and also by the neglect of the second-order contribution to  $S_{ie}(k)$  and of the  $\chi_4$  term to  $\Delta S_{ee}(k)$ . Although it is difficult to give quantitative estimates of the errors introduced by these approximations, it is clear that they will not substantially modify the conclusion that electron-ion effects on the electronic structure factors are generally very small. Certainly we can be sure that for small  $k$ , the expressions for  $\Delta S_{ee}(k)$  and  $S_{ie}(k)$  are essentially exact.

One further effect that has not been included in this treatment of the problem is the blurring of the Fermi surface of the electrons due to disorder scattering by the ions. The magnitude of this blurring,  $\Delta k_F$ , will be related to the reciprocal of the electronic mean free path,  $\lambda$ , which is usually many atomic spacings in nearly-free electron liquid metals (in sodium it is  $\sim 73$  atomic spacings, in aluminium  $\sim 11$ )<sup>(1d)</sup>. Thus the effect will be small, but should introduce an exponential factor  $e^{-\Delta k_F r}$  into the electron-electron pair function  $g_{ee}(r)$ . This will damp the small amplitude, long-range oscillations that arise in  $g_{ee}(r)$  due to the singularities in the jellium response functions  $\chi$  and  $\chi_4$  that enter the theory (c.f. § 3.1).

The conclusion from the above discussion is, that if the proposal of EMM to extract  $S_{ee}(k)$  from a combination of scattering data is carried out for liquid sodium and aluminium, the result will be, to the accuracy of a few percent, an experimental determination of the jellium structure factor  $S(k)$  at the electron density of these metals.

The author does not underestimate the experimental difficulties involved in obtaining X ray, neutron and electron scattering data to the required high accuracy; these difficulties are highlighted in the following sections. However

the conclusion is interesting in the light of the current controversy over the correct form of  $S(k)$  in interacting jellium (see § 4.7).

#### § 4.6 Comparison of X ray and neutron structure factor data for liquid aluminium

In the absence of suitable electron diffraction data it is not possible to carry out fully the proposal of EMM (see § 1.5), but it is still interesting to use the above calculations of  $S_{ee}(k)$  and  $S_{ie}(k)$  to estimate the expected theoretical difference,  $\Delta(k)$ , between the structure factors as obtained by X ray and neutron diffraction. We recall that EMM pointed out the existence of systematic differences of up to 10% in the two sets of data.

According to the theory of EMM,  $\Delta(k)$  is given by (c.f. (1.37) )

$$\begin{aligned} \Delta(k) &= S_X(k)/f_a^2(k) - S_N(k) \\ &= \frac{Z}{f_a^2(k)} S_{ee}(k) + \frac{2Z \frac{1}{2} f_c(k) S_{ie}(k)}{f_a^2(k)} + \left[ \frac{f_c^2(k)}{f_a^2(k)} - 1 \right] S_{ii}(k) \end{aligned} \quad (4.10)$$

where  $f_a(k)$  and  $f_c(k)$  are respectively the free atom and free ion form factors.

If we now use (4.1) and (4.2) for  $S_{ee}(k)$  and  $S_{ie}(k)$ , (4.10) becomes

$$\begin{aligned} \Delta(k) &= \frac{Z S(k)}{f_a^2(k)} + \left[ \frac{(\chi(k) V_{ie}(k) + f_c(k))^2}{f_a^2(k)} - 1 \right] S_{ii}(k) \end{aligned} \quad (4.11)$$

Note that  $\Delta(k) \rightarrow 0$  as  $k \rightarrow 0$ .

The quantity  $F(k) = f_c(k) + \chi(k) V_{ie}(k)$  that appears in (4.11) can be interpreted on the basis of the following rigid pseudo atom picture. Ions immersed in an electron gas will gather around them a screening charge of electrons. Within the linear response approximation, ion plus screening cloud will behave as a single unit, which Ziman<sup>(105)</sup> has called a neutral pseudo atom. The electron density of the pseudoatom is described by the form factor  $F(k)$ . The screening clouds of

neighbouring pseudoatoms must add up in the interstitial regions to give the roughly constant density of the original electron gas. The intrinsic correlations of this electron gas account for the first term in (4.11) while the term  $F^2(k) S_{ii}(k)$  arises by virtue of the apparent rigid attachment of the electrons to the ions. The difference between  $F(k)$  and  $f_a(k)$  is usually called the 'solid state effect' as it is the result of the delocalisation of the valence electrons when free atoms are brought together to form condensed matter. Within the present approximation, this, together with  $S(k)$  are responsible for the differences between X ray and neutron structure factor data. Note that the first term in (4.11) appears to become large at large  $k$ , when  $S(k) \sim 1$  and  $f_a^2(k)$  becomes small. However at these large momentum transfers the validity of (4.11) is doubtful because the distinction between core and valence electrons is less meaningful.

$\Delta(k)$  has been calculated from (4.11) for liquid aluminium and is shown in figure 4.3a.  $f_a(k)$  and  $f_c(k)$  have been taken from the wavefunction calculations of Fukamachi<sup>(18)</sup>. Professor Singwi has kindly supplied the author with tabulated values of  $S(k)$  for  $r_s = 2$  and 4.  $S(k)$  for  $r_s = 2$  (which is appropriate to aluminium) is shown in figure 4.4.

In figure 4.3b,  $\Delta^{\text{exp}}(k)$  is shown. This is the difference between the X ray data of Waseda and the neutron data of Jović for liquid aluminium. Note that the neutron principal peak height is 2.34 compared with an X ray height of 2.47, although this does not correspond to the maximum discrepancy.

It is clear from figure 4.3 that  $\Delta(k)$  and  $\Delta^{\text{exp}}(k)$  show very little agreement with each other,  $\Delta^{\text{exp}}(k)$  being in general an order of magnitude greater and showing markedly different structure (except that both show a dip at the position of the principal peak). The results for liquid sodium (not presented in detail because of the inaccuracy of the neutron data) also suggest that the

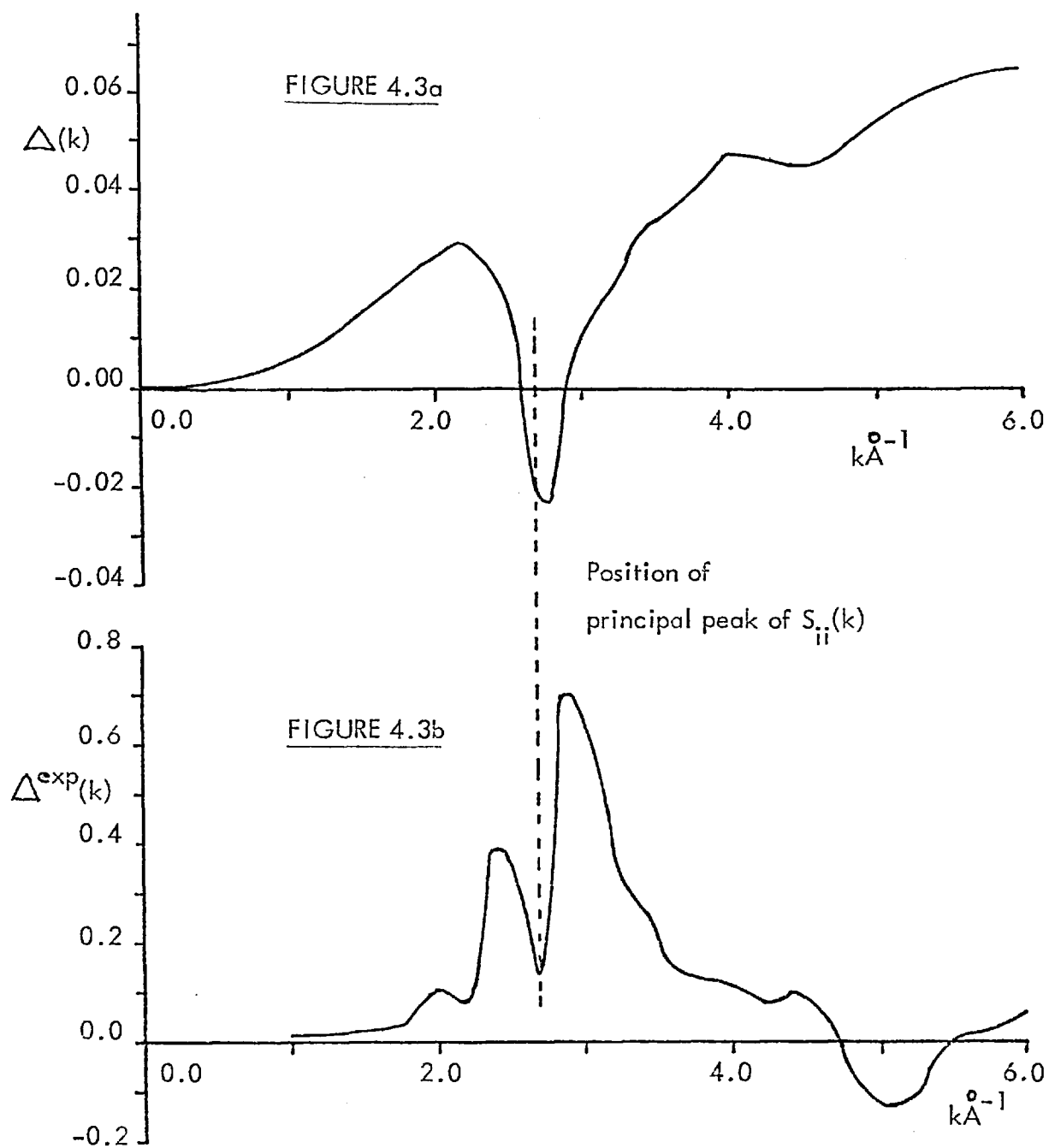


FIGURE 4.3 THE DIFFERENCE BETWEEN THE X RAY AND NEUTRON STRUCTURE FACTORS OF LIQUID ALUMINIUM.

(a)  $\Delta(k)$  AS CALCULATED FROM EQUATION (4.11).

(b)  $\Delta^{\text{exp}}(k)$  USING THE X RAY DATA OF WASEDA<sup>(37)</sup> AND THE NEUTRON DATA OF JOVIC<sup>(36)</sup>.

Note that the scale is 10X larger in (b) than in (a).



calculated difference between the neutron and X ray structure factors is much less than that which is observed. Thus the systematic enhancement by up to 10% of the X ray data noticed by EMM is so far unexplained.

#### § 4.7 Further discussion

The conclusion drawn in the preceding section would seem to imply that either inaccuracies in the X ray and neutron data make a quantitative comparison between them inappropriate, or that the theory is inadequate, or both.

It is not intended here to give a detailed discussion of the relative merits and demerits of X rays *vis a vis* neutrons for studying liquid metal structure, but some comments will be made. Both methods require the use of corrections based on theoretical models to actually extract the structure factor from the raw data. In the case of neutrons, corrections are needed for incoherent scattering, multiple scattering and inelastic scattering; in the case of X rays, the effects of Compton scattering must be subtracted and the data divided by the square of the atomic form factor. Greenfield et al<sup>(35)</sup> have given convincing arguments for the superior accuracy of at least their X ray measurements, particularly in the low k region. On the other hand, Enderby<sup>(17)</sup> and Faber<sup>(1e)</sup> argue favourably for the intrinsic accuracy of neutron experiments, although they recognise that measurements which do not go to sufficiently low k can lead to large normalisation errors. There is no doubt room for improvement in the accuracy of both X ray and neutron data and assuming the correctness of the theory presented here, experimentalists should be concerned that there is not closer agreement between the two.

But what impressed EMM was the systematic enhancement of the X ray data for a wide variety of liquid metals and the fact that this enhancement was not observed for other classes of liquids such as liquefied rare gases and molecular liquids (see table 1.1 on page 23 ). They pointed out that a rigid pseudoatom

model was unlikely to be able to explain this discrepancy. It would in fact give the neutron peak higher than the X ray peak (as observed in the aluminium calculations) because of the reduction of  $F(k)$  below  $f_a(k)$ . Thus EMM were led to suggest that there must be a degree of non-rigidity in the valence electron distribution so that these electrons are able to form an incipient structure (i.e. one only present on a short time scale) with a longer range order than the ions. This would show up as liquid-like peaks in the electron structure factor. From such a model they predicted that the neutron peak height should be intermediate between the X ray and electron diffraction peak heights as is apparently observed for bismuth.

It is difficult to see how to incorporate these ideas into the theory of  $S_{ee}(k)$  developed in this thesis. There seems little doubt that the electron-ion contributions to  $S_{ee}(k)$  are very small and therefore the only modification that can be made is to the jellium structure factor  $S(k)$ .

Current theories of  $S(k)$  based on the GRPA show no liquid-like structure;  $S(k)$  rises monotonically to  $\sim 1$  at  $2k_F$  (see figure 4.4 on page 66). However there is growing evidence that these theories are still inadequate because they neglect the important frequency dependence of the local field correction  $G(q)$  (see equation (4.8)). Doubts were originally raised by Platzman et al's inelastic X ray scattering measurements of the dynamic electron structure factor,  $S(\underline{k}, \omega)$ , in several solid metals<sup>(106)</sup> (see also H ohberger et al<sup>(107)</sup>). These workers unexpectedly observed in beryllium, aluminium, lithium and also graphite that reasonably well defined plasmon excitations persisted into the wavenumber range between  $k_F$  and  $2k_F$ . Furthermore the plasmon dispersion relation,  $\omega(\underline{k})$ , appeared to flatten and even to acquire negative slope. These observations (which seem not to depend on lattice structure) conflict with the mean field (GRPA) theories of

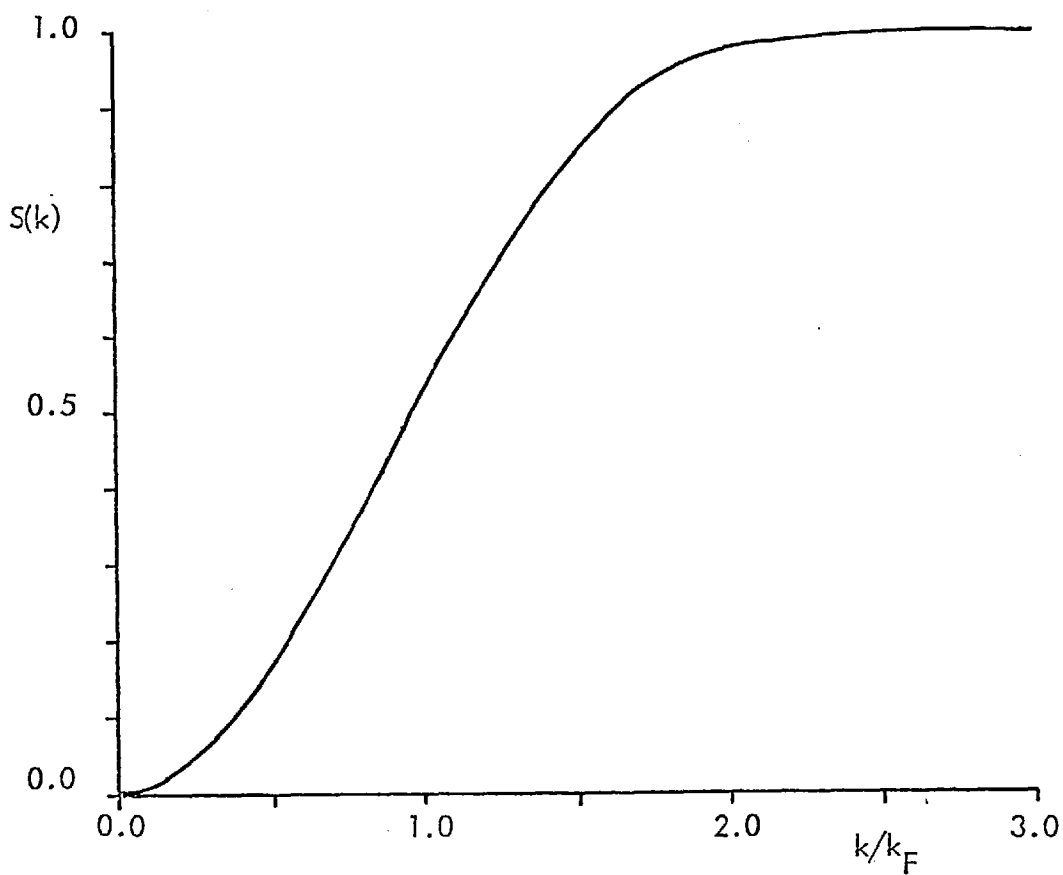


FIGURE 4.4 THE JELLIUM STRUCTURE FACTOR,  $S(k)$ ,

FOR  $r_s = 2$ . Data supplied by Professor K.S. Singwi.

interacting electrons. According to these theories plasmons are ill-defined in this region because they are unstable to decay into single- and multi-particle excitations. Recently Singwi et al<sup>(108)</sup> have suggested an explanation for the observed phenomena in terms of electron life-time effects.

The relevance of these observations to the present discussion can be made apparent by means of a simple model. If we suppose that the electron excitations are predominantly plasmon-like with dispersion relation  $\omega(\underline{k})$  and we also neglect plasmon damping, then the two sum rules on  $S(\underline{k}, \omega)$  given by<sup>(109)</sup>

$$S(\underline{k}) = \frac{1}{n_e} \int d\omega S(\underline{k}, \omega) \quad (4.12)$$

$$\frac{\hbar k^2}{2m} = \frac{1}{n_e} \int d\omega \omega S(\underline{k}, \omega) \quad (4.13)$$

are both satisfied by the form

$$S(\underline{k}, \omega) = n_e S(\underline{k}) \delta(\omega - \omega(\underline{k})) \quad (4.14)$$

provided

$$\omega(\underline{k}) = \frac{\hbar k^2}{2m S(\underline{k})} \quad (4.15)$$

On the basis of (4.15), an explanation of the observed flattening of  $\omega(\underline{k})$  in the region  $k_F \lesssim k \lesssim 2k_F$ , is a corresponding enhancement of  $S(\underline{k})$  in this region.

Although this model is naive in neglecting the large contribution to  $S(\underline{k}, \omega)$  due to single- and multi-particle excitations, it does point towards the conclusion that the jellium structure factor  $S(\underline{k})$  may show some liquid-like structure due to short-range electron correlations.

It must not be supposed that the deviations of the observed electron structure factor from that for instance shown in figure 4.4, are large. Certainly there is no suggestion that the electrons possess the substantial degree of order characteristic of a Wigner lattice<sup>(110)</sup>; this is unlikely because the electron densities of real

metallic systems are well above that suspected for the Wigner transition. However an idea of the magnitude of the effect can be seen from figure 4.5. The full curve shows  $S(k)$  for solid beryllium as obtained from (4.12) using the experimental measurements of  $S(\underline{k}, \omega)$  by Platzman et al<sup>(111)</sup>. The dotted curve shows the theoretical  $S(k)$  for an electron gas corresponding to the density of beryllium, according to the RPA. It can be seen that the observed  $S(k)$  shows a bump at  $k/k_F \sim 0.8$  and also is enhanced by up to 10% at  $k/k_F \sim 2$ . It should be remembered however, that beryllium shows distinct anisotropy in some of its properties<sup>(112)</sup> and thus electron-ion interactions are clearly more important than in nearly-free electron metals. Quantitative conclusions from figure (4.5) must therefore be treated with caution.

The implications of these results for  $S_{ee}(k)$  in liquid metals are still uncertain. Even if  $S(k)$  does show some liquid-like behaviour, there is still the problem that the enhancement of the X ray structure factor appears to be independent of the atomic number of the liquid metal. It might have been expected that in metals in which the proportion of core electrons to valence electrons is high, the X ray scattering would be entirely dominated by the former. But as EMM have pointed out, the division of electrons into valence electrons (those which are dominated by electron-electron interactions) and core electrons (those for which the electron-ion interaction is comparatively strong) may not in this context correspond to the customary separation.

In summary, this discussion has shown that although recent experiments have modified our view of the electron structure factor in homogeneous electron systems, there is no firm evidence that in such systems there is present the degree of electron ordering that would be necessary to explain the enhancement of the X ray structure factor data over the corresponding neutron data in liquid metals. Little further progress can be made in the absence of reliably accurate neutron and X ray

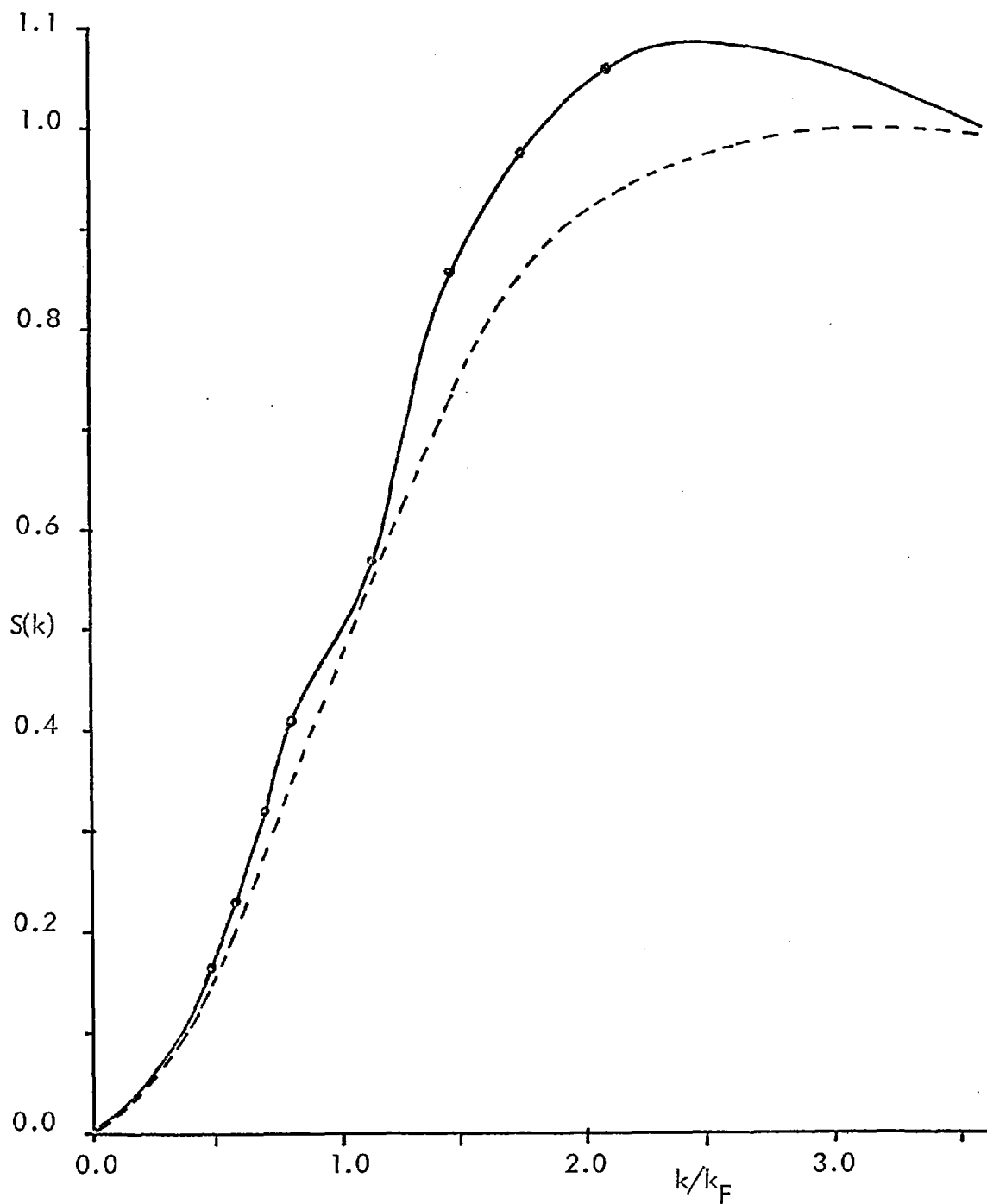


FIGURE 4.5 ELECTRON STRUCTURE FACTOR FOR SOLID BERYLLIUM.

FULL CURVE, EXPERIMENTAL RESULTS OF PLATZMAN ET AL<sup>(111)</sup>.

BROKEN CURVE,  $S(k)$  AS GIVEN BY THE RPA AT THE ELECTRON DENSITY OF BERYLLIUM.

scattering data.

## § 4.8 Final summary and conclusions

The aims of the work described above and in the preceding chapters have been,

- (1) to derive expressions for the electronic pair correlation functions and static structure factors in nearly-free electron metals,
- (2) to apply these expressions to a calculation of  $S_{ee}(k)$  and  $S_{ie}(k)$  in simple liquid metals, and
- (3) to use these calculations to try and understand the observed differences between X ray and neutron structure factor data on liquid metals.

The first aim has been achieved in chapter 2. There, a perturbation expansion for the electron-electron two particle correlation function, correct to second-order in a weak electron-ion interaction, is derived using a functional derivative technique. The unperturbed system is taken as a jellium of electrons superimposed on, but not interacting with, a jellium of ions. General results are obtained for an inhomogeneous system in which the ions are free to move. However they are shown to simplify (a) when the ions are 'frozen', as in rigid solids, and (b) in liquid metals, which are homogeneous on average. Only (b) has been investigated in detail. Using the adiabatic approximation (which relies on the small electronic to ionic mass), expressions to second-order in the electron-ion interaction  $V_{ie}$ , are derived for the electron-electron and electron-ion structure factors,  $S_{ee}(k)$  and  $S_{ie}(k)$ , in liquid metals. These expressions involve ion-ion correlation functions, and response functions of the electron jellium.

The condition of overall charge neutrality in liquid metals has been shown by several authors to imply that as  $k \rightarrow 0$ ,  $S_{ee}(k)$  and  $S_{ie}(k)$  are simply related to the ion-ion structure factor  $S_{ii}(k)$  according to

$$\lim_{k \rightarrow 0} \left\{ S_{ii}(k) = \frac{1}{Z^{\frac{1}{2}}} S_{ie}(k) = \frac{1}{Z} S_{ee}(k) \right\}$$

where  $Z$  is the valency. Specific terms in the expressions derived for  $S_{ie}(k)$  and  $S_{ee}(k)$  are shown to give these exact limits. These 'charge neutrality' terms are the first-order term in the case of  $S_{ie}(k)$  and one of the two second-order terms in the case of  $S_{ee}(k)$  (there being no first order term). Clearly it is then required to prove that the other terms contributing to  $S_{ie}(k)$  and  $S_{ee}(k)$  are zero as  $k \rightarrow 0$ . This has been done for the second-order contribution to  $S_{ie}(k)$ . However, no general proof has been found that the additional second-order term contributing to  $S_{ee}(k)$  is zero in this limit.

This term involves a complicated four-body response function of jellium,  $\chi_4$ . In chapter 3, two approximations to  $\chi_4$  are constructed, one using density functional arguments and the other using diagrammatic analysis. Both approximations do in fact lead to the conclusion that the  $\chi_4$  term contributes nothing to  $S_{ee}(k)$  as  $k \rightarrow 0$ . But as the physical interpretation of this property of  $\chi_4$  is different for the two approximations, the exact nature of  $\chi_4$  is still uncertain and requires further elucidation. Furthermore, it has not yet proved possible to evaluate fully either approximation to  $\chi_4$ . But as  $\chi_4$  is a measure of the irreducible short-range correlations between four adjacent electrons, its contribution to  $S_{ee}(k)$  is expected to be small. Trigger<sup>(23)</sup>, in his analysis of  $S_{ee}(k)$  by a different method, does not explicitly consider this term at all, and also concludes that the 'charge neutrality' term is the dominant electron-ion contribution to  $S_{ee}(k)$  for all  $k$ .

In § 4.1 to § 4.5 of chapter 4, calculations of these dominant electron-ion contributions to  $S_{ee}(k)$  and  $S_{ie}(k)$  are presented for liquid sodium and aluminium. In these calculations, the Ashcroft empty core pseudopotential was used for the electron-ion interaction;  $S_{ii}(k)$  was taken from neutron diffraction experiments; and the jellium linear density response function was taken from the GRPA results of Singwi<sup>(33)</sup> et al.



In liquid sodium, the electron-ion contribution to  $S_{ee}(k)$  is never greater than its  $k = 0$  value of 0.0240, and similarly in liquid aluminium, not greater than the  $k = 0$  value of 0.06. These contributions are, at most, one or two percent of  $S_{ee}(k)$ , except in the charge neutrality ( $k \rightarrow 0$ ) limit, when the otherwise dominant, jellium contribution to  $S_{ee}(k)$ , tends to zero. The electron-ion contribution does, however, show marked structure, which reflects that of both the ion-ion structure factor and the pseudopotential. In particular, the smallness of the electron-ion effects is explicable in the case of (a) sodium, because the principal peak of  $S_{ii}(k)$ , being beyond  $2k_F$ , has very little impact, and (b) aluminium, because the principal peak, although before  $2k_F$ , has its effect annulled by its coincidence with the node in the pseudopotential.

$S_{ie}(k)$  is also small, its magnitude not exceeding 0.1 in either liquid sodium or aluminium. However, a feature common to both metals is a rapid change of sign of  $S_{ie}(k)$  at the position of the pseudopotential node.

Two conclusions follow from these results, both of which arise in the context of the proposal by EMM<sup>(10)</sup> to experimentally determine  $S_{ee}(k)$  and  $S_{ie}(k)$  by combining the results of X ray, neutron and electron scattering experiments on liquid metals (see § 1.5).

Firstly, in liquid sodium and aluminium, the electron-ion contributions to  $S_{ee}(k)$  are so small as to imply that a measurement of  $S_{ee}(k)$  by the method of EMM will be effectively a measure of the jellium structure factor at the electron density of these metals. It should be pointed out however, that highly accurate data will be required for this purpose, which is certainly not available at present in the case of electron diffraction.

Secondly, as has been discussed in § 4.6 and § 4.7, the very small electron-ion effects calculated here, in no positive way help to explain the systematic

enhancement (as observed by EMM) of the principal peak of the X ray structure factor over that obtained by neutron diffraction experiments on liquid metals. Assuming that this enhancement is not simply a manifestation of inaccurate X ray or neutron data, it follows that its explanation requires the existence of some degree of incipient ordering amongst the valence electrons, which will be detected by the X rays but not by the neutrons. This ordering should show up as liquid-like peaks in the jellium structure factor although current GRPA theories of jellium predict no such behaviour. However there is growing experimental evidence from the work of Platzman<sup>(106)</sup> and others, that these theories are inadequate in their treatment of dynamic short-range electron correlations. Furthermore, these experiments explicitly show some structure in the measured electron structure factor, although it is still uncertain whether this is of a magnitude that will help explain the discrepancies between the X ray and neutron data. Clearly future work in this field should aim to clarify this point further.

## CHAPTER 5

A SIMPLE MODEL OF MOMENTUM DENSITY IN DILUTE BINARY ALLOYS§5.1 Introduction

It is well known that observations of Compton scattering of high energy photons by electronic systems (see § 5.4) give useful information about the momentum density of the electrons. In this chapter it is proposed that such measurements are a possible means of investigating impurity screening in dilute random alloys of nearly-free electron metals.

The basic idea is simple. If, for instance, a small concentration of magnesium is present in a host lattice of lithium, the excess charge of the  $Mg^{2+}$  ions over the  $Li^+$  ions creates an attractive impurity potential and leads to the build up of a localised electron screening charge centred on the magnesium ions. In such a screening charge the electron density will be strongly varying and to represent the density gradients, the electronic wave functions must contain high Fourier components. These will manifest themselves as a tail above the usual Fermi cut-off in the momentum density and also in the Compton profile.

Clearly a detailed quantitative treatment of self-consistent screening and momentum density in disordered alloys taking into account crystal structure, multiple scattering and impurity clustering would be very complicated, although recent attempts along these lines have been made by Bansil and Mijarens<sup>(40)</sup> using the average  $t$ -matrix approximation. However the method adopted here is to illustrate the particular phenomenon described above by means of a simple non-structural theory of charge distribution in dilute alloys first discussed by Friedel<sup>(41)</sup>. The momentum density and Compton profile are then derived from this charge density by a semi-classical Thomas-Fermi argument. Calculations are presented for an alloy of 10% magnesium in lithium and some comments made on other effects which may mask

observation of the screening charge by this method. Finally, contact is made with the recent density functional theory of momentum density of Platzman and Lam<sup>(42)</sup>.

### §5.2 The Friedel model of primary solid solutions

The Friedel<sup>(41)</sup> model of localised screening in dilute random alloys is based upon the following definitions and assumptions.

a) Impurity ions, each with an excess charge of  $Z|e|$  are distributed in the solvent metal with an atomic concentration  $c$ . Each impurity is situated at the centre of a sphere of radius  $R$  such that

$$c = \frac{\Omega}{\frac{4}{3}\pi R^3} \quad (5.1)$$

where  $\Omega$  is the atomic volume of the pure solvent. Clustering of impurities (and hence the overlap of the impurity spheres) is neglected, as is distortion of the solvent lattice.

b) Within each impurity sphere the additional  $Z$  electrons and the extra ionic charge give rise to a self consistent Hartree potential  $V(r)$  which satisfies Poisson's equation in the form

$$\nabla^2 V(\underline{r}) = -4\pi \left\{ \rho(E_f^0 + \Delta E_f, \underline{r}) - \rho_0(E_f^0, \underline{r}) - Z \delta(\underline{r}) \right\} \quad (5.2)$$

Here  $\rho_0(E_f, \underline{r})$  is the pure solvent electron density (i.e. the density of electrons with energy less than the Fermi energy  $E_f$ );  $\rho(E_f^0 + \Delta E_f, \underline{r})$  is the alloy electron density, in general with a Fermi level shift; and the delta function takes account of the excess charge at the impurity site. Note that the electrostatic potential is  $V(r)/-|e|$ , although in the atomic units used here,  $|e| = \hbar = m_e = 1$ . This equation is to be solved with the boundary conditions

$$V(R) = 0 \quad (5.3a)$$

$$V'(R) = 0 \quad (5.3b)$$

These conditions ensure the overall charge neutrality of the impurity spheres as well as continuity at the boundaries of two adjacent spheres.

c) The alloy and pure solvent electron densities are related by means of the generalised Thomas-Fermi approximation, i.e. by putting

$$\rho(E_f^o + \Delta E_f, r) \sim \rho_o(E_f^o + \Delta E_f - V(r), r) \quad (5.4)$$

This is exact if  $V(r)$  is a constant (and  $\Delta E_f = 0$ ) but is expected to be a reasonable approximation also if  $V(r)$  is slowly varying. In order to be able to solve (5.2)

simply, it is still necessary to linearise the expression for the extra electron density

$\Delta \rho(r)$  by assuming the potential is weak, and using the expansion

$$\begin{aligned} \Delta \rho(r) &\sim \rho_o(E_f^o + \Delta E_f - V(r), r) - \rho_o(E_f^o, r) \\ &\sim [\Delta E_f - V(r)] \left. \frac{\partial \rho_o(E_f, r)}{\partial E_f} \right|_{E_f^o} + O(V^2(r)) \end{aligned} \quad (5.5)$$

Assuming that the solvent metal approximates to a free electron metal, the derivative occurring in (5.4) (the density of states at the Fermi level) can be replaced by its free-electron value

$$\left. \frac{\partial \rho_o(E_f)}{\partial E_f} \right|_{E_f^o} = \frac{m_e p_F^o}{\pi^2} \quad (5.6)$$

where  $p_F^o$  is the Fermi momentum of the pure solvent. Poisson's equation now reads

$$\nabla^2 V(r) = -q^2 (\Delta E_f - V(r)) + 4\pi Z \delta(r) \quad (5.7)$$

where  $q = \left[ \frac{4 m_e p_F^o e^2}{\pi} \right]^{\frac{1}{2}}$  is the Thomas-Fermi screening parameter for the solvent.

The potential  $V(r)$  (which is in fact spherically symmetrical) and the Fermi level shift are now straightforwardly obtained by integrating equation (5.7) subject to the conditions (5.3). The result is

$$V(r) = \Delta E_f - \frac{Z}{r \Delta} \left\{ q R \cosh q(R-r) - \sinh q(R-r) \right\} \quad (5.8)$$

$$\Delta E_f = \frac{Z q}{\Delta} \quad (5.9)$$

where

$$\Delta = q R \cosh q R - \sinh q R$$

From (5.5) we obtain for the extra electron density

$$\Delta \rho(r) = \frac{q^2}{4\pi} (\Delta E_f - V(r)) = \frac{q^2}{4\pi} \frac{Z}{r\Delta} \left\{ qR \cosh q(R-r) - \sinh q(R-r) \right\} \quad (5.10)$$

and it is easily verified that this gives a total of  $Z$  electrons in the impurity sphere.

Some important consequences of these results were pointed out by Friedel. The Fermi level shift  $\Delta E_f$  given by (5.8) is for finite concentrations non zero but much smaller than that predicted on the basis of what will be called the mean density model. In this model, a rigid free-electron band is simply filled with the available electrons, ignoring screening, and the Fermi level is calculated from the mean electron density.

Such a model gives a Fermi level shift

$$\Delta E_f^m = \frac{1}{2} \left[ 3\pi^2 \left( \rho_0 + \frac{Zc}{\Omega} \right) \right]^{\frac{2}{3}} - \frac{1}{2} \left[ 3\pi^2 \rho_0 \right]^{\frac{2}{3}} \xrightarrow{\text{small}} \frac{Zc \pi^2}{\Omega \rho_0^{\frac{2}{3}}} \quad (5.11)$$

which for small concentrations is linear in the concentration, whereas in the Friedel theory,  $\Delta E_f$  approaches zero much faster (indeed exponentially) in the limit of infinite dilution. That this is reasonable can be seen from the following argument for the case of an attractive impurity potential (see also the end of § 5.3). The band energy of the solvent metal will be lowered by the attractive potential, but there are also now more electrons to put into it. These effects virtually cancel out at low concentrations and no significant Fermi level shift arises until the concentration is high enough ( $qR \lesssim 10$ ) that there is no unperturbed solvent between the impurities.

Another way to see what is happening is to examine the extra electron density (c.f. equation (5.10) )

$$\Delta \rho(r) = \frac{q^2 \Delta E_f}{4\pi} - \frac{q^2 V(r)}{4\pi} \quad (5.12)$$

The first term in (5.12) is a constant density term which contributes a charge

$Q = \frac{1}{3} q^2 R^3 \Delta E_f$  towards the total of  $Z$  in each impurity sphere.  $Q$  is simply the

uniform charge necessary to raise the free electron Fermi level by  $\Delta E_f$ . The

second term, proportional to  $V(r)$ , is the screening cloud which because of the

boundary conditions vanishes at  $r = R$ . Since  $Q/Z$  is in general small (in the

calculation below for 10% LiMg,  $Q/Z = 0.07$ ), the bulk of the extra electrons are in the screening cloud. Furthermore the electron density of the screening cloud is strongly varying and well localised around the impurity ion, since the Thomas-Fermi screening length  $q^{-1}$  (roughly the range of the impurity potential) is in general less than an atomic radius.

Before going on to discuss momentum density it is necessary to comment briefly on the weaknesses of the Friedel model. The treatment of screening by linearised Thomas-Fermi theory is clearly unsatisfactory, especially close to the impurity sites (the model in fact gives an infinite electron density at  $r = 0$ ). Non-linear effects of the rapidly varying Coulomb-like potential will be important in this region. Also, as Friedel himself later demonstrated, the monotonically decaying exponential impurity potentials characteristic of linearised Thomas-Fermi theory are replaced in proper wave mechanical theories by longer range and oscillatory potentials (Friedel oscillations). The model, being essentially based on perturbation theory, is only applicable to dilute alloys in which the impurities are more or less screened independently and the wave functions of the pure solvent (i.e. plane waves in the above) are still a good basis set. As Friedel showed in his original paper, despite these criticisms his model gives a surprisingly good account of the electronic properties of a wide range of dilute alloys. We shall now proceed to show how the strongly varying electron density in the screening cloud manifests itself in the alloy momentum distribution.

### § 5.3 Momentum density in the Friedel model

Continuing in the spirit of Thomas-Fermi theory, that is, on the assumption that the electron gas is sufficiently slowly varying to be treated as locally homogeneous, we define a local Fermi momentum  $p_F(r)$  by means of the free electron relation

$$p_F(r) = \left(3\pi^2\right)^{\frac{1}{3}} \left[\rho_0 + \Delta\rho(r)\right]^{\frac{1}{3}} \quad (5.13)$$

where  $\rho_0$  is the mean density of the pure solvent and  $\Delta\rho(r)$  is given by (5.12).

The probability of electrons at radius  $r$  having momentum of magnitude between  $p$  and  $p + dp$ ,  $I(p, r)dp$ , is then given by the familiar Fermi sphere argument in terms of the unit step function  $\theta(x)$  as

$$I(p, r) = \frac{4\pi p^2}{4/3\pi \rho_F^3(r)} \theta(\rho_F(r) - p) dp \quad (5.14)$$

At radius  $r$ , the density of electrons is  $\rho_0 + \Delta\rho(r)$ , so in the spherical shell of volume  $4\pi r^2 dr$ , the number of electrons with momentum between  $p$  and  $p + dp$  is

$$I(p, r) dp \cdot 4\pi r^2 (\rho_0 + \Delta\rho(r)) dr = \frac{4p^2}{\pi} \theta(\rho_F(r) - p) r^2 dp dr \quad (5.15)$$

where (5.13) has been used. Integrating over the whole impurity sphere (which contains  $N$  electrons, say) the normalised momentum distribution for the alloy,

$I(p)$ , is given by

$$I(p) = \frac{1}{N} \int_0^R 4\pi r^2 (\rho_0 + \Delta\rho(r)) I(p, r) dr = \frac{4p^2}{\pi N} \int_0^R \theta(\rho_F(r) - p) r^2 dr \quad (5.16)$$

If  $p < \rho_F(R)$ , the integration extends over the whole sphere. If  $p > \rho_F(R)$ , only the sufficiently high density regions with  $\rho_F(r) \geq p$  contribute. We therefore define  $r(p)$  such that

$$r(p) = R \quad p \leq \rho_F(R)$$

$$r(p) \text{ is the solution of } p = \rho_F(r) \text{ if } p > \rho_F(R)$$

The curve  $r = r(p)$  is shown schematically in figure 4.1 and the range of integration for a particular  $p > \rho_F(R)$  is shown shaded.

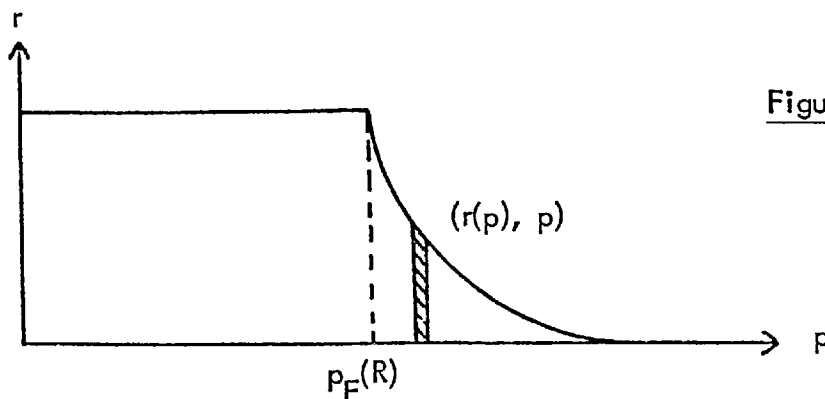


Figure 4.1



The curve can alternatively be regarded as  $p = p_F(r)$  and illustrates the increase of local Fermi momentum towards the centre of the impurity sphere.

The final result for  $I(p)$  is

$$I(p) = \frac{4p^2}{\pi N} \int_0^{r(p)} r^2 dr = \frac{4p^2}{3\pi N} r^3(p) \quad (5.17)$$

This should be compared with the result,  $I^m(p)$  expected on the basis of the mean density model. This would give

$$I^m(p) = \frac{4p^2}{3\pi N} R^3 \theta(p_F^m - p) \quad (5.18)$$

where  $p_F^m$  is given by  $\left[ 3\pi^2 \left( \rho_0 + \frac{Zc}{\Omega} \right) \right]^{\frac{1}{3}}$  (c.f. equation (5.11)).

$I(p)$  has been calculated from (5.17) for an alloy of 10% magnesium in lithium.

The parameters for this system are (in atomic units)

Atomic radius of lithium, $R_a$	$= \left( \frac{3\Omega}{4\pi} \right)^{\frac{1}{3}} = 3.26$
Thomas-Fermi screening length, $q^{-1}$	$= 1.15$
Impurity sphere radius, $R$	$= 7.02$
Lithium Fermi momentum, $p_F^0$	$= 0.5890$
Alloy 'Fermi momentum', $p_F(R)$	$= 0.5903$
Mean density Fermi momentum, $p_F^m$	$= 0.6080$

Dilute Li Mg is expected to be as good a candidate as any for the Friedel model, lithium being a fair approximation to a free electron metal and its lattice being very little distorted by even quite high concentrations of magnesium.

A plot of  $I(p)$  against  $p/p_F(R)$  is shown in figure 4.2.  $I(p)$  follows the normal free electron-like parabola, but instead of being sharply cut-off to zero at  $p_F(R)$ , there exists a high momentum tail. Shown dotted is  $I^m(p)$  calculated from (5.18). This curve does have a sharp cut-off but at the higher momentum  $p_F^m$  ( $p_F^m/p_F(R) \sim 1.03$ ). Since the area under each curve is unity, this clearly illustrates that the occupation of high momentum states necessary for localised screening is only compatible with a smaller change in the Fermi level.

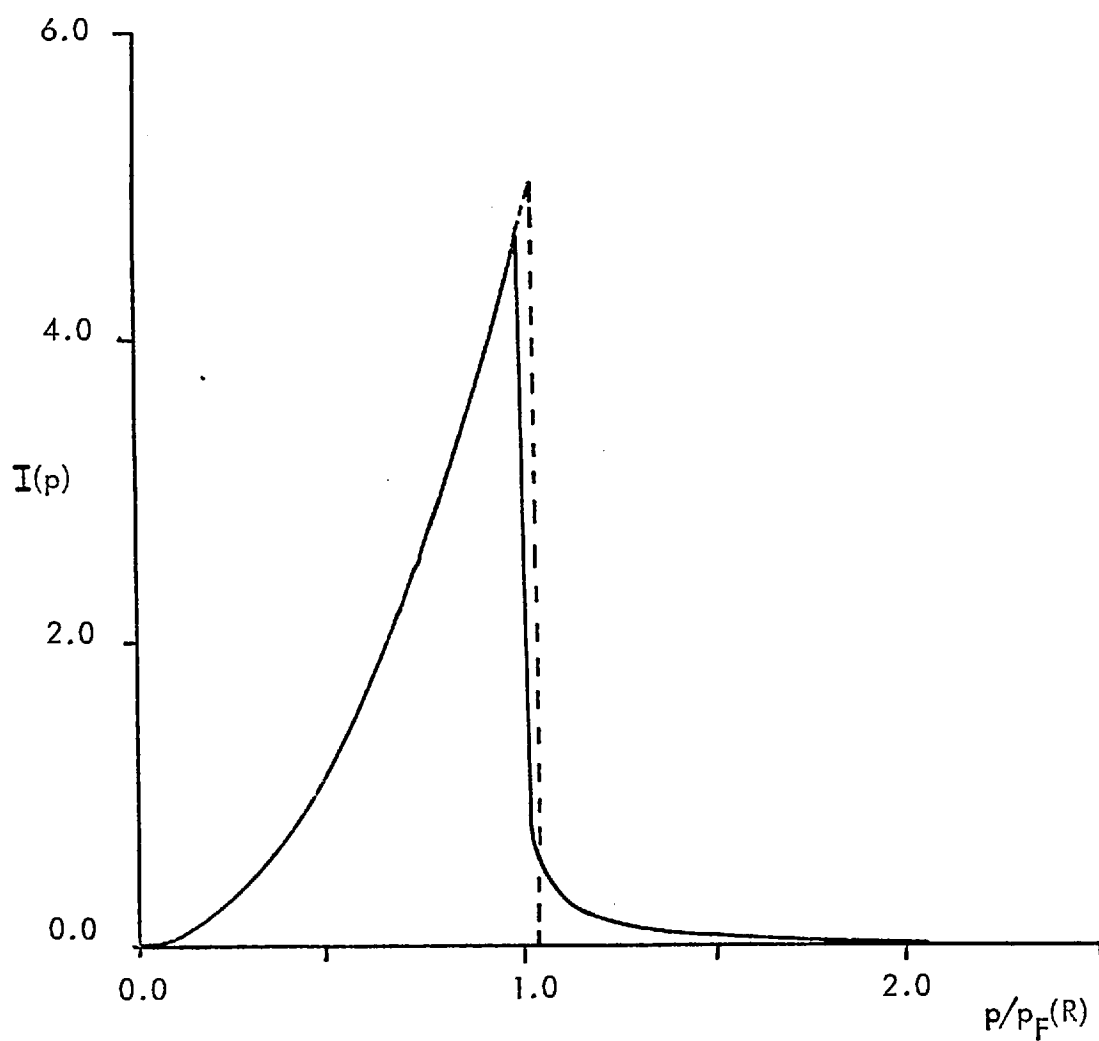


FIGURE 4.2 THE MOMENTUM DISTRIBUTION FOR 10% Li Mg.

FULL CURVE,  $I(p)$  AS GIVEN BY EQUATION (5.17).

DOTTED CURVE,  $I^m(p)$  AS GIVEN BY EQUATION (5.18).

## § 5.4 Compton profile

One possible means of observing the effect described above is by Compton scattering experiments. In such experiments the energy spectrum of monochromatic X or  $\gamma$  rays scattered through a fixed large angle ( $\sim 180^\circ$ ) by an electronic system is measured. The recoil energy of the electrons is considerably higher than typical atomic energies and this enables the general expression for the X ray scattering cross section (equation (1.29)) to be simplified by means of the 'impulse approximation' (see for instance Platzman and Tzoar<sup>(43)</sup>). The result for Compton scattering is

$$\frac{\partial^2 \sigma}{\partial \omega \partial \Omega} \propto \frac{m_e}{|k|} J(q) \quad (5.19)$$

where the Compton profile (CP)  $J(q)$  is defined in terms of the exact momentum density  $N(\underline{p})$  of the system by

$$J(q) = \int d\underline{p} N(\underline{p}) \delta(p_z - q) \quad (5.20)$$

Here the reduced variable  $q = \frac{m\omega}{|k|} - \frac{|k|}{2}$ ,  $\omega$  being the energy transfer,  $\underline{k}$  the momentum transfer (taken as the z-axis) and the  $\delta$ -function expressing conservation of energy. From (5.20) it follows that the measured CP gives direct information about cross sections perpendicular to the  $\underline{k}$  direction of the three dimensional momentum density.

For a system with spherical symmetry it is easy to show that (5.20) reduces to

$$J(q) = \frac{1}{2} \int_q^\infty d\rho \frac{I(\rho)}{\rho} \quad (5.21)$$

where  $I(\rho)$  is the probability density for an electron having momentum of magnitude  $\rho$ .

Using the expression (5.16) for  $I(\rho)$  in the Friedel model, we find

$$\begin{aligned} J(q) &= \frac{2}{\pi N} \int_0^R r^2 \int_q^\infty \rho \theta(\rho_F(r) - \rho) d\rho dr \\ &= \frac{1}{\pi N} \int_0^R r^2 (\rho_F^2(r) - q^2) \theta(\rho_F(r) - q) dr \end{aligned} \quad (5.22)$$

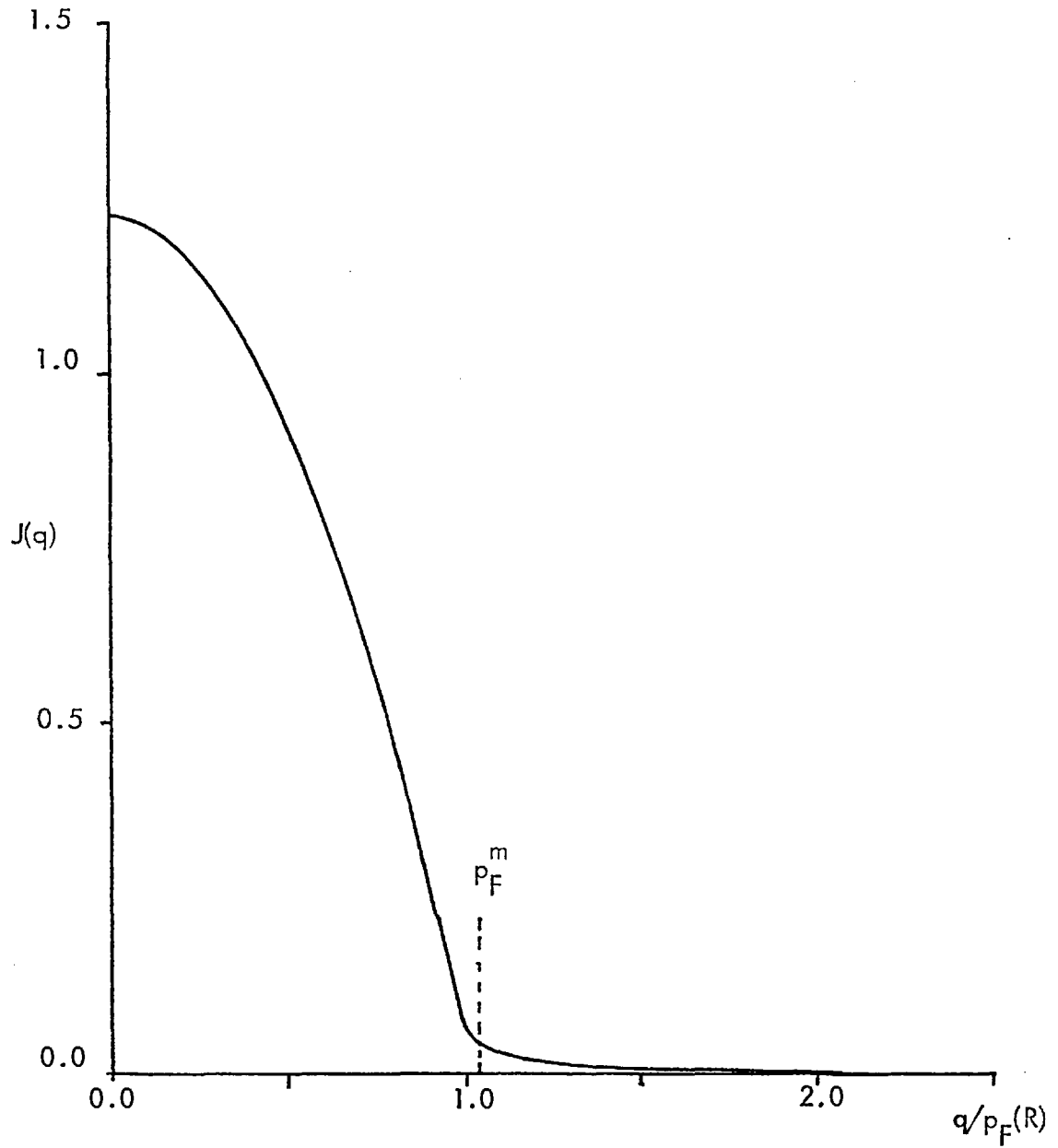


FIGURE 4.3 THE COMPTON PROFILE  $J(q)$  FOR 10% Li Mg  
AS CALCULATED FROM EQUATION (5.22).

$J(q)$  calculated for the same Li Mg alloy is shown in figure 4.3. Again the usual free-electron like inverted parabola has an additional high momentum tail above  $q = p_F(R)$ .  $J(0)$  is about 1% lower than the value expected from the mean density model which would give for the CP,

$$\overline{J}^m(q) = \frac{R^3}{3\pi N} \left( (p_F^m)^2 - q^2 \right) \theta(p_F^m - q) \quad (5.23)$$

However it should be noted that the usual experimental procedure of fitting a parabola of the form of (5.23) to the observed CP to obtain the Fermi momentum, would, if applied to figure 4.3, give a value much nearer  $p_F^m$  than  $p_F(R)$ . In order to distinguish the two models one must look for the high momentum tail and the shoulder in  $J(q)$  at  $p_F(R)$ .

### § 5.5 Difficulties in observing the high momentum components

In the example above, the effect of screening on the CP is not large and it is important to ask whether in real alloys its observation will not be masked by other contributions to the high momentum tail in the momentum distribution. Such contributions arise from:

- (a) the strongly varying electron density in the ionic cores;
- (b) inhomogeneities in the solvent metal electron density arising from the Bloch wave nature of the electronic wave functions;
- (c) electron correlations (which in the homogeneous electron gas have the effect of weakening the discontinuity in the momentum distribution at the Fermi level by shifting occupancy of states from below to above it);
- (d) the blurring of the Fermi surface in alloys due to lifetime effects. (These are difficult to estimate and will not be discussed further).

The effect of the ionic cores is usually subtracted out using calculations of their contribution to the CP from free ion wavefunctions. Eisenberger et al<sup>(44)</sup> (see also Pandey and Lam<sup>(45)</sup>) have shown that both (b) and (c), as well as core

orthogonalisation, are important in lithium and sodium metals, giving contributions to the CP tail of roughly the same magnitude as estimated above for the screening effect. Clearly the best procedure would be to watch the change in CP as magnesium is added to lithium, although it is still doubtful whether one could with any accuracy single out a contribution due to the screening of magnesium ions. The effect would be greater in more concentrated alloys and where valency difference is larger, but this has not been pursued in detail because of the limited validity of the Friedel model and its extension to the calculation of momentum density presented here.

It should be noted that positron annihilation experiments also give information about momentum density in electronic systems<sup>(46)</sup>. Stewart<sup>(47)</sup> carried out some investigations of this sort on the Li Mg system, although the lowest magnesium concentration used was 19%. Interestingly, he speculated that the lack of fit of his angular correlation curves to theoretical curves based on the mean density model may be due to just the effect of screening calculated above. However, interpretation of positron experiments is complicated by uncertain many-body corrections due to the electron-positron interaction. Also the tendency of the positron to avoid the positive ionic core regions means that any effect of the localised screening charge will be partially missed. As a result, Compton scattering experiments are probably better suited to observing this effect.

## § 5.6 Conclusion

On the basis of the Friedel model it has been shown using semi-classical arguments how impurity screening in dilute nearly-free electron alloys gives rise to high momentum tails in the momentum distribution and Compton profile of the alloy. No quantitative conclusions can be drawn with any confidence because of the simplicity of the model. However, it is likely that observation of the effect

will be difficult because of other factors which give contributions of roughly the same magnitude to the tail in the Compton profile.

It is interesting to note that Platzman and Lam<sup>(42)</sup> have recently shown that density functional theory (see Appendix C) can be extended to the calculation of the momentum density  $N(\underline{p})$  and Compton profile  $J(q)$  of inhomogeneous systems. Where the electron density  $n(r)$  is slowly varying they propose use of local density approximations of the form

$$N(\underline{p}) = \int N^0(\underline{p}, n(\underline{r})) n(\underline{r}) d\underline{r} \quad (5.24)$$

$$J(q) = \int J^0(q, n(\underline{r})) n(\underline{r}) d\underline{r} \quad (5.25)$$

where  $N^0(\underline{p}, n)$  and  $J^0(q, n)$  are respectively the exact momentum density and Compton profile of an interacting electron gas of constant density  $n$ . These expressions, used successfully by Platzman and Lam in the case of atoms, are clearly analogous to equations (5.16) and (5.22) derived above using Thomas-Fermi theory. They differ in including electron correlation effects rather than relying on free electron theory. To use (5.24) and (5.25) in the alloy problem, one would need a better approximation to the alloy electron density than for instance given by the Friedel model. In this connection it is worth mentioning the work of Ratti and Ziman<sup>(48)</sup>. These authors calculate self consistent charge densities in binary alloys by solving the non-linear Thomas-Fermi equation, but only in the interstitial regions where the density is at its most uniform. The model has the advantage of being applicable to concentrated alloys.

## CHAPTER 6

### PERIODIC POTENTIALS FOR RANDOM BINARY ALLOYS

#### § 6.1 Introduction

The theory of the electronic structure of pure crystalline metals and ordered alloys is enormously simplified by the use of Bloch's theorem which characterises the nature of electronic wave functions in the presence of a periodic potential. Very accurate methods now exist for the calculation of the one-electron band structures of such systems, progress in recent years being largely concerned with the inclusion of electron correlation effects in a self consistent manner. However it only needs one impurity or defect in the crystal to annul the translational symmetry of the potential and make Bloch's theorem strictly inapplicable. Of course single impurities can be satisfactorily treated by perturbation theory. But this is in general inappropriate to the case of concentrated disordered alloys where the crystal momentum  $\hbar\mathbf{k}$  which characterises Bloch wave functions is no longer a good quantum number. Such systems necessitate the development of alternative methods of calculating electronic properties, such as the density of states, this being an important field of current research. Progress has been made in recent years by using Green's function techniques and multiple scattering theory, the most promising methods being the coherent potential approximation (for a recent review see Yonezawa and Morigaki<sup>(49)</sup>) and the continued fraction method (see Jacobs<sup>(50)</sup>).

The purpose of this chapter is to demonstrate that in principle some of the configurationally averaged properties of random binary alloys can be obtained from a set of periodic potentials used in conjunction with existing band structure techniques.

The model of a random binary alloy that will be used is as follows. Atoms of type A and B are placed at random on the sites of a perfect lattice, it being assumed that the lattice can accommodate the two kinds of atom without distortion. The



concentration of the  $N_A$  A atoms is  $c$ , and that of the  $N - N_A$  B atoms is  $1 - c$ .

Atoms of type A and B respectively have atomic-like localised potentials  $V_A(\underline{r})$  and  $V_B(\underline{r})$  associated with them. A particular configuration of atoms is denoted by  $\underline{R}_\alpha$ , and in this configuration the alloy potential is given by

$$V_{\underline{R}_\alpha} = \sum_{i=1}^N V_B(\underline{r} - \underline{R}_i) + \sum_{j=1}^{N_A} \bar{V}(\underline{r} - \underline{R}_j) \quad (6.1)$$

where  $\bar{V}(\underline{r}) = V_A(\underline{r}) - V_B(\underline{r})$  and the second sum is only over A sites. The correct procedure now, is to use (6.1) for a general configuration in the Schrödinger equation and to calculate electronic properties from the wave functions so obtained. Only then should configuration averaging be carried out to give the measurable properties of the alloy. This procedure is in general inpracticably difficult for the reasons given above.

The earliest attempt to simplify the alloy problem by using a periodic potential was by Nordheim<sup>(51)</sup> who introduced the 'virtual crystal' approximation. This involves the replacement of (6.1) in the Schrödinger equation by its configurational average, the virtual crystal potential  $V_{vc}(\underline{r})$  given by

$$\begin{aligned} V_{vc}(\underline{r}) &= \langle V_{\underline{R}_\alpha}(\underline{r}) \rangle = \sum_{i=1}^N V_B(\underline{r} - \underline{R}_i) + c \sum_{i=1}^N \bar{V}(\underline{r} - \underline{R}_i) \\ &= \sum_{i=1}^N \left\{ c V_A(\underline{r} - \underline{R}_i) + (1 - c) V_B(\underline{r} - \underline{R}_i) \right\} \end{aligned} \quad (6.2)$$

where here and elsewhere  $\langle \rangle$  denotes configurational averaging. This is now a periodic potential as each atom irrespective of type has associated with it the average potential  $c V_A(\underline{r}) + (1 - c) V_B(\underline{r})$ .

This prescription clearly has no a priori justification whatsoever, since the configurational averaging is done in the wrong order with respect to the solving of the Schrödinger equation. As a result all effects of disorder scattering have been eliminated. Nevertheless the virtual crystal approximation has been used with some success in the prediction of a number of Fermi surface properties (such as the de Haas-

van Alphen effect) in dilute CuZn alloys by March, Gibbs, Stocks and Faulkner (MGSF, <sup>(52)</sup>).

### § 6.2 Energy dependent periodic potentials for random alloys

We now follow the argument given by MGSF as a justification for the use of energy dependent periodic potentials in the calculation of the configurationally properties of random alloys. In particular we focus on the quantity  $\langle \rho_{R\alpha}(\underline{r}, E) \rangle$  that is the configurationally averaged density of electrons with energy less than  $E$ . From this, the averaged electron density is obtained by putting  $E = E_F$ , the Fermi energy. Furthermore, the number of electrons with energy less than  $E$ ,  $N(E)$  is given by

$$N(E) = \int d\underline{r} \langle \rho_{R\alpha}(\underline{r}, E) \rangle \quad (6.3)$$

with  $N(E_F)$  being the total number of electrons,  $N_e$ . The alloy density of states,  $n(E)$  is given by

$$n(E) = \frac{\partial N(E)}{\partial E} \quad (6.4)$$

We have assumed that the alloy lattice is undistorted and so the electron density  $\langle \rho_{R\alpha}(\underline{r}, E_F) \rangle$  must have the periodicity of the background lattice. For example, in the case of dilute CuZn alloys, the background lattice will be the face-centred cubic lattice of copper, though perhaps with an expanded lattice parameter. Appealing to density functional theory (see Appendix C, proposition (6)) it now follows that there must exist a periodic potential denoted by  $V_{E_F}(\underline{r})$  which is expressible as a functional of the density  $\langle \rho_{R\alpha}(\underline{r}, E_F) \rangle$  and from which this density can be generated according to

$$\langle \rho_{R\alpha}(\underline{r}, E_F) \rangle = \sum_{i=1}^{N_e} \phi_i^{E_F*}(\underline{r}) \phi_i^{E_F}(\underline{r}) \quad (6.5)$$

i.e. by summing the squares of the lowest  $N_e$  normalised eigenfunctions (which will be Bloch-like) of the Schrödinger equation with potential  $V_{E_F}(\underline{r})$ .

Of course the potential  $V_{E_F}(\underline{r})$  will also generate a complete density of

states curve but having the van Hove singularities characteristic of the background lattice. This therefore cannot be the alloy density of states, which is expected to have a much more complicated structure. To obtain this, the following procedure is necessary. For each energy  $E$  a different periodic potential  $V_E(\underline{r})$  is required to generate the periodic density  $\langle \rho_{\underline{r}}(\underline{r}, E) \rangle$ . The periodic potential  $V_{E^*}(\underline{r})$  can thus, by means of (6.3), be used to obtain the single point on the integrated density of states curve corresponding to  $E = E^*$ . The complete  $N(E)$  is built up point by point by solving an infinite number of periodic potential problems and the alloy density of states derived by differentiating this composite curve with respect to  $E$ . Note that for given  $E$ , the potential  $V_E(\underline{r})$  only depends on  $\underline{r}$  and not on the energy eigenvalue occurring in the Schrödinger equation.

In a pure metal,  $V_E(\underline{r})$  must obviously be independent of  $E$ , as a single periodic potential is sufficient to obtain the complete density of states. However for a random alloy it is to be expected that  $V_E(\underline{r})$  strongly varies with  $E$ . In this way it is possible to see how the considerable fine structure known to exist in the density of states of alloys due to clustering<sup>(53)</sup> can be reproduced.

How to construct the periodic potentials  $V_E(\underline{r})$  is not at all clear and for this reason an alternative set of periodic potentials for alloys is discussed below. The above argument however allows the virtual crystal approximation to be viewed in a different light. MGSF suggest that the virtual crystal potential is a reasonable first approximation to the potential  $V_{E_F}(\underline{r})$ . Furthermore if the energy dependence near the Fermi level is not great this approximation should give fair agreement with some Fermi surface properties (as indeed they find for CuZn). However, the authors do point out that the variation with  $E$  of the periodic potential must be included to properly describe the copper and zinc d band resonances.

### § 6.3 $\beta$ -dependent periodic potential for random alloys

For a particular alloy configuration  $\underline{R}_\alpha$  let the electronic wave functions obtained from the Schrödinger equation with potential (6.1) be  $\psi_i(\underline{r})$  and the corresponding energies be  $E_i$ . Then instead of working with  $\rho_{\underline{R}_\alpha}(\underline{r}, E)$  as above, we now introduce the generalised partition function (diagonal element of the Bloch density matrix),  $C_{\underline{R}_\alpha}(\underline{r}, \beta)$ , defined by

$$C_{\underline{R}_\alpha}(\underline{r}, \beta) = \sum_{\text{all } i} e^{-\beta E_i} \psi_i^*(\underline{r}) \psi_i(\underline{r}) \quad (6.6)$$

where  $\beta = (kT)^{-1}$ . It is easily shown (see March, Young and Sampanthar, (29) p 14) that in general  $\rho(\underline{r}, E)$  is the inverse Laplace transform with respect to  $\beta$  of  $C(\underline{r}, \beta) / \beta$ . Furthermore  $C(\underline{r}, \beta)$  can be obtained explicitly to all orders in perturbation theory in terms of a one-body potential  $V(\underline{r})$  (March and Murray (58)) and this expansion can, in principle, be inverted to give

$$V(\underline{r}) = g[C(\underline{r}, \beta)] \quad (6.7)$$

where  $g$  is a universal functional. Since  $V(\underline{r})$  is independent of  $\beta$ , we note that for all  $\beta_1, \beta_2$

$$g[C(\underline{r}, \beta_1)] = g[C(\underline{r}, \beta_2)] \quad (6.8)$$

For a particular alloy configuration we therefore have

$$V_{\underline{R}_\alpha}(\underline{r}) = g[C_{\underline{R}_\alpha}(\underline{r}, \beta)] \quad (6.9)$$

We now suppose, in the spirit of MGSF, that for a given  $\beta$ , there exists a periodic potential  $V_\beta(\underline{r})$  which yields from the Schrödinger equation Bloch wave functions  $\phi_{\underline{k}}^\beta(\underline{r})$  with energy  $\epsilon_{\underline{k}}^\beta$  from which we construct

$$C_\beta(\underline{r}, \beta) = \sum_{\text{all } \underline{k}} \exp(-\beta \epsilon_{\underline{k}}^\beta) \phi_{\underline{k}}^{\beta*}(\underline{r}) \phi_{\underline{k}}^\beta(\underline{r}) \quad (6.10)$$

Then defining

$$C_\beta(\underline{r}, \beta) \doteq \langle C_{\underline{R}_\alpha}(\underline{r}, \beta) \rangle \quad (6.11)$$

and noting from (6.7) that

$$V_{\beta}(\underline{r}) = g [ C_{\beta}(\underline{r}, \beta) ] \quad (6.12)$$

it follows from (6.8) and (6.11) that

$$V_{\beta}(\underline{r}) = g [ \langle C_{\underline{R}\alpha}(\underline{r}, \beta) \rangle ] \quad (6.13)$$

It is interesting to compare this result with the virtual crystal potential which from (6.2) and (6.9) can be written in the form

$$V_{vc}(\underline{r}) = \langle V_{\underline{R}\alpha}(\underline{r}) \rangle = \langle g [ C_{\underline{R}\alpha}(\underline{r}, \beta) ] \rangle \quad (6.14)$$

The difference between (6.13) and (6.14) is, as might be expected, the ordering of the configurational averaging, and in (6.13) this introduces a  $\beta$ -dependence into the potential not present in (6.14).

To recapitulate this argument, (6.13) gives a formal expression for an infinite set of periodic potentials, one for each value of  $\beta$ . For a particular  $\beta^*$ , the periodic potential  $V_{\beta^*}(\underline{r})$  will generate via (6.10) and (6.11) just the one value of  $\langle C_{\underline{R}\alpha}(\underline{r}, \beta) \rangle$  corresponding to  $\beta = \beta^*$ . The complete  $\langle C_{\underline{R}\alpha}(\underline{r}, \beta) \rangle$  is therefore built up by solving an infinite number of periodic potential problems in an analogous way to the obtaining of  $N(E)$  from the energy-dependent potentials in §6.2. Since the taking of Laplace transforms commutes with configurational averaging, one can in principle then obtain  $\langle \rho_{\underline{R}\alpha}(\underline{r}, E) \rangle$  and hence the density of states.

#### §6.4 Two approximate forms for the $\beta$ -dependent potentials

The objective of the approach described in the preceding section is to find periodic potentials  $V_{\beta}(\underline{r})$  in the form

$$V_{\beta}(\underline{r}) = F [ V_A(\underline{r}), V_B(\underline{r}), \beta, c ] \quad (6.15)$$

This can be done in two approximate cases where the functional  $g$  (see (6.7)) is known.

a) Slowly varying alloy potential

If the alloy potential is slowly varying we can suppose it simply has the effect of locally shifting the electron energy levels and hence the generalised partition function is approximately of the form

$$C_{R_\alpha}(\underline{r}, \beta) = C_1(\underline{r}, \beta) e^{-\beta \sum_{i=1}^{N_\alpha} \bar{V}(\underline{r} - \underline{R}_i)} \quad (6.16)$$

where  $C_1(\underline{r}, \beta)$  is calculated from the periodic potential  $\sum_{i=1}^N V_B(\underline{r} - \underline{R}_i)$  and is therefore independent of configuration. From (6.16) it follows that

$$\begin{aligned} V_{R_\alpha}(\underline{r}) &= \sum_{i=1}^N V_B(\underline{r} - \underline{R}_i) - \frac{1}{\beta} \ln \frac{C_{R_\alpha}(\underline{r}, \beta)}{C_1(\underline{r}, \beta)} \\ &\equiv g[C_{R_\alpha}(\underline{r}, \beta)] \end{aligned} \quad (6.17)$$

From (6.13)

$$\begin{aligned} V_\beta(\underline{r}) &= g[\langle C_{R_\alpha}(\underline{r}, \beta) \rangle] \\ &= \sum_{i=1}^N V_B(\underline{r} - \underline{R}_i) - \frac{1}{\beta} \ln \left\langle e^{-\beta \sum_{i=1}^{N_\alpha} \bar{V}(\underline{r} - \underline{R}_i)} \right\rangle \end{aligned} \quad (6.18)$$

To evaluate the average in (6.18) we introduce

$$f_i = e^{-\beta \bar{V}(\underline{r} - \underline{R}_i)} - 1 \quad (6.19)$$

Then

$$\begin{aligned} \left\langle e^{-\beta \sum_{i=1}^{N_\alpha} \bar{V}(\underline{r} - \underline{R}_i)} \right\rangle &= \left\langle \prod_{i=1}^{N_\alpha} (1 + f_i) \right\rangle \\ &= \left\langle 1 + \sum_{i=1}^{N_\alpha} f_i + \frac{1}{2!} \sum_{i \neq j}^{N_\alpha} \sum_{i \neq j}^{N_\alpha} f_i f_j \right. \\ &\quad \left. + \frac{1}{3!} \sum_{i \neq j \neq k}^{N_\alpha} \sum_{i \neq j \neq k}^{N_\alpha} f_i f_j f_k + \dots \right\rangle \end{aligned} \quad (6.20)$$

Because the summations in (6.20) are over clusters in which all sites are distinct, averaging simply implies the substitution  $\sum_{i=1}^{N_\alpha} \rightarrow c \sum_{i=1}^N$  and so we find

$$\left\langle \prod_{i=1}^{N_\alpha} (1 + f_i) \right\rangle = \prod_{i=1}^N (1 + c f_i) \quad (6.21)$$

Substituting in (6.18), the final result for the  $\beta$ -dependent periodic potentials in the form (6.15) is

$$V_{\beta}(\underline{r}) = \sum_{i=1}^N \left\{ V_{\beta}(\underline{r}-\underline{R}_i) - \frac{1}{\beta} \ln \left[ 1 + c \left( \frac{e^{-\beta V(\underline{r}-\underline{R}_i)}}{-1} \right) \right] \right\} \quad (6.22)$$

b) Effective potential approximation

Hilton, March and Curtis<sup>(54)</sup> have found it useful to express the generalised partition function in terms of an effective potential  $U(\underline{r}, \beta)$  defined by

$$C(\underline{r}, \beta) = C_0(\beta) e^{-\beta U(\underline{r}, \beta)} \quad (6.23)$$

where  $C_0(\beta)$  is the partition function per unit volume for free electrons  $\left(\frac{1}{2\pi\beta}\right)^{\frac{3}{2}}$ .

These authors show that if any one of the conditions (i)  $U$  small, (ii)  $\nabla U$  small,

(iii)  $\beta$  small, is satisfied then

$$U(\underline{r}, \beta) = \int V_{R_{\alpha}}(\underline{r}_1) G(\underline{r}-\underline{r}_1, \beta) d\underline{r}_1 \quad (6.24)$$

where

$$G(\underline{r}-\underline{r}_1, \beta) = \frac{1}{\pi\beta} \frac{e^{-\frac{\beta}{2}|\underline{r}-\underline{r}_1|^2}}{|\underline{r}-\underline{r}_1|} \quad (6.25)$$

(6.24) can be inverted by convolution to give

$$V_{R_{\alpha}}(\underline{r}) = \int U(\underline{r}_1, \beta) J(\underline{r}-\underline{r}_1, \beta) d\underline{r}_1 \quad (6.26)$$

where

$$J(\underline{r}, \beta) = \int e^{-i\underline{q} \cdot \underline{r}} \frac{1}{G(\underline{q}, \beta)} \frac{d\underline{q}}{(2\pi)^3} \quad (6.27)$$

Here  $G(\underline{q}, \beta)$  is the Fourier transform of (6.25). From (6.26) and (6.23) we now have

$$V_{R_{\alpha}}(\underline{r}) = -\frac{1}{\beta} \int \ln \left[ \frac{C_{R_{\alpha}}(\underline{r}, \beta)}{C_0(\underline{r}, \beta)} \right] J(\underline{r}-\underline{r}_1, \beta) d\underline{r}_1 \quad (6.28)$$

and from (6.13)

$$V_{\beta}(\underline{r}) = -\frac{1}{\beta} \int \ln \left[ \langle e^{-\beta U(\underline{r}, \beta)} \rangle \right] J(\underline{r}-\underline{r}_1, \beta) d\underline{r}_1 \quad (6.29)$$

Now

$$\langle e^{-\beta U(\underline{r}, \beta)} \rangle = e^{-\beta \sum_{i=1}^N U_B(\underline{R}_i, \underline{r}, \beta)} \langle e^{-\beta \sum_{i=1}^{N_A} \bar{U}(\underline{R}_i, \underline{r}, \beta)} \rangle \quad (6.30)$$

where

$$U_B(\underline{R}_i, \underline{r}, \beta) = \int V_B(\underline{r} - \underline{R}_i) G(\underline{r} - \underline{r}_1, \beta) d\underline{r}_1 \quad (6.31)$$

and  $\bar{U} = U_A - U_B$ . Applying the same averaging method to (6.30) as used above,

we finally find that

$$V_\beta(\underline{r}) = \sum_{i=1}^N \left\{ V_B(\underline{r} - \underline{R}_i) - \frac{1}{\beta} \int \ln \left[ 1 + c \left( e^{-\beta \bar{U}(\underline{R}_i, \underline{r}, \beta)} - 1 \right) \right] J(\underline{r} - \underline{r}_1, \beta) d\underline{r}_1 \right\} \quad (6.32)$$

Both the results (6.22) and (6.32) have two important properties. Firstly,

as must be the case for a theory of concentrated alloys, they are correctly

invariant under the interchange of components A and B i.e. under the transformation

$c \rightarrow 1-c$ ,  $V_B \rightarrow V_A$ ,  $\bar{V} \rightarrow -\bar{V}$ . For instance, under this transformation (6.32)

becomes

$$V_\beta(\underline{r}) = \sum_{i=1}^N \left\{ V_A(\underline{r} - \underline{R}_i) - \frac{1}{\beta} \int \ln \left[ c + (1-c) e^{\beta U(\underline{R}_i, \underline{r}, \beta)} \right] J(\underline{r} - \underline{r}_1, \beta) d\underline{r}_1 \right\} \quad (6.33)$$

By making use of the identity

$$\ln(1 - c + ce^{-x}) + x = \ln(c + (1-c)e^x) \quad (6.34)$$

and also the inverse of (6.31) it is easily seen that (6.32) and (6.33) are identical.

Secondly, both (6.22) and (6.32) reduce to the virtual crystal potential

(6.2) in the limit of small  $\beta$  and as  $V_A \rightarrow V_B$  (that is, small  $\bar{V}$  and  $\bar{U}$ ). All

$\beta$ -dependence is then lost. This can be verified for (6.32) by observing that

$$V_{VC}(\underline{r}) = \sum_{i=1}^N \left\{ V_B(\underline{r} - \underline{R}_i) + c \int \bar{U}(\underline{R}_i, \underline{r}, \beta) J(\underline{r} - \underline{r}_1, \beta) d\underline{r}_1 \right\} \quad (6.35)$$

It is interesting to note that MGSF showed quite generally that the coherent

potential approximation (CPA) also reduces to the virtual crystal approximation

in the limit of small differences between  $V_A$  and  $V_B$ . However, neither the CPA

nor the  $\beta$ -dependent potentials discussed here agree with the virtual crystal

approximation as  $c \rightarrow 0$  for general  $V_A$  and  $V_B$ .



## § 6.5 Conclusions

In this chapter an argument has been presented which justifies the use of a set of E-dependent or  $\beta$ -dependent periodic potentials in the calculation of  $\langle \rho_{\underline{R}\alpha}(\underline{r}, E) \rangle$  or  $\langle C_{\underline{R}\alpha}(\underline{r}, \beta) \rangle$  for random binary alloys. The argument throws new light on the virtual crystal approximation which, considered on its own is theoretically unsound, but in the present context can be seen as a limiting form of the E- or  $\beta$ -dependent potentials.

The achievement of the approach developed here is to allow the well-known techniques of solving the periodic potential problem to be used in the case of random alloys. However this gain is balanced by the need to solve a large number of periodic potential problems in order to obtain a complete picture of the electronic structure of the alloy. This is particularly true of the  $\beta$ -dependent potentials, as in this case, if one is really interested in calculating  $\langle \rho_{\underline{R}\alpha}(\underline{r}, E) \rangle$  and the density of states,  $\langle C_{\underline{R}\alpha}(\underline{r}, \beta) \rangle$  is needed for a wide range of  $\beta$  values in order to be able to take the inverse Laplace transform satisfactorily. For this reason it is doubtful whether the  $\beta$ -dependent periodic potentials are of much practical value.

Unfortunately little progress has been made in the construction of the more directly useful E-dependent potentials. However it is to be hoped that except over certain ranges of energy, the variation with energy of the potential is small enough to allow useful information to be obtained from a limited number of calculations.

## CHAPTER 7

CORRELATED BOND PERCOLATION ON THE BETHE LATTICE§ 7.1 Introduction to percolation theory

The theory of percolation processes in random media is an intriguing branch of probability theory which has found application in a wide range of physical problems. For general reviews, see Frisch and Hammersley<sup>(70)</sup>, Shante and Kirkpatrick<sup>(71)</sup> and Essam<sup>(72)</sup>.

A typical percolation problem is as follows. The sites of an infinite perfect lattice are occupied at random with probability  $p$  and a cluster is defined as a group of neighbouring occupied sites surrounded by vacancies. How does the mean size of clusters (irrespective of shape) vary with  $p$  and what is the percolation probability  $P(p)$  that a particular site is part of a cluster of infinite size? This is the so called site percolation problem, but alternatively one could focus attention on the nearest neighbour bonds of the lattice and take  $p$  as the probability that a given bond is present (bond percolation problem).

These percolation problems are tantalisingly simple to formulate but as yet no analytic solution for a general  $d$ -dimensional lattice exists, although certain percolation properties of particular lattices are known exactly. However the general features of the solution have been elucidated. If one begins with an empty lattice and then occupies sites (or bonds) at random, thus steadily increasing the fraction  $p$  of sites occupied, the mean size of clusters clearly increases with  $p$  as existing clusters grow in size and coalesce. At  $p = 1$  the mean cluster size is obviously infinite, but it turns out that for infinite lattices there is a well defined critical percolation probability  $p_c$  at which the mean size of clusters first diverges.

$p_c$  is best defined in terms of the percolation probability  $P(p)$  as

$$p_c = \sup \{ p : P(p) = 0 \} \quad (7.1)$$

This says that for  $p < p_c$  all occupied sites are with certainty contained in finite clusters and hence  $P(p)$  is identically zero. Above  $p_c$  there exist infinite clusters (Kikuchi<sup>(73)</sup> has argued that in fact there can only be one such cluster) and  $P(p)$  increases from zero at  $p = p_c$  to one at  $p = 1$  (which it approaches asymptotically as  $P(p) \sim p$ ) as the infinite clusters extend over the whole lattice.

In general the bond ( $b$ ) and site ( $s$ ) problems for a given lattice result in different percolation properties (for instance  $p_c^s \geq p_c^b$ ), although the Bethe lattice (see below) is an exception. Results for the common 3-d lattices have to be obtained by Monte Carlo methods<sup>(74), (75)</sup> or series expansions<sup>(76)</sup> and numerical estimates of  $p_c$  for these lattices are given in Table 7.1 (where  $z$  is the co-ordination number of the lattice).

lattice	$p_c^s$	$p_c^b$	$z$	$z p_c^b$
diamond	0.425	0.388	4	1.55
s.c.	0.307	0.247	6	1.48
b.c.c.	0.243	0.178	8	1.42
f.c.c.	0.195	0.119	12	1.43
h.c.p.	0.204	0.124	12	1.49

Table 7.1 Numerical estimates of the critical percolation probability for some 3-d lattices

One lattice for which analytic results are available is the Bethe lattice (infinite Cayley tree). A Bethe lattice of co-ordination number  $z = \sigma + 1$  is a branching structure in which  $z$  bonds leave each site but one and only one path links any two sites (see figure 7.1). The Bethe lattice is infinitely dimensional in the sense that it cannot be embedded in any finite dimensional space while maintaining the same topology. However it is the simplicity of

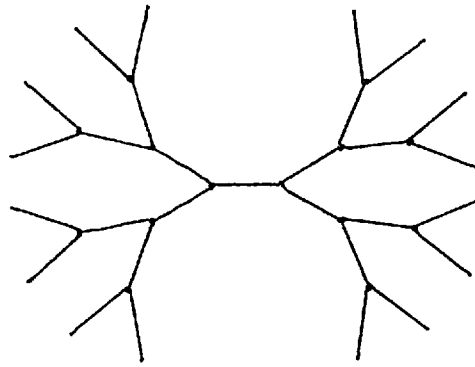


Figure 7.1 Part of a Bethe lattice of co-ordination number 3.

its topology that makes it susceptible to exact analysis (Fisher and Essam<sup>(77)</sup>). It can be shown rigorously that for a Bethe lattice of co-ordination number  $\sigma + 1$ ,

$$p_c^b = p_c^s = \frac{1}{\sigma} \quad (7.2)$$

Intuitively, (7.2) is simply saying (in the bond case) that an infinite cluster can be built up provided an occupied bond has on average at least one of the  $\sigma$  independent bonds leaving a particular end also occupied. Figure 7.2 shows the percolation probability  $P(p)$ , the probability of a site belonging to a finite cluster  $F(p)$  and the mean size of (finite) clusters  $S(p)$ , for a Bethe lattice with  $z = 4$ , although curves for other lattices are similar in form.

One reason for studying the percolation problem is because of the interesting critical behaviour around  $p_c$ . Critical exponents have been introduced for the percolation probability  $P(p)$  and mean cluster size  $S(p)$ , of the form

$$\begin{aligned} P(p) &\propto (p - p_c)^k & p \rightarrow p_c^+ \\ S(p) &\propto (p_c - p)^{-(i+1)} & p \rightarrow p_c^- \end{aligned} \quad (7.3)$$

where  $k = 1$ ,  $i = 0$  for the Bethe lattice and for 3-d lattices  $0.3 \leq k \leq 0.4$  (Kirkpatrick<sup>(75)</sup>). Recently, various authors have begun to apply modern ideas about critical phenomena to the percolation problem, for instance scaling

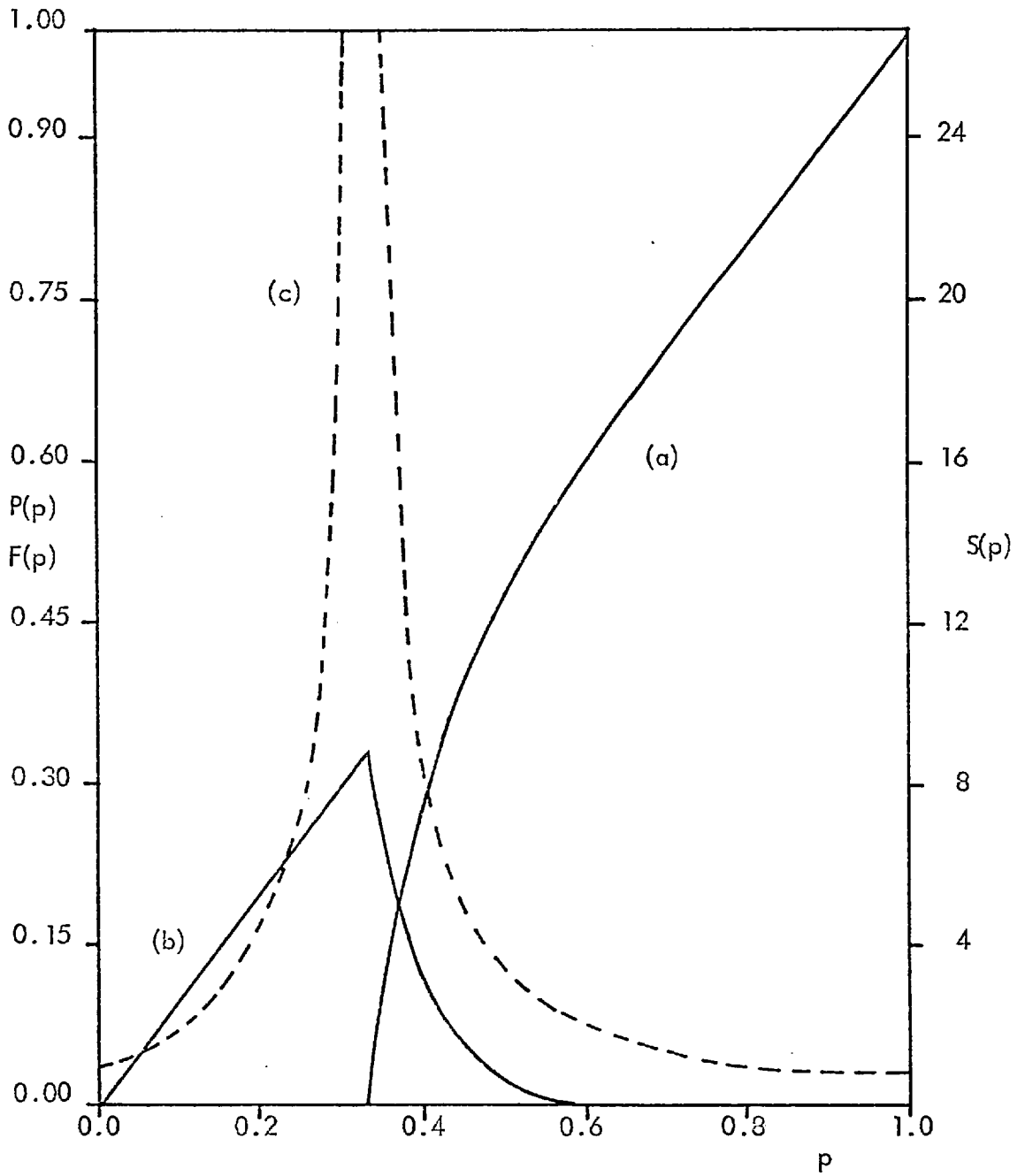


FIGURE 7.2 PERCOLATION PROPERTIES OF A BETHE LATTICE

OF CO-ORDINATION NUMBER 4

(a) PERCOLATION PROBABILITY,  $P(p)$

(b) PROBABILITY OF A SITE BELONGING TO A FINITE CLUSTER,  $F(p)$

(c) MEAN SIZE OF FINITE CLUSTERS,  $S(p)$

Diagram taken from reference (71).

hypotheses<sup>(78)</sup> and the renormalisation group<sup>(79)</sup>.

As a physical example of the site percolation problem, consider an alloy in which the concentration of magnetic impurities (assumed distributed at random) is  $p$  (Essam<sup>(72)</sup>, p149). If the magnetic interaction is short range, isolated clusters of impurities spins will behave independently and so there can be no ferromagnetic ordering at any temperature while there are only finite sized clusters i.e. for  $p < p_c^s$ .  $p_c^s$  is thus a lower bound for the occurrence of spontaneous magnetisation. If a nearest neighbour Ising interaction is assumed, the spontaneous magnetisation at zero temperature is proportional to  $P^s(p)$ .

A resistor on a lattice in which a fraction  $(1-p)$  of the resistors (bonds) is removed at random is an illustration of the bond percolation problem. Clearly if  $p < p_c^b$  there can be no conducting paths extending right through the network and the ensemble averaged conductivity  $\langle \sigma(p) \rangle$  of such a system is zero. For  $p > p_c^b$ ,  $\langle \sigma(p) \rangle$  is non zero but as first pointed out by Last and Thouless<sup>(80)</sup> and confirmed by Kirkpatrick<sup>(81)</sup> and Stinchcombe<sup>(82)</sup>, it increases more slowly than the percolation probability with a power law behaviour in the critical region of the form

$$\langle \sigma(p) \rangle \propto (p - p_c^b)^t \quad (7.4)$$

with  $t \sim 1.6$  for 3-d lattices and  $t = 2$  for the Bethe lattice. The reason for this is that although there is an infinite conducting path through the network for  $p > p_c^b$ , the resistance of such a path remains very high until a substantial number of parallel conducting paths exist. For recent work on resistor networks see (83), (84). The derivation of the name percolation theory becomes apparent if one identifies the bonds in the bond problem with open or blocked water pipes or channels in a porous rock. Only if  $p > p_c^b$  can water percolate through such a system.

The percolation problem can be generalised in a number of interesting ways. Odagaki et al<sup>(85)</sup> and Coniglio<sup>(86)</sup> have recently considered the temperature dependent percolation problem, that is when sites of a lattice are occupied not at random, but in accordance with the statistical mechanical distributions characteristic of lattice gas or Ising systems. Ziman<sup>(87)</sup> constructed a semi classical bond percolation model of electronic conduction in disordered systems by assuming that the ability of an electron to percolate from one atomic cell to another depended on the height of the intercell potential barriers, which in a disordered system would be random quantities. Ziman suggested that the empirical relation

$$z p_c^b \sim \frac{d}{(d-1)} \quad (7.5)$$

( $d$  is the lattice dimension and  $z$  its co-ordination number) which holds quite well for 2 and 3 dimensional perfect lattices (see table 7.1) could be extended to irregular structures where only a mean co-ordination is defined. Scher and Zallen<sup>(88)</sup> went further and extended percolation ideas to continuous media by considering the motion of a classical particle of energy  $E$  in a random continuous potential. They estimated that the volume fraction of classically accessible space (i.e. with potential less than  $E$ ) had to exceed a critical fraction  $v_c \sim 0.15$  (3 dimensions) before the particle could percolate throughout the system. This critical volume fraction is also relevant to the problem of when a random inhomogeneous mixture of conducting and insulating material will actually conduct electricity<sup>(89)</sup>. The sharp metal-insulator transition observed at low temperatures by Cusack et al<sup>(90)</sup> in metal-rare gas mixtures has been interpreted on this basis but so far there is no conclusive evidence that these systems are in fact inhomogeneous. An alternative explanation in terms of the Mott transition has been proposed by Berggren and Lindell<sup>(91)</sup>. Clearly the validity of the classical percolation theory of conduction is in doubt when the conducting regions are small

compared to the electronic mean free path. In this case quantum mechanical tunnelling through classically forbidden regions must be considered. Indeed electronic conduction in systems in which the disorder is on an atomic scale as in alloys, amorphous semiconductors, liquids and supercritical fluid metals is perhaps more usefully discussed in terms of a division of the electronic states in a band into localised and non-localised states separated by a mobility edge<sup>(92),(93)</sup>, than in percolation terms.

A final example of the application of percolation theory is to the problem of thermally-activated hopping conduction in doped semiconductors. Miller and Abrahams<sup>(94)</sup> and Ambegaokar et al<sup>(95)</sup> (see also Suprato and Butcher<sup>(96)</sup>) have shown that provided the localised impurity states are far enough apart, phonon assisted transitions between two states at sites  $\underline{R}_i, \underline{R}_j$  and with energies  $E_i, E_j$ , can be described by an impedance  $Z_{ij}$  where

$$Z_{ij} \propto e^{-\beta/2 [ |E_i| + |E_j| + |E_i - E_j| ] - 2\alpha | \underline{R}_i - \underline{R}_j |} \quad (7.6)$$

The problem is thus reduced to finding the conductivity of a random network with impedances  $Z_{ij}$  and several methods have been suggested for doing this ( (95), (97) ). The results appear to confirm Mott's original suggestion<sup>(98)</sup> that the conductivity in these systems at low temperatures should obey the relation  $\ln \sigma \propto T^{-1/4}$ .

For the purpose of the work to be described below the interest in the model just outlined lies in the fact that Kirkpatrick<sup>(81)</sup> abstracted from it the so called correlated bond percolation problem, which as its name suggests, introduces a degree of correlation between bonds that is not present in the random bond percolation model.



## §7.2 The correlated bond percolation problem

The problem to be discussed in the remainder of this chapter is as follows. Each site  $i$  of a lattice is associated with a random variable  $E_i$  which is uniformly distributed on  $[-1, 1]$ . A bond joins neighbouring sites  $i$  and  $j$  provided

$$E_{ij} = \frac{1}{4} (|E_i| + |E_j| + |E_i - E_j|) \leq E \quad (7.7)$$

where  $0 \leq E \leq 1$ . What is the percolation probability  $P(E)$  that a given site is part of an infinite chain of sites linked by bonds, and is there a well defined critical value of  $E$ ,  $E_c$ , such that percolation can occur only for  $E > E_c$ ?

To help understand the problem, figure 7.3 shows the values of  $E_i, E_j$  which imply a bond between neighbouring sites  $i$  and  $j$ .

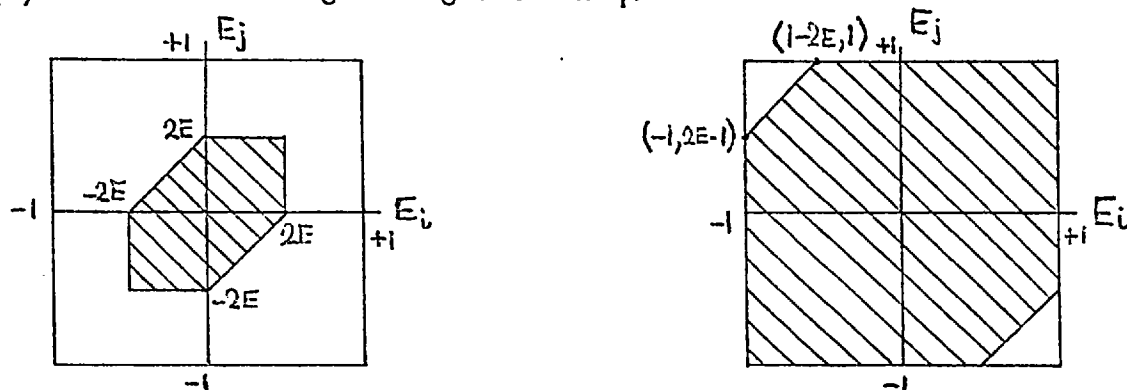


Figure 7.3 Neighbouring sites  $i$  and  $j$  have a bond joining them provided  $(E_i, E_j)$  is in the shaded region. Left,  $E < \frac{1}{2}$ ; right  $E > \frac{1}{2}$ .

From figure (7.3) it is clear that only sites with  $|E_i| \leq \min(2E, 1)$  can have bonds from them. Also, the probability  $p(E)$  that two neighbouring sites are joined by a bond irrespective of any other connections is equal to the shaded area divided by the total area of the square of allowed values of  $E_i, E_j$ , that is

$$p(E) = \begin{cases} 3E^2 & 0 \leq E \leq \frac{1}{2} \\ E(2-E) & \frac{1}{2} \leq E \leq 1 \end{cases} \quad (7.8)$$

If there were no correlations between bonds one would simply have a random bond percolation problem with  $E_c$  given by

$$p(E_c) = p_c^b \quad (7.9)$$

where  $p_c^b$  is the critical percolation probability for the bond problem on the lattice concerned.

However correlations of a form which tend to cluster bonds together do exist. If a site  $i$  has a bond entering it, then  $|E_i| \leq \min(2E, 1)$ . Therefore the conditional probability  $p'(E)$ , that given  $i$  has one bond entering it, it also has a bond leaving it to a second neighbouring site, is given by

$$p'(E) = \begin{cases} \frac{3}{2}E & 0 \leq E \leq \frac{1}{2} \\ E(2-E) & \frac{1}{2} \leq E \leq 1 \end{cases} \quad (7.10)$$

Thus if  $E \leq \frac{1}{2}$ , a site with one bond entering it is actually more likely to have another bond leaving it than if the occupation of bonds is assumed independent. Clustering of bonds and the likelihood of percolation is therefore enhanced in the correlated bond problem.

In order to obtain analytic results we now specialise to the case of correlated bond percolation on the Bethe lattice of co-ordination number  $\sigma + 1$ . As mentioned in § 7.1, the condition for percolation to occur on a Bethe lattice is that a site which has a bond entering it must have open on average at least one of the  $\sigma$  other bonds leaving it. When correlations are important, one must be careful to use a conditional probability here, of the form (7.10). Thus we arrive at the following estimate for the percolation threshold,

$$\begin{aligned} \sigma p'(E_c) &= 1 \\ E_c &= \frac{2}{3\sigma} \quad (\sigma > 1) \end{aligned} \quad (7.11)$$

It will be seen below that even when correlations are exactly taken into account,  $E_c$  turns out to be only slightly less than this estimate. Note that a Bethe lattice with  $\sigma = 1$  corresponds to a linear chain. As there is no possibility of bypassing an absent bond, percolation cannot occur on a linear chain unless  $E = 1$ .

### § 7.3 Percolation probability for the correlated bond model on the Bethe lattice

Using a method analogous to that devised by Essam<sup>(72)</sup> to discuss random bond percolation, we now show how to obtain the percolation probability  $P(E)$  for the correlated bond model on the Bethe lattice.

Suppose the central site has associated parameter  $E_0$ . Since the  $\sigma + 1$  branches leaving this site are independent of each other if  $E_0$  is fixed, we may write

$$P(E) = 1 - \frac{1}{2} \int_{-1}^1 Q_E^{\sigma+1}(E_0) dE_0 \quad (7.12)$$

Here,  $Q_E(E_0)$  is the probability that no infinite chain leaves a site with parameter  $E_0$  along a particular branch. The  $\frac{1}{2}$  arises from the uniform probability distribution of  $E_0$  on  $[-1, 1]$ .

Let  $p_E(E_i, E_j) = 1 - q_E(E_i, E_j)$  be the probability that a bond connects neighbouring sites with parameters  $E_i, E_j$ . From (7.7),

$$p_E(E_i, E_j) = \theta(E - E_{ij}) \quad (7.13)$$

It now follows that  $Q_E(E_0)$  satisfies the following non-linear integral equation,

$$Q_E(E_0) = \frac{1}{2} \int_{-1}^1 q_E(E_0, E_i) dE_i + \frac{1}{2} \int_{-1}^1 p_E(E_0, E_i) Q_E^{\sigma}(E_i) dE_i \quad (7.14)$$

In (7.14) the first term is the probability that the bond in a given direction leaving  $E_0$  is absent. The second term is the probability that this bond is

present but that the  $\sigma$  remaining branches leaving  $E_i$  are all dead ends. With

the help of figure 7.3 and noting that  $Q_E(E_0)$  is even in  $E_0$ , (7.14) may be written

$$Q_E(E_0) = \begin{cases} 1 - 2E + \frac{1}{2}E_0 + \int_0^{2E} Q_E^{\sigma}(E_i) dE_i - \frac{1}{2} \int_{2E-E_0}^{2E} Q_E^{\sigma}(E_i) dE_i & 0 \leq E_0 \leq 2E \\ 1 & 2E < E_0 \leq 1 \end{cases} \quad (7.15a)$$

$$Q_E(E_0) = \begin{cases} \int_0^1 Q_E^\sigma(E_i) dE_i & 0 \leq E_0 \leq 2E-1 \\ \frac{1-2E+E_0}{2} + \int_0^1 Q_E^\sigma(E_i) dE_i - \frac{1}{2} \int_{2E-E_0}^1 Q_E^\sigma(E_i) dE_i & E_0 > 2E-1 \end{cases} \quad (7.15b)$$

From the discussion above (c.f. equation (7.11)) we expect  $E_c < \frac{1}{2}$  (for  $\sigma > 1$ ) and so we now focus attention on (7.15a). It is easily seen that  $Q_E(E_0) = 1$  is always a solution of (7.15a). However, we expect that there exists an  $E_c$  such that for  $E > E_c$  there is another solution with  $Q_E(E_0) < 1$  (provided  $|E_0| \leq 2E$ ) indicating that percolation can take place with a non-zero probability.  $E_c$  is thus a bifurcation point of the integral equation<sup>(99)</sup>.

Let  $\chi_E(\alpha) = 1 - Q_E(E_0/2E)$ , then for  $\alpha \leq 1$  (7.15a) becomes

$$\chi_E(\alpha) = 2E \int_0^1 [1 - (1 - \chi_E(t))^\sigma] dt - E \int_{1-\alpha}^1 [1 - (1 - \chi_E(t))^\sigma] dt \quad (7.16)$$

(7.16) is of the form of an eigenvalue equation with eigenvalue  $E$  and has the properties

- (i)  $\chi_E(\alpha) = 0$  is a solution of (7.16),
- (ii) Any non-zero solution of (7.16) is a monotonic decreasing function of  $\alpha$ , since  $\frac{d\chi_E(\alpha)}{d\alpha} = -E [1 - (1 - \chi_E(1-\alpha))^\sigma] \leq 0$ ,
- (iii)  $\chi_E(0) = 2\chi_E(1)$ .

From (ii) and (iii) it follows that  $E_c$  is a well defined quantity in the sense that considered as a function of  $E$  for fixed  $\alpha$ , the second solution required to (7.16) is such that  $\chi_E(\alpha) \rightarrow 0$  as  $E \rightarrow E_c^+$  for all  $\alpha$ . In other words, the threshold  $E_c$  does not vary with  $\alpha$ . We therefore make the ansatz that for small  $E - E_c$ ,

$$\chi_E(\alpha) \sim \delta^\nu (y(\alpha) + \delta z(\alpha) + \dots) \quad (7.17)$$

where  $\delta = E - E_c$  and

$$y(\alpha) = \lim_{\delta \rightarrow 0^+} \frac{\chi_E(\alpha)}{\delta^\nu} \neq 0 \quad (7.18)$$

The exponent  $\nu$  will later be shown to be 1. Substituting (7.17) in (7.16) and using (7.18) gives a linear integral equation for  $y(\alpha)$ ,

$$y(\alpha) = 2E_c\sigma \int_0^1 y(t) dt - E_c\sigma \int_{1-\alpha}^1 y(t) dt \quad (7.19)$$

This equation is best solved by reduction to a second order differential equation.

Putting

$$C = 2E_c\sigma \int_0^1 y(t) dt = y(0) \quad (7.20)$$

(7.19) can be written (with  $X = \sigma E_c$ )

$$y(\alpha) = C - X \int_0^\alpha y(1-t) dt \quad (7.21)$$

Differentiating with respect to  $\alpha$  gives

$$\begin{aligned} \frac{dy(\alpha)}{d\alpha} &= -X y(1-\alpha) \\ &= -X \left[ C - X \int_\alpha^1 y(t) dt \right] \end{aligned} \quad (7.22)$$

Differentiating again gives

$$\frac{d^2 y(\alpha)}{d\alpha^2} = -X^2 y(\alpha) \quad (7.23)$$

The solution of (7.23) is clearly of the form

$$y(\alpha) = A \sin X\alpha + B \cos X\alpha \quad (7.24)$$

Substituting back in (7.19) we find

$$y(\alpha) = C \left( \cos X\alpha - \frac{1}{2} \sin X\alpha \right) \quad (7.25)$$

where  $C$  is a non-zero constant as yet undetermined and  $X$  must satisfy the condition

$$\frac{(1 - \sin X)}{\cos X} = \frac{1}{2} \quad (7.26)$$

The relevant solution of (7.26) gives for the percolation threshold

$$E_c = \sin^{-1}\left(\frac{3}{5}\right)/\sigma = 0.6435/\sigma \quad (7.27)$$

This exact result is to be compared with the value  $E_c = \frac{2}{3\sigma}$  obtained by simple arguments in § 7.2 (equation (7.11)). The small difference arises

when full account is taken of the variation with  $E_i$  of the conditional probability that further bonds leave a site  $i$  given that a bond enters  $i$ .

To obtain the exponent  $\nu$  and the constant  $C$  it is necessary to make use of the non-linearity of (7.16). This may be done by solving for the next order term in the expansion (7.17). Substituting (7.17) in (7.16) we find as  $\delta \rightarrow 0^+$

$$\begin{aligned} & \delta^\nu y(\alpha) + \delta^{\nu+1} z(\alpha) \\ & \sim F_\alpha \left[ 2E \left\{ \sigma (\delta^\nu y(t) + \delta^{\nu+1} z(t)) - \frac{\sigma(\sigma-1)}{2} (\delta^\nu y(t) + \delta^{\nu+1} z(t))^2 \right\} \right] \end{aligned} \quad (7.28)$$

where  $F_\alpha$  is the linear functional given by

$$F_\alpha [g(t)] = \left( \int_0^1 - \frac{1}{2} \int_{1-\alpha}^1 \right) dt g(t) \quad (7.29)$$

Putting  $\sigma E = X + \sigma \delta$ , the terms in  $\delta^\nu$  in (7.28) give back (7.19) for  $y(\alpha)$  as  $\delta \rightarrow 0^+$ , while the terms in  $\delta^{\nu+1}$  give for  $z(\alpha)$ ,

$$z(\alpha) = F_\alpha \left[ 2Xz(t) + 2\sigma y(t) - X(\sigma-1)y^2(t) \right] \quad (7.30)$$

Note however that in (7.30) the term in  $y^2(\alpha)$  is only included if  $\nu = 1$

(i.e. if  $2\nu = \nu+1$ ). Following a similar procedure to that used above, (7.30) may be reduced to a second order differential equation,

$$\frac{d^2 z(\alpha)}{d\alpha^2} = -X^2 z(\alpha) - 2\sigma X y(\alpha) + X^2(\sigma-1) y(\alpha) \left[ y(1-\alpha) + \frac{1}{2} y(\alpha) \right] \quad (7.31)$$

where again the last term only occurs if  $\nu = 1$ . Now if this term is excluded, a solution to (7.31) is easily found to be

$$z(\alpha) = Ay(\alpha) + By(1-\alpha) - \sigma\alpha y(1-\alpha) \quad (7.32)$$

However if (7.32) is now substituted into (7.30) (with the  $y^2(t)$  term missing) no non-zero solution of this form can be found to the integral equation. This is essentially because the lack of  $y^2$  terms in (7.32) and the integral equation it should satisfy means that the constant  $C = y(0)$  (see (7.25)) cancels out of the integral equation and hence is not available as an additional degree of freedom to help (7.32) satisfy the equation. We therefore conclude that  $\nu = 1$ .

It then follows, after considerable algebra, that the solution to (7.30) is

$$z(\alpha) = D y(\alpha) - \sigma \left(\alpha - \frac{1}{2}\right) y(1-\alpha) + \frac{\sigma}{12} (\sigma-1) C^2 - \frac{1}{3} (\sigma-1) y(\alpha) \left( y(1-\alpha) + \frac{1}{2} y(\alpha) \right) \quad (7.33)$$

where  $C$  is now fixed by the requirement that

$$C = \frac{15}{4} \frac{\sigma}{(\sigma-1)} \quad (7.34)$$

$D$  is a constant undetermined to this order.

Having found  $y$  and  $C$ , we are now in a position to obtain the critical behaviour of the percolation probability  $P(E)$  (defined by (7.12) ),

$$\begin{aligned} P(E) &= 1 - \int_0^1 Q_E^{\sigma+1}(E_0) dE_0 \\ &\sim 2E_c(\sigma+1) \int_0^1 \delta y(\alpha) d\alpha + O(\delta^2) \\ &\sim \frac{15}{4} \frac{(\sigma+1)}{(\sigma-1)} (E-E_c) + O(E-E_c)^2 \end{aligned} \quad (7.35)$$

where (7.20) and (7.34) have been used. The percolation probability thus behaves linearly in the critical region.

In order to obtain  $P(E)$  for general  $E$ , one must solve the non-linear integral equation (7.15) numerically. This has been done for various  $\sigma$  using a straightforward iterative procedure, the integrations being computed using the trapezium rule with 40 subdivisions. Convergence was found to be very fast except near the critical region. However extrapolation of the results from just above  $E_c$  gave very good agreement with the theoretical values of  $C$  and  $E_c$ .  $\chi_E(\alpha)$  and  $P(E)$  for  $\sigma = 4$  are shown in figure 7.4 and figure 7.5 respectively. Note that the calculations have only been carried out for  $E \leq 0.5$ .

## § 7.4 Conclusion

The exact solution to the correlated bond percolation problem on the Bethe lattice has been presented. This has involved the analysis of an interesting non-linear integral equation for the percolation probability (see (7.15) ). The bifurcation point

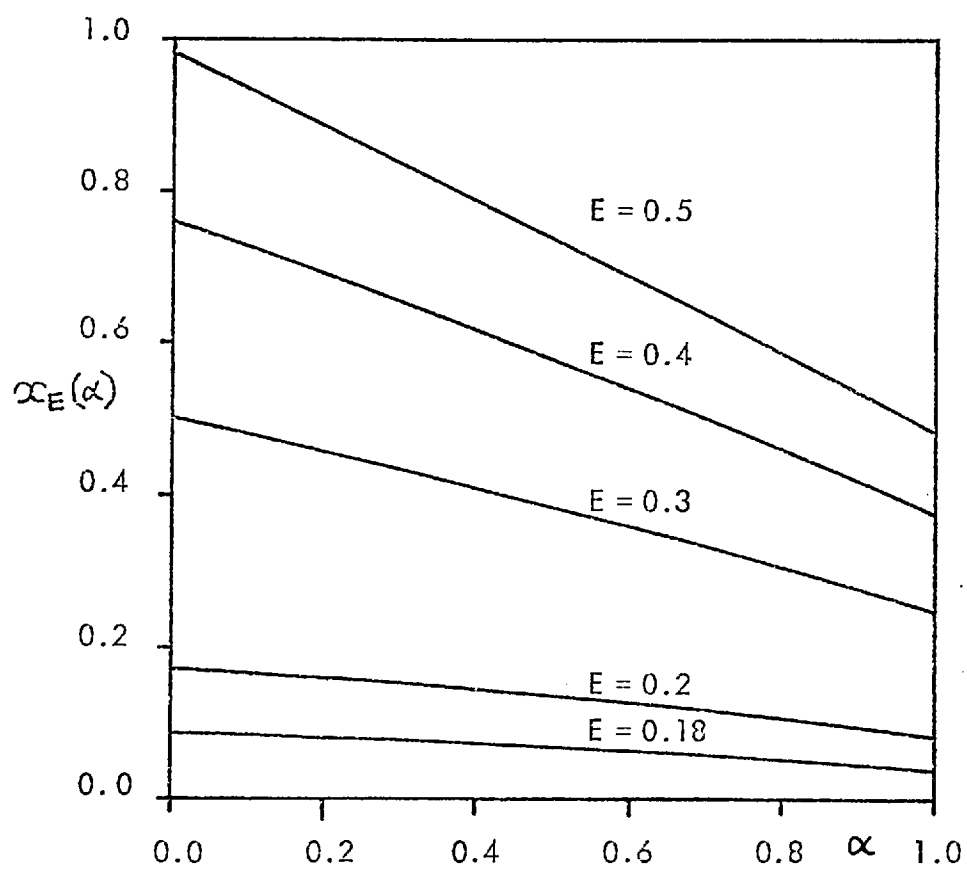


FIGURE 7.4  $\alpha_E(\alpha)$ , FOR VARIOUS  $E$ , FOR A BETHE LATTICE OF CO-ORDINATION NUMBER 5. The percolation threshold is at  $E = 0.1609$ .



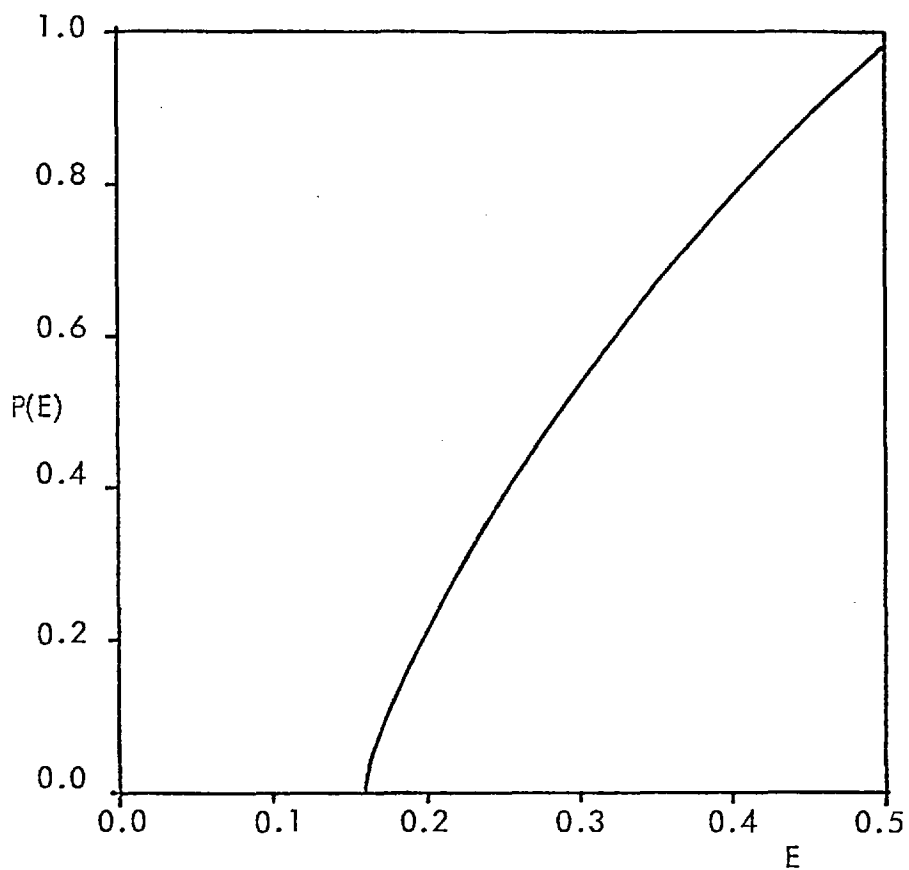


FIGURE 7.5 THE PERCOLATION PROBABILITY,  $P(E)$ , FOR THE CORRELATED BOND MODEL ON THE BETHE LATTICE OF CO-ORDINATION NUMBER 5. The percolation threshold is at  $E = 0.1609$ .

of this equation (i.e. the eigenvalue at which two different solutions of the equation coincide) corresponds to the percolation threshold,  $E_c$ , of the problem. Only for  $E > E_c$  is the percolation probability,  $P(E)$ , non zero.  $E_c$  has been found to depend on the co-ordination number  $\sigma + 1$  of the Bethe lattice according to

$$E_c = \frac{1}{\sigma} \sin^{-1}\left(\frac{3}{5}\right)$$

This exact result is only slightly different from the estimate (7.11) obtained by simple arguments. These arguments may therefore be usefully extended to other lattices for which analytic results are not available.

It has also been shown that  $P(E)$  behaves linearly in the critical region (see (7.35) ). This is the same as found for random bond percolation<sup>(77)</sup> and temperature dependent percolation<sup>(85)</sup> on the Bethe lattice, thus lending further support to the hypothesis that critical exponents for a particular dimensionality of lattice (in this case, infinite) are independent of the details of the percolation problem.

An interesting extension to the work presented here would be to use the methods of Heinrichs and Kumar<sup>(100)</sup> to calculate the conductivity of a correlated bond resistor network.

## APPENDIX A

EVALUATION OF THE FREE-PARTICLE FOUR-BODY RESPONSE FUNCTION  $\chi_4^0$ 

The free-particle response function  $\chi_4^0$  appears in both the approximations derived for the interacting  $\chi_4$  in chapter 3. It is therefore of interest to try and evaluate  $\chi_4^0$ . This function is defined in  $\underline{r}$ -space by (c.f. (3.1) )

$$\chi_4^0(\underline{r}_1, \underline{r}_2; \underline{r}_3, \underline{r}_4) = (-i)^2 \int_{-\infty}^{\infty} dt_3 dt_4 \langle 0 | T \rho_e(\underline{r}_4 t_4) \rho_e(\underline{r}_3 t_3) \rho_e(\underline{r}_1 t_1) \rho_e(\underline{r}_2 t_2) | 0 \rangle_c \quad (\text{A1})$$

where  $|0\rangle$  is the non-interacting ground state. In this appendix,  $\chi_4^0$  is evaluated by two different methods although no closed analytic expression is obtained for its Fourier transform form,  $\chi_4^0(\underline{k}, \underline{q}-\underline{k}; \underline{q}-\underline{q}, -\underline{q})$ .

§ A1 Derivation using Wick's theorem

We consider the Green's function  $\Gamma_4^0$  defined by

$$\Gamma_4^0(X_1, X_2, X_3, X_4) = (-i)^2 \langle 0 | T \rho_e(X_1) \rho_e(X_2) \rho_e(X_3) \rho_e(X_4) | 0 \rangle_c \quad (\text{A2})$$

where  $X_i = (\underline{r}_i, t_i)$ . In terms of the electron field operators  $\psi_\sigma^\dagger(X_i)$  and  $\psi_\sigma(X_i)$ ,  $\rho_e(X_i)$  can be written in the form

$$\rho_e(X_i) = \sum_{\sigma} \psi_\sigma^\dagger(X_i) \psi_\sigma(X_i) \quad (\text{A3})$$

$\sigma$  being a spin index. Thus (A2) becomes

$$\begin{aligned} \Gamma_4^0(X_1, X_2, X_3, X_4) &= (-i)^2 \sum_{\sigma_1 \sigma_2 \sigma_3 \sigma_4} \langle T \psi_{\sigma_4}^\dagger(X_4) \psi_{\sigma_4}(X_4) \psi_{\sigma_3}^\dagger(X_3) \psi_{\sigma_3}(X_3) \psi_{\sigma_2}^\dagger(X_2) \psi_{\sigma_2}(X_2) \psi_{\sigma_1}^\dagger(X_1) \psi_{\sigma_1}(X_1) \rangle \\ &= (-i)^2 \sum_{\sigma_1 \sigma_2 \sigma_3 \sigma_4} \langle T \psi_{\sigma_4}^\dagger(X_4) \psi_{\sigma_4}(X_4) \psi_{\sigma_3}^\dagger(X_3) \psi_{\sigma_3}(X_3) \psi_{\sigma_2}^\dagger(X_2) \psi_{\sigma_2}(X_2) \psi_{\sigma_1}^\dagger(X_1) \psi_{\sigma_1}(X_1) \rangle \end{aligned} \quad (\text{A4})$$

Using Wick's theorem for time-ordered products,  $\Gamma_4^0$  can be decomposed to give

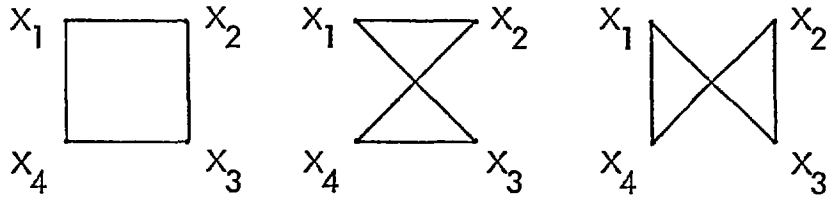
$$\begin{aligned} \Gamma_4^0(X_1, X_2, X_3, X_4) &= 2 \cdot 2 \cdot \left\{ G^\sigma(X_1-X_2) G^\sigma(X_2-X_3) G^\sigma(X_3-X_4) G^\sigma(X_4-X_1) \right. \\ &\quad + G^\sigma(X_1-X_3) G^\sigma(X_3-X_4) G^\sigma(X_4-X_2) G^\sigma(X_2-X_1) \\ &\quad \left. + G^\sigma(X_1-X_3) G^\sigma(X_3-X_2) G^\sigma(X_2-X_4) G^\sigma(X_4-X_1) \right\} \quad (\text{A5}) \end{aligned}$$

In (A5) one of the factors of 2 arises from a spin sum, the other from the fact that each of the three terms appears twice in the Wick's theorem decomposition.

$G^0(X_1, -X_2)$  is the free-particle Green's function for one spin and is given by

$$iG^0(X_1, -X_2) = \langle 0 | T \Psi_\sigma(X_1) \Psi_\sigma^\dagger(X_2) | 0 \rangle \quad (A6)$$

The three terms in (A5) clearly correspond to the Feynman diagrams



We now note that

$$\begin{aligned} N_{4+}^0(\underline{k}, \underline{k}-\underline{k}; \underline{q}-\underline{q}, -\underline{q}) \\ = \int \frac{d\omega}{(2\pi)} e^{i\omega S} \left\{ \int e^{i\underline{k} \cdot (\underline{r}_1 - \underline{r}_2)} e^{i\underline{k} \cdot (\underline{r}_2 - \underline{r}_3)} e^{i\underline{q} \cdot (\underline{r}_3 - \underline{r}_4)} e^{-i\omega(t_1 - t_2)} \right. \\ \left. \times \prod_4^0(\underline{r}_4 t_4, \underline{r}_3 t_3, \underline{r}_1 t_1, \underline{r}_2 t_2) d(\underline{r}_1 - \underline{r}_2) d(\underline{r}_2 - \underline{r}_3) d(\underline{r}_3 - \underline{r}_4) \right. \\ \left. \times d(t_1 - t_2) dt_3 dt_4 \right\} \end{aligned} \quad (A7)$$

where the  $e^{i\omega S}$  maintains the correct time ordering as in (A1). The expression in the curly brackets was denoted by  $\prod_4^0$  in chapter 3 (c.f. (3.20)).

Substituting (A5) in (A7) we find

$$\begin{aligned} N_{4+}^0(\underline{k}, \underline{k}-\underline{k}; \underline{q}-\underline{q}, -\underline{q}) \\ = 4 \int \frac{d\underline{p}}{(2\pi)^3} \int \frac{d\omega}{(2\pi)} e^{i\omega S} \int \frac{d\omega'}{(2\pi)} \left\{ G^0(\underline{p}-\underline{k}, \omega'+\omega) G^0(\underline{p}-\underline{k}, \omega') G^0(\underline{p}-\underline{q}, \omega') G^0(\underline{p}, \omega') \right. \\ + G^0(\underline{p}-\underline{k}, \omega'+\omega) G^0(\underline{p}-\underline{k}, \omega') G^0(\underline{p}+\underline{q}-\underline{k}, \omega') G^0(\underline{p}, \omega') \\ \left. + G^0(\underline{p}, \omega'+\omega) G^0(\underline{p}+\underline{q}-\underline{k}, \omega'+\omega) G^0(\underline{p}-\underline{k}+\underline{q}, \omega') G^0(\underline{p}-\underline{k}, \omega') \right\} \end{aligned} \quad (A8)$$

where

$$G^0(\underline{p}, \omega) = \frac{\theta(k_F - |\underline{p}|)}{\omega - p^2/2m - i\epsilon} + \frac{\theta(|\underline{p}| - k_F)}{\omega - p^2/2m + i\epsilon} \quad (A9)$$

Three kinds of frequency integral in (A8).

(a) The first two terms have a factor

$$\int e^{i\omega S} G^{\circ}(\underline{p}-\underline{k}, \omega) \frac{d\omega}{(2\pi)} = i \theta(k_F - |\underline{p}-\underline{k}|) \quad (\text{A10})$$

(b) The first two terms also have a factor of the form

$$\begin{aligned} \int \frac{d\omega}{(2\pi)} G^{\circ}(\underline{p}_1, \omega) G^{\circ}(\underline{p}_2, \omega) G^{\circ}(\underline{p}_3, \omega) &= i J_3(\underline{p}_1, \underline{p}_2, \underline{p}_3) \\ &= \int \frac{d\omega}{(2\pi)} \left[ \frac{\theta(k_F - p_1) + \theta(p_1 - k_F)}{\omega - p_1^2/2m - i\epsilon} + \frac{\theta(p_1 - k_F)}{\omega - p_1^2/2m + i\epsilon} \right] \left[ \frac{\theta(k_F - p_2) + \theta(p_2 - k_F)}{\omega - p_2^2/2m - i\epsilon} + \frac{\theta(p_2 - k_F)}{\omega - p_2^2/2m + i\epsilon} \right] \left[ \frac{\theta(k_F - p_3) + \theta(p_3 - k_F)}{\omega - p_3^2/2m - i\epsilon} + \frac{\theta(p_3 - k_F)}{\omega - p_3^2/2m + i\epsilon} \right] \end{aligned} \quad (\text{A11})$$

In (A11), only the six product terms that have poles both sides of the real axis contribute to the integration. The other two terms give zero as the contour can be closed in the half-plane in which there are no poles. After some algebra it follows that

$$\frac{J_3(\underline{p}_1, \underline{p}_2, \underline{p}_3)}{4} = \frac{\theta(k_F - p_1)}{(p_1^2 - p_2^2)(p_1^2 - p_3^2)} + \frac{\theta(k_F - p_2)}{(p_2^2 - p_1^2)(p_2^2 - p_3^2)} + \frac{\theta(k_F - p_3)}{(p_3^2 - p_2^2)(p_3^2 - p_1^2)} \quad (\text{A12})$$

(c) The last term in (A11) has two factors of the form

$$\begin{aligned} i J_2(\underline{p}_1, \underline{p}_2) &= \int \frac{d\omega}{2\pi} G^{\circ}(\underline{p}_1, \omega) G^{\circ}(\underline{p}_2, \omega) \\ &= 2 \left[ \frac{\theta(k_F - p_1) - \theta(k_F - p_2)}{p_2^2 - p_1^2} \right] \end{aligned} \quad (\text{A13})$$

Collecting together the results we find

$$\begin{aligned} \chi_4^{\circ}(\underline{k}, \underline{G}-\underline{k}; \underline{q}, \underline{G}-\underline{q}) &= -4 \int \frac{d\underline{p}}{(2\pi)^3} \left\{ \begin{aligned} &\theta(k_F - |\underline{p}-\underline{k}|) J_3(\underline{p}, \underline{p}-\underline{G}, \underline{p}-\underline{G}+\underline{q}) \\ &+ \theta(k_F - |\underline{p}-\underline{k}|) J_3(\underline{p}, \underline{p}-\underline{G}, \underline{p}-\underline{q}) \\ &+ J_2(\underline{p}-\underline{k}, \underline{p}-\underline{k}+\underline{q}) J_2(\underline{p}, \underline{p}+\underline{q}-\underline{G}) \end{aligned} \right\} \end{aligned} \quad (\text{A14})$$

The integrals in (A14) are to be interpreted as principal parts where necessary.

Note that (A14) is unchanged under the transformations  $\underline{k} \rightarrow \underline{G} - \underline{k}$  and  $\underline{q} \rightarrow \underline{G} - \underline{q}$ .

If  $\underline{G} = 0$ , this implies symmetry between  $\underline{r}_1$  and  $\underline{r}_2$  and between  $\underline{r}_3$  and  $\underline{r}_4$  in the  $\underline{r}$ -space form of  $N_4^0$ .

For liquid metal calculations the  $\underline{G} \rightarrow 0$  limit of (A14) is required. This involves the expression  $J_3(\underline{p}, \underline{p}, \underline{p} \pm \underline{q})$  which can be readily defined if it is noticed from (A12) that

$$\begin{aligned} \frac{J_3(\underline{p}_1, \underline{p}_2, \underline{p}_3)}{4} &= \frac{\theta(k_F - p_1)}{(p_1^2 - p_3^2)(p_3^2 - p_2^2)} + \frac{\theta(k_F - p_3)}{(p_3^2 - p_2^2)(p_3^2 - p_1^2)} \\ &+ \frac{\theta(k_F - p_1) - \theta(k_F - p_2)}{(p_2^2 - p_3^2)(p_1^2 - p_2^2)} \end{aligned} \quad (\text{A15})$$

Hence

$$\lim_{p_2 \rightarrow p_1} \frac{J_3(\underline{p}_1, \underline{p}_2, \underline{p}_3)}{4} = \frac{\theta(k_F - p_3) - \theta(k_F - p_1)}{(p_3^2 - p_1^2)^2} + \frac{1}{2k_F} \frac{\delta(p_1 - k_F)}{(p_3^2 - p_1^2)} \quad (\text{A16})$$

Unfortunately, because of the complex form of (A14) it has not been possible to evaluate fully  $N_4^0(k, \underline{r} - k; \underline{q} - \underline{G}, -\underline{q})$  or the  $\underline{G} = 0$  limit (although some other limits are derived in Appendix B). However the  $\underline{r}$ -space form of  $N_4^0$  can be obtained by making use of the Fourier transforms

$$\frac{k_F^2}{8\pi^3} \frac{J_1(k_F|\underline{r}_1| + k_F|\underline{r}_2|)}{|\underline{r}_1||\underline{r}_2|} = \iint J_2(\underline{p}_1, \underline{p}_2) e^{-i\underline{p}_1 \cdot \underline{r}_1} e^{-i\underline{p}_2 \cdot \underline{r}_2} \frac{d\underline{p}_1}{(2\pi)^3} \frac{d\underline{p}_2}{(2\pi)^3} \quad (\text{A17})$$

$$\begin{aligned} \frac{k_F^2}{8\pi^4} \frac{J_1(k_F|\underline{r}_1| + k_F|\underline{r}_2| + k_F|\underline{r}_3|)}{|\underline{r}_1||\underline{r}_2||\underline{r}_3|} \\ = \iiint J_3(\underline{p}_1, \underline{p}_2, \underline{p}_3) e^{-i\underline{p}_1 \cdot \underline{r}_1} e^{-i\underline{p}_2 \cdot \underline{r}_2} e^{-i\underline{p}_3 \cdot \underline{r}_3} \frac{d\underline{p}_1}{(2\pi)^3} \frac{d\underline{p}_2}{(2\pi)^3} \frac{d\underline{p}_3}{(2\pi)^3} \end{aligned} \quad (\text{A18})$$

$$\frac{k_F^2}{2\pi^2} \frac{J_1(k_F|\underline{r}_1|)}{|\underline{r}_1|} = \int \theta(k_F - p_1) e^{-i\underline{p}_1 \cdot \underline{r}_1} \frac{d\underline{p}_1}{(2\pi)^3} \quad (\text{A19})$$

In (A18), (A19) and (A20),  $J_1(k_F r)$  is the spherical Bessel function given by

$$J_1(k_F r) = \frac{\sin k_F r - k_F r \cos k_F r}{(k_F r)^2} \quad (\text{A20a})$$

$$J_1(k_F r) = \frac{1}{k_F^2} \int_0^{k_F} x \sin x r dx \quad (\text{A20b})$$

The integral representation in (A20b) is useful in demonstrating (A18) - (A20).

Using these Fourier transforms,  $\chi_4(\underline{r}_1, \underline{r}_2; \underline{r}_3, \underline{r}_4)$  is obtained from (A14) as

$$\begin{aligned} \chi_4(\underline{r}_1, \underline{r}_2; \underline{r}_3, \underline{r}_4) &= -\frac{k_F^4}{2\pi^6} \left[ \frac{J_1(k_F |\underline{r}_1 - \underline{r}_2|)}{|\underline{r}_1 - \underline{r}_2|} \frac{J_1(k_F |\underline{r}_1 - \underline{r}_3| + k_F |\underline{r}_3 - \underline{r}_4| + k_F |\underline{r}_4 - \underline{r}_2|)}{|\underline{r}_1 - \underline{r}_3| |\underline{r}_3 - \underline{r}_4| |\underline{r}_4 - \underline{r}_2|} \right. \\ &\quad \left. + \frac{1}{2} \frac{J_1(k_F |\underline{r}_1 - \underline{r}_3| + k_F |\underline{r}_3 - \underline{r}_2|)}{|\underline{r}_1 - \underline{r}_3| |\underline{r}_3 - \underline{r}_2|} \frac{J_1(k_F |\underline{r}_1 - \underline{r}_4| + k_F |\underline{r}_4 - \underline{r}_2|)}{|\underline{r}_1 - \underline{r}_4| |\underline{r}_4 - \underline{r}_2|} \right] \quad (\text{A21}) \end{aligned}$$

§ A2 Second derivation using the Dirac density matrix

The Dirac density matrix  $\gamma(\underline{r}_1, \underline{r}_2)$  is defined for a general electron system

by

$$\gamma(\underline{r}_1, \underline{r}_2) = \sum_{\sigma} \langle \psi_{\sigma}^{\dagger}(\underline{r}_1) \psi_{\sigma}(\underline{r}_2) \rangle \quad (\text{A22})$$

and it immediately follows from (A3)

$$\gamma(\underline{r}, \underline{r}) = \langle \rho_e(\underline{r}) \rangle \quad (\text{A21})$$

For a system of  $N$  non-interacting spin  $\frac{1}{2}$  fermions it is easily shown that

$$\gamma(\underline{r}_1, \underline{r}_2) = 2 \sum_{i=1}^{\frac{1}{2}N} \psi_i^*(\underline{r}_1) \psi_i(\underline{r}_2) \quad (\text{A22})$$

where  $\psi_i$  are the normalised one particle wave functions. For a homogeneous system of free electrons, the  $\psi_i$ 's are plane waves and in this case

$$\gamma^0(\underline{r}_1, \underline{r}_2) = \frac{k_F^2}{\pi^2} \frac{J_1(k_F |\underline{r}_1 - \underline{r}_2|)}{|\underline{r}_1 - \underline{r}_2|} \quad (\text{A23})$$

It follows from (A22) that  $\gamma^0$  has the property of idempotency, that is

$$\int \gamma^0(\underline{r}_1, \underline{r}_2) \gamma^0(\underline{r}_2, \underline{r}_3) d\underline{r}_2 = 2 \gamma^0(\underline{r}_1, \underline{r}_3) \quad (\text{A24})$$

As discussed by March, Young and Sampanthar<sup>(29)</sup> in the case of free particles,

the Dirac density matrix completely determines all higher order correlation functions.

In particular, the cluster part of the two particle correlation function,  $P_{ee}^c(\underline{r}_1, \underline{r}_2)$  for free particles is given by

$$P_{ee}^c(\underline{r}_1, \underline{r}_2) = -\frac{1}{2} \left[ \gamma^0(\underline{r}_1, \underline{r}_2) \right]^2 \quad (\text{A25})$$

March and Murray<sup>(58)</sup> have given a perturbation expansion for  $\gamma^0(\underline{r}_1, \underline{r}_2)$  in the presence of an external potential  $U(\underline{r})$ . To second order in  $U(\underline{r})$ , the change in  $\gamma^0(\underline{r}_1, \underline{r}_2)$  from its homogeneous gas value (A23) is given by

$$\begin{aligned} \delta\gamma^0(\underline{r}_1, \underline{r}_2) = & -\frac{k_F^2}{2\pi^3} \int \frac{J_1(k_F|\underline{r}_1-\underline{r}_3|+k_F|\underline{r}_3-\underline{r}_2|)}{|\underline{r}_1-\underline{r}_3| |\underline{r}_3-\underline{r}_2|} U(\underline{r}_3) d\underline{r}_3 \\ & + \frac{k_F^2}{4\pi^4} \iint \frac{J_1(k_F|\underline{r}_1-\underline{r}_3|+k_F|\underline{r}_3-\underline{r}_4|+k_F|\underline{r}_4-\underline{r}_2|)}{|\underline{r}_1-\underline{r}_3| |\underline{r}_3-\underline{r}_4| |\underline{r}_4-\underline{r}_2|} \\ & \times U(\underline{r}_3) U(\underline{r}_4) d\underline{r}_3 d\underline{r}_4 \end{aligned} \quad (\text{A26})$$

The corresponding change in  $P_{ee}^c(\underline{r}_1, \underline{r}_2)$  can be obtained from (A25) as

$$\begin{aligned} \delta P_{ee}^c(\underline{r}_1, \underline{r}_2) = & -\gamma^0(\underline{r}_1, \underline{r}_2) \delta\gamma^0(\underline{r}_1, \underline{r}_2) \\ & -\frac{1}{2} \left[ \delta\gamma^0(\underline{r}_1, \underline{r}_2) \right]^2 \end{aligned} \quad (\text{A27})$$

If (A26) is now substituted in (A27), the resulting expansion clearly corresponds to equation (2.28) of chapter 2, provided  $\chi_3$  and  $\chi_4$  in that equation are replaced by their free particle values. By comparing terms in these expansions we find

$$\chi_3^0(\underline{r}_1, \underline{r}_2; \underline{r}_3) = \frac{k_F^4}{2\pi^5} \frac{J_1(k_F|\underline{r}_1-\underline{r}_2|)}{|\underline{r}_1-\underline{r}_2|} \frac{J_1(k_F|\underline{r}_1-\underline{r}_3|+k_F|\underline{r}_3-\underline{r}_2|)}{|\underline{r}_1-\underline{r}_3| |\underline{r}_3-\underline{r}_2|} \quad (\text{A28})$$

and  $\chi_4^0(\underline{r}_1, \underline{r}_2; \underline{r}_3, \underline{r}_4)$  is exactly as given in (A21).

Finally, we deduce from (A21) and (A26) that the free-particle linear and quadratic density response functions  $\chi^0$  and  $\chi_2^0$  are given in  $\underline{r}$ -space by

$$\chi^0(\underline{r}_1, \underline{r}_2) = -\frac{k_F^2}{2\pi^3} \frac{J_1(2k_F|\underline{r}_1-\underline{r}_2|)}{|\underline{r}_1-\underline{r}_2|^2} \quad (\text{A29})$$



$$N_{\chi_2^0}(\underline{r}_1, \underline{r}_2, \underline{r}_3) = \frac{k_F^2}{2\pi^4} \frac{J_1(k_F|\underline{r}_1-\underline{r}_2| + k_F|\underline{r}_2-\underline{r}_3| + k_F|\underline{r}_3-\underline{r}_1|)}{|\underline{r}_1-\underline{r}_2| |\underline{r}_2-\underline{r}_3| |\underline{r}_3-\underline{r}_1|} \quad (\text{A30})$$

## APPENDIX B

SOME EXACT LONG WAVELENGTH LIMITS OF THE RESPONSE FUNCTIONS

$$\underline{N}_2^0, \underline{N}_3^0, \underline{N}_4^0, H_4^0$$

Firstly it is shown that

$$\lim_{k \rightarrow 0} H_4^0(k, \underline{q}-k; \underline{q}-\underline{q}, -\underline{q}) = 0 \quad (\text{B1})$$

where  $H_4^0$  is the free particle response function defined in  $\underline{r}$ -space by (c.f. (3.4) )

$$\begin{aligned} \delta P_{ee}^c(\underline{r}_1, \underline{r}_2) &= \int H_3^0(\underline{r}_1, \underline{r}_2; \underline{r}_3) \delta \rho_e(\underline{r}_3) d\underline{r}_3 \\ &+ \frac{1}{2} \int H_4^0(\underline{r}_1, \underline{r}_2; \underline{r}_3, \underline{r}_4) \delta \rho_e(\underline{r}_3) \delta \rho_e(\underline{r}_4) d\underline{r}_3 d\underline{r}_4 \\ &+ O(\delta e_e^2) \end{aligned} \quad (\text{B2})$$

Secondly, the result (B1) is used to give some exact long wavelength limits of the other free particle response functions.

### § B1 Proof of (B1)

According to (A25),  $P_{ee}^c(\underline{r}_1, \underline{r}_2)$  for free particles is given in terms of the Dirac density matrix  $\gamma^0(\underline{r}_1, \underline{r}_2)$  by

$$P_{ee}^c(\underline{r}_1, \underline{r}_2) = -\frac{1}{2} [\gamma^0(\underline{r}_1, \underline{r}_2)]^2 \quad (\text{B3})$$

Using the idempotency of  $\gamma^0$  (as expressed in (A24) ) and the fact that its diagonal element is the electron density, it follows that for free particles

$$\int \delta P_{ee}^c(\underline{r}_1, \underline{r}_2) d\underline{r}_1 = -\delta \rho_e(\underline{r}_2) \quad (\text{B4})$$

Comparing (B4) and (B2) we find

$$\int H_3^0(\underline{r}_1, \underline{r}_2; \underline{r}_3) d\underline{r}_1 = -\delta(\underline{r}_2 - \underline{r}_3) \quad (\text{B5})$$

$$\int H_4^0(\underline{r}_1, \underline{r}_2; \underline{r}_3, \underline{r}_4) d\underline{r}_1 = 0 \quad (\text{B6})$$

The Fourier transform of (B6) is the same as (B1).

### § B2 Long wavelength limits of $N_2^0, N_3^0, N_4^0$

If both sides of (B4) are expanded to second-order in the external potential

the following relationships between response functions are obtained

$$\int \chi_3^c(\underline{r}_1, \underline{r}_2; \underline{r}_3) d\underline{r}_1 = -\chi^o(\underline{r}_2, \underline{r}_3) \quad (\text{B7})$$

$$\int \chi_4^o(\underline{r}_1, \underline{r}_2; \underline{r}_3, \underline{r}_4) d\underline{r}_1 = -\chi_2^o(\underline{r}_2, \underline{r}_3, \underline{r}_4) \quad (\text{B8})$$

In Fourier space, these become

$$\lim_{\underline{k} \rightarrow 0} \chi_3^o(\underline{k}, \underline{q}-\underline{k}; -\underline{q}) = -\chi^o(\underline{q}) \quad (\text{B7a})$$

$$\lim_{\underline{k} \rightarrow 0} \chi_4^o(\underline{k}, \underline{q}-\underline{k}; \underline{q}, -\underline{q}) = -\chi_2^o(\underline{q}, \underline{q}-\underline{q}, -\underline{q}) \quad (\text{B8a})$$

(B8a) can in fact be verified from the expression for  $\chi_4^o$  given by (A14).

We are now in a position to derive some explicit long wavelength results for  $\chi_1^o, \chi_2^o, \chi_3^o$  and  $\chi_4^c$ .

(a) From expression (A30) for  $\chi_2^o$ ,

$$\begin{aligned} \chi_2^o(0, \underline{q}, -\underline{q}) &= \frac{k_F^2}{2\pi^4} \int e^{i\underline{q} \cdot \underline{r}_1} \frac{J_1(k_F|\underline{r}_1| + k_F|\underline{r}_2| + k_F|\underline{r}_1 + \underline{r}_2|)}{|\underline{r}_1||\underline{r}_2||\underline{r}_1 + \underline{r}_2|} d\underline{r}_1 d\underline{r}_2 \\ &= \frac{k_F}{\pi^3} \int e^{i\underline{q} \cdot \underline{r}_1} \frac{J_0(2k_F|\underline{r}_1|)}{|\underline{r}_1|} d\underline{r}_1 \\ &= \frac{1}{\pi^2 q} \ln \left| \frac{q+2k_F}{q-2k_F} \right| \end{aligned} \quad (\text{B9})$$

In (B9),  $J_0(x) = \frac{\sin x}{x}$  and use has been made of the result that for arbitrary  $C$ ,

$$\int \frac{J_1(k_F|\underline{r}_1 - \underline{r}_2| + C + k_F|\underline{r}_1 - \underline{r}_2|)}{|\underline{r}_1 - \underline{r}_2||\underline{r}_1 - \underline{r}_2|} d\underline{r} = \frac{2\pi}{k_F} J_0(k_F|\underline{r}_2 - \underline{r}_1| + C) \quad (\text{B10})$$

(b) (B9) and (B8a) immediately imply that

$$\lim_{\underline{k} \rightarrow 0} \chi_4^o(\underline{k}, \underline{q}-\underline{k}; \underline{q}, -\underline{q}) = -\frac{1}{\pi^2 q} \ln \left| \frac{q+2k_F}{q-2k_F} \right| \quad (\text{B11})$$

(c) From expression (A28) for  $\chi_3^o$ ,

$$\begin{aligned} \chi_3^o(\underline{k}, -\underline{k}; 0) &= \frac{k_F^4}{2\pi^5} \iint e^{i\underline{k} \cdot \underline{r}_1} \frac{J_1(k_F|\underline{r}_1|)}{|\underline{r}_1|} \frac{J_1(k_F|\underline{r}_1 + \underline{r}_2| + k_F|\underline{r}_1|)}{|\underline{r}_1 + \underline{r}_2||\underline{r}_2|} d\underline{r}_1 d\underline{r}_2 \\ &= \frac{k_F^3}{\pi^4} \int e^{i\underline{k} \cdot \underline{r}_1} \frac{J_1(k_F|\underline{r}_1|)}{|\underline{r}_1|} J_0(k_F|\underline{r}_1|) d\underline{r}_1 \end{aligned}$$

$$= \frac{k_F^2}{\pi^2} \theta(2k_F - k) \left(1 - \frac{k}{2k_F}\right) \quad (\text{B12})$$

where (B10) has again been used.

(d) From expression (A29) for  $\chi^0$ ,

$$\begin{aligned} \chi^0(\underline{G}) &= -\frac{k_F^2}{2\pi^3} \int e^{i\underline{G} \cdot \underline{r}} \frac{J_1(2k_F|\underline{r}|)}{r^2} d\underline{r} \\ &= -\frac{k_F^2}{\pi^2} \left[ \frac{1}{2} + \frac{k_F}{2G} \left[ 1 - \frac{G^2}{4k_F^2} \right] \ln \left| \frac{G+2k_F}{G-2k_F} \right| \right] \end{aligned} \quad (\text{B13})$$

and

$$\chi^0(0) = -\frac{k_F^2}{\pi^2} \quad (\text{B14})$$

Note that (B13) agrees with equation (4.6) of chapter 4.

(e) Using expression (A21) for  $\chi_4^0$ ,

$$\begin{aligned} \chi_4^0(\underline{k}, \underline{k}; 0, 0) &= -\frac{k_F^4}{2\pi^6} \left\{ \iiint e^{i\underline{k} \cdot \underline{x}} \left[ \frac{J_1(k_F|\underline{x}|)}{|\underline{x}|} \frac{J_1(k_F|\underline{x}+\underline{y}| + k_F|\underline{z}| + k_F|\underline{y}+\underline{z}|)}{|\underline{x}+\underline{y}||\underline{z}||\underline{y}+\underline{z}|} \right. \right. \\ &\quad \left. \left. + \frac{1}{2} \frac{J_1(k_F|\underline{x}+\underline{y}| + k_F|\underline{y}|)}{|\underline{x}+\underline{y}||\underline{y}|} \frac{J_1(k_F|\underline{x}+\underline{y}+\underline{z}| + k_F|\underline{y}+\underline{z}|)}{|\underline{x}+\underline{y}+\underline{z}||\underline{y}+\underline{z}|} \right] \right. \\ &\quad \left. \times d\underline{x} d\underline{y} d\underline{z} \right\} \end{aligned}$$

$$\begin{aligned} &= -\frac{k_F^3}{\pi^5} \iint e^{i\underline{k} \cdot \underline{x}} \frac{J_1(k_F x)}{x} \frac{J_0(k_F|\underline{x}+\underline{y}| + k_F|\underline{y}|)}{|\underline{x}+\underline{y}|} d\underline{x} d\underline{y} \\ &\quad - \frac{k_F^2}{\pi^4} \int e^{i\underline{k} \cdot \underline{x}} J_0^2(k_F x) d\underline{x} \\ &= -\frac{2k_F}{\pi^4} \int e^{i\underline{k} \cdot \underline{x}} \frac{J_1(2k_F x)}{x} d\underline{x} \end{aligned} \quad (\text{B15})$$

$$= -\frac{1}{\pi^2 k_F} \theta(2k_F - k)$$

In deriving (B15) use has been made of (B10) and also the result

$$\int \frac{J_0(k_F|x+y| + k_F|y|)}{|y|} dy = \frac{\pi}{k_F^2} \cos k_F x \quad (\text{B16})$$

(f) In chapter 3 it was shown that

$$H_4^\circ(\underline{k}, -\underline{k}; \underline{q}, -\underline{q}) = \left\{ \chi_4^\circ(\underline{k}, -\underline{k}; \underline{q}, -\underline{q}) - \frac{\chi_3^\circ(\underline{k}, -\underline{k}; 0) \chi_2^\circ(0, \underline{q}, -\underline{q})}{\chi^\circ(0)} \right\} \quad (\text{B17})$$

Using (B9), (B12) and (B14) the second term of the RHS of (B17) is

$$\frac{\chi_3^\circ(\underline{k}, -\underline{k}; 0) \chi_2^\circ(0, \underline{q}, -\underline{q})}{\chi^\circ(0)} = -\frac{\theta(2k_F - k)(1 - \frac{k}{2k_F}) \ln \left| \frac{q + 2k_F}{q - 2k_F} \right|}{\pi^2 q} \quad (\text{B18})$$

From (B15) and (B18) it follows that

$$H_4^\circ(\underline{k}, -\underline{k}; 0, 0) = -\theta(2k_F - k) \frac{k}{2\pi^2 k_F^2}$$

which clearly goes to zero as  $\underline{k} \rightarrow 0$  as required by (B1).

Finally, Brovman and Kagan<sup>(27a)</sup>, and Pethick<sup>(30)</sup> have shown that

$$\chi_2(\underline{G}, -\underline{G}, 0) = \lim_{\underline{k} \rightarrow 0} \chi(\underline{k}) \frac{\partial \chi(\underline{G})}{\partial n_e} = \chi_2(0, \underline{G}, -\underline{G}) \quad (\text{B19})$$

is an exact relation for the interacting jellium density response functions  $\chi$  and  $\chi_2$ . Since  $\lim_{\underline{k} \rightarrow 0} \chi(\underline{k}) = 0$ , this shows that  $\chi_2(\underline{G}, -\underline{G}, 0)$  is zero. This fact has been used in § 2.9 and § 3.2. (B19) is in fact equally applicable to free particles, for which it takes the form (using (B14) )

$$\chi_2^\circ(0, \underline{G}, -\underline{G}) = -\frac{1}{k_F} \frac{\partial}{\partial k_F} \chi^\circ(\underline{G}) \quad (\text{B20})$$

Use of (B13) in (B20) gives an alternative proof of (B10). Brovman and Kagan<sup>(27b)</sup>

have given an explicit form for the complete  $\chi_2^\circ(\underline{k}, \underline{G}-\underline{k}, -\underline{G})$ .

APPENDIX C

SUMMARY OF DENSITY FUNCTIONAL THEORY

Density functional theory (DFT) is a formally exact theory of inhomogeneous many-electron systems which however is expressed in a form that lends itself to a number of useful approximations. It dates from two classic papers by Hohenberg and Kohn (HK, 55) and Kohn and Sham (KS, 56) where it was shown that a secure theoretical foundation could be given to the early attempts of Thomas<sup>(102)</sup> and Fermi<sup>(103)</sup> to characterise the ground state properties of inhomogeneous electron systems by their electron density. For a general review of DFT see March<sup>(57)</sup>.

DFT is based on the following two part theorem proved by HK.

- (1) The ground state energy  $E$  of an interacting  $N$ -electron system in the presence of an external potential  $V(\underline{r})$  may be written in the form

$$E = F[n] + \int V(\underline{r}) n(\underline{r}) d\underline{r} \equiv E[n] \quad (C1)$$

where  $F[n]$  is a universal functional of the density  $n(\underline{r})$  (i.e. independent of  $N$  and  $V(\underline{r})$ ).

- (2) Subject to the conservation of particle number, i.e.

$$\int n(\underline{r}) d\underline{r} = N \quad (C2)$$

the ground state energy is stationary (a minimum) with respect to first order changes in the density, that is in functional derivative notation,

$$\frac{\delta E[n]}{\delta n(\underline{r})} = 0 \quad (C3)$$

This theorem is straightforwardly proved using the variational principle for the ground state wave function (assumed non-degenerate) and involves the use of the lemmas:

- (3) The external potential  $V(\underline{r})$  is to within a constant a unique functional of the exact ground state electron density  $n(\underline{r})$ .

(4) The ground state wave function is a unique functional of the density  $n(\underline{r})$ .

Indeed (4) is the strongest proposition within the theory and has the corollary:

(5) All ground state properties of an inhomogeneous electron system can be expressed as unique functionals of the density  $n(\underline{r})$ .

(1) is a special case of (5) which has also been used in chapter 3 as justification for the expansion (3.4).

KS made the important step of writing the energy functional in (1) in the form

$$E[n] = \int V(\underline{r})n(\underline{r})d\underline{r} + T_S[n] + \frac{1}{2} \iint d\underline{r}d\underline{r}' \frac{n(\underline{r})n(\underline{r}')}{|\underline{r}-\underline{r}'|} + E_{xc}[n] \quad (C4)$$

where  $T_S[n]$  is the total kinetic energy of a gas of non-interacting electrons of density  $n(\underline{r})$  (see <sup>(59)</sup> for a discussion of this functional),  $E_{xc}[n]$  is the total exchange and correlation energy (including a kinetic energy contribution) and the third term is the classical coulomb energy. Using (2) we find the Euler equation

$$\int \delta n(\underline{r}) \left\{ \frac{\delta E[n]}{\delta n(\underline{r})} - \mu \right\} = 0 \quad (C5)$$

where  $\mu$  is a Lagrange multiplier which is easily identified as the chemical potential. (C5) gives

$$\mu = \frac{\delta E[n]}{\delta n(\underline{r})} = \frac{\delta T_S[n]}{\delta n(\underline{r})} + V^{HK}(\underline{r}) \quad (C6)$$

where  $V^{HK}(\underline{r})$  is the sum of the usual Hartree potential  $V_H(\underline{r})$  and the exchange and correlation potential  $V_{xc}(\underline{r})$ , i.e.

$$V^{HK}(\underline{r}) = V(\underline{r}) + \int \frac{n(\underline{r}')d\underline{r}'}{|\underline{r}-\underline{r}'|} + V_{xc}(\underline{r}) \quad (C7)$$

$$V_{xc}(\underline{r}) = \frac{\delta E_{xc}[n]}{\delta n(\underline{r})} \quad (C8)$$

KS showed that  $V^{HK}(\underline{r})$  could be considered as a one body potential for the many electron system in the sense that the electron density  $n(\underline{r})$  is generated from it

by summing the squares of the  $N$  lowest one particle wave functions obtained from the Schrödinger equation

$$\left\{ -\frac{1}{2} \nabla^2 + V^{\text{HK}}(\underline{r}) \right\} \psi_i(\underline{r}) = \epsilon_i \psi_i(\underline{r}) \quad (\text{C9})$$

This result is summarised in the proposition.

(6) Given any density  $n(\underline{r})$  such that  $\int d\underline{r} n(\underline{r}) = \text{an integer}$ , there exists a one body potential which will generate via the Schrödinger equation the same density.

Note that the functions  $\psi_i$  and energies  $\epsilon_i$  in (C9) strictly have no other physical significance than through the relations

$$n(\underline{r}) = \sum_i^N \psi_i^*(\underline{r}) \psi_i(\underline{r}) \quad (\text{C10})$$

$$E = \sum_{i=1}^N \epsilon_i - \frac{1}{2} \iint \frac{n(\underline{r}) n(\underline{r}')}{|\underline{r} - \underline{r}'|} d\underline{r} d\underline{r}' - \int V_{\text{xc}}(\underline{r}) n(\underline{r}) d\underline{r} + E_{\text{xc}}[n] \quad (\text{C11})$$

However some authors<sup>(60)</sup> have irresistibly (though not without some justification<sup>(101)</sup>) used approximations to  $V^{\text{HK}}(\underline{r})$  as a means of introducing exchange and correlation into band structure calculations, the very successful '  $\rho^{\frac{1}{3}}$  ' exchange potential of Slater<sup>(61)</sup> being an example of this.

In order to make use of the exact equations (C7) to (C10) it is necessary to solve them self-consistently given some approximation to  $E_{\text{xc}}[n]$  and an initial  $n(\underline{r})$ . A frequently used form for  $E_{\text{xc}}[n]$  is the so called local approximation given by

$$E_{\text{xc}}[n] = \int \epsilon_{\text{xc}}^{\circ}[n(\underline{r})] d\underline{r} \quad (\text{C12})$$

where  $\epsilon_{\text{xc}}^{\circ}[n]$  is the exchange and correlation energy density of an interacting homogeneous electron gas. This approximation is expected to be useful when the electron density is slowly varying. Several authors ( (56), (59), (62) ) have discussed gradient corrections to (C12), the most general form of  $E_{\text{xc}}[n]$  that has



been proposed<sup>(56)</sup> <sup>(63)</sup> being

$$E_{xc}[n] \sim \int d\mathbf{r} \left[ \epsilon_{xc}^0[n(\mathbf{r})] - \frac{1}{2} \int d\mathbf{r}' B_{xc}(\mathbf{r}'; n(\mathbf{r})) [n(\mathbf{r} + \frac{1}{2}\mathbf{r}') - n(\mathbf{r} - \frac{1}{2}\mathbf{r}')]^2 \right] \quad (C13)$$

$$B_{xc}(\mathbf{r}'; n(\mathbf{r})) = B_{xc}(\mathbf{r}'; k_F) \Big|_{k_F = (3\pi^2 n(\mathbf{r}))^{1/3}}$$

The second term in (C13) partially sums the gradient expansion of the exchange and correlation energy and the kernel  $B_{xc}$  can be related in Fourier transform to the local field factor  $G(q)$  in the expression for the dielectric constant of the homogeneous electron gas (see equation (4.7)). In fact

$$B_{xc}(q; k_F) = -\frac{2\pi}{q^2} G(q) \quad (C14)$$

and therefore requires a theory of exchange and correlation transcending the RPA for its calculation.

Since its inception DFT has been increasingly applied to the calculation of a large number of physical properties of various electronic systems. Some examples are : charge density in atoms<sup>(64)</sup>; charge density at surfaces<sup>(65)</sup>; band structure calculations<sup>(60), (66)</sup>; spin density<sup>(67)</sup>; momentum density<sup>(42), (68)</sup>, phonon spectra<sup>(69)</sup>.

REFERENCES

- (1) T.E. Faber, An Introduction to the Theory of Liquid Metals, Cambridge (1972).  
(1a) p113 ; (1b) p323 ; (1c) p315 ; (1d) p5 ; (1e) p124.
- (2) N.H. March, Liquid Metals, Pergamon (1968).
- (3) M.D. Johnson and N.H. March, *Phys. Lett.* 3, 313, (1963).
- (4) G.K. Corless and N.H. March, *Phil. Mag.* 6, 1285, (1961).
- (5) The Properties of Liquid Metals : Proceedings of the Second International Conference, Tokyo, 1972, ed. S. Takeuchi, Taylor and Francis (1973).  
See especially the first section on the structure of liquid metals and alloys.
- (6) M. Watabe and M. Hasegawa, in (5), p133.
- (7) J. Chihara, in (5), p137.
- (8) N.H. March and M.P. Tosi, *Ann. Phys.* 81, 414, (1973).
- (9) M.P. Tosi, M. Parrinello and N.H. March, *Nuovo Cimento* 23, 135, (1974).
- (10) P.A. Egelstaff, N.H. March, N.C. McGill, *Can. J. Phys.* 52, 1651, (1974).
- (11) J.G. Kirkwood and F.P. Buff, *J. Chem. Phys.* 19, 774, (1951).
- (12) P. Gray, *J. Phys.* F3, L43, (1973).
- (13) M. Parrinello and M.P. Tosi, *J. Phys.* C6, L254, (1973).
- (14) N.H. March, M.P. Tosi and A.B. Bhatia, *J. Phys.* C6, L59, (1973).
- (15) M.P. Tosi and N.H. March, *Nuovo Cimento* 15B, 308, (1973).
- (16) P.M. Platzman and N. Tzoar, *Phys. Rev.* 136, A11, (1964).
- (17) J.E. Enderby, in Physics of Simple Liquids, ed. H.N.V. Temperley, J.S. Rowlinson and G.S. Rushbrooke, North Holland (1968). Chapter 14.
- (18) T. Fukamachi, Technical report B12, Institute for Solid State Physics, University of Tokyo (1971).
- (19) A.L. Fetter and J.D. Walecka, Quantum Theory of Many-Particle Systems, McGraw-Hill (1971). (19a) p21, (19b) p151.

- (20) L. Hedin and S. Lundqvist, in Solid State Physics, Vol. 23, eds. F. Seitz, D. Turnbull and H. Ehrenreich, Academic Press (1969).
- (21) L.P. Kadanoff and G. Baym, Quantum Statistical Mechanics, Benjamin Press (New York, 1962). p43.
- (22) S. Cusack, N.H. March, M. Parrinello and M.P. Tosi, J. Phys. F6, 749, (1976).
- (23) S.A. Trigger, Phys. Lett. 56A, 325, (1976).
- (24) M.C. Abramo and M.P. Tosi, Nuovo Cimento 10B, 21, (1972).
- (25) E. Feenberg, Theory of Quantum Fluids, Academic (1969). Chapter 2.
- (26) W. Kohn, Phys. Rev. Lett. 2, 393, (1959).
- (27) E.G. Brovman and Y.M. Kagan, Sov. Phys. Usp. 17, 128, (1974).
- (27a) E.G. Brovman and Y.M. Kagan, Sov. Phys. JEPT. 30, 721, (1970).
- (27b) E.G. Brovman and A. Kholas, Sov. Phys. JEPT. 39, 924, (1974).
- (28) J.C. Stoddart, N.H. March and M.J. Stott, Phys. Rev. 186, 683, (1969).
- (29) N.H. March, W.H. Young and S. Sampanthar, The Many-Body Problem in Quantum Mechanics, Cambridge (1967). Chapter 1.
- (30) C.J. Pethick, Phys. Rev. B2, 1789, (1970).
- (31) V. Heine, and M. Cohen and V. Heine in Solid State Physics, Vol. 24, (1970). Details as for (20).
- (32) N.W. Ashcroft, Phys. Lett. 23, 48, (1966).
- (33) K.S. Singwi, M.P. Tosi, R.H. Land and A. Sjölander, Phys. Rev. 176, 589, (1968).
- (34) N.S. Gringrich and L. Heaton, J. Chem. Phys. 34, 873, (1961).
- (35) A.J. Greenfield, J. Wellendorf and N. Wiser, Phys. Rev. A4, 1607, (1971).
- (36) D. Jović, Boris Kidrić Institute of Nuclear Sciences, Belgrade, Yugoslavia, private communication.
- (37) Y. Waseda, Tohoku University, Japan, private communication.

- (38) Quoted by I.H. Umar, A. Meyer, M. Watabe and W.H. Young, *J. Phys.* F4, 1691, (1974).
- (39) K. Honma, Niigata University, Japan, private communication.
- (40) P.E. Mijnarends and A. Bansil, reported at 13th annual Solid State Physics Conference (Institute of Physics), Manchester, January 1976.
- (41) J. Friedel, *Adv. in Phys.* 3, 446, (1954).
- (42) L. Lam and P.M. Platzman, *Phys. Rev.* B9, 5122 and 5128, (1974).
- (43) P.M. Platzman and N. Tzoar, *Phys. Rev.* 139, A410, (1965).
- (44) P. Eisenberger, L. Lam, P.M. Platzman and P.H. Schmidt, *Phys. Rev.* B6, 3671, (1972).
- (45) K.C. Pandey and L. Lam, *Phys. Lett.* A43, 319, (1973).
- (46) R.N. West, Positron Studies of Condensed Matter, Taylor and Francis, London, 1974.
- (47) A.T. Stewart, *Phys. Rev.* 133, A1651, (1964).
- (48) V.K. Ratti and J.M. Ziman, *J. Phys.* F4, 1684, (1974).
- (49) F. Yonezawa and K. Morigaki, *Prog. Theor. Phys.* supplement no. 53, (1973).
- (50) R.L. Jacobs, *J. Phys.* F4, 1351, (1974).
- (51) L.W. Nordheim, *Ann. d. Physik*, 9, 641, (1931).
- (52) N.H. March, P. Gibbs, G.M. Stocks and J.S. Faulkner, *J. Physique* 33, C3, (1972).
- (53) M. Weissmann and N. Cohen, *J. Phys.* C9, 473, (1976).
- (54) D. Hilton, N.H. March and A.R. Curtis, *Proc. Roy. Soc.* A300, 391, (1971).
- (55) P.C. Hohenberg and W. Kohn, *Phys. Rev.* 136, B864, (1964).
- (56) W. Kohn and L. Sham, *Phys. Rev.* 140, A1133, (1965).
- (57) N.H. March, in Orbital Theories of Molecules and Solids, ed. N.H. March, Clarendon Press (Oxford, 1974).

- (58) N.H. March and A.M. Murray, Proc. Roy. Soc. A261, 119, (1961).
- (59) J.C. Stoddart, A.M. Beattie and N.H. March, Int. J. Quantum Chem. 4, 35, (1971).
- (60) Computational Methods in Band Theory, eds. P.J. Marcus, J.F. Janak and A.R. Williams, Plenum Press (London, 1971).
- (61) J.C. Slater, Phys. Rev. 81, 385, (1951).
- (62) G. Niklasson, A. Sjölander and K.S. Singwi, Phys. Rev. B11, 113, (1975).
- (63) J.C. Stoddart, P. Stoney, N.H. March and I.B. Ortenburger, Nuovo Cimento 23B, 15, (1974).
- (64) B.Y. Tong and L.J. Sham, Phys. Rev. 144, 1, (1966).
- (65) N.D. Lang in Solid State Physics, Vol. 28, (1973). Details as for (20).
- (66) R.C. Perrin, R. Taylor and N.H. March, J. Phys. F5, 1490, (1975).
- (67) J.C. Stoddart and N.H. March, Ann. Phys. 64, 174, (1971).
- (68) N.H. March and J.C. Stoddart, in Computational Solid State Physics, eds. F. Herman, N.W. Dalton, and T. Koehler, Plenum Press (London, 1972).
- (69) W. Jones and N.H. March, Proc. Roy. Soc. A317, 359, (1970).
- (70) H.L. Frisch and J.M. Hammersley, J. Soc. Indust. Appl. Math., 11, 894, (1963)
- (71) V.K.S. Shante and S. Kirkpatrick, Adv. Phys. 20, 325, (1971).
- (72) J.W. Essam, in Phase Transitions and Critical Phenomena, Vol. 2, eds. C. Domb and M.S. Green, Academic Press (New York, 1972), Chapter 6.
- (73) R. Kikuchi, J. Chem. Phys. 53, 2713, (1970).
- (74) P. Dean and N.F. Bird, Mathematics Division report Ma61 of the National Physical Laboratory, Teddington, Middlesex, England, (1966).
- (75) S. Kirkpatrick, Solid State Commun. 12, 1279, (1973).
- (76) J.W. Essam and M.E. Fisher, J. Chem. Phys. 38, 802, (1963).
- (77) M.E. Fisher and J.W. Essam, J. Math. Phys. 2, 609, (1961).

- (78) J.P. Straley, *J. Phys.* C9, 783, (1976).
- (79) A.P. Young and R.B. Stinchcombe, *J. Phys.* C8, L535, (1975).
- (80) B.J. Last and D.J. Thouless, *Phys. Rev. Lett.* 27, 1719, (1971).
- (81) S. Kirkpatrick, *Rev. Mod. Phys.* 45, 574, (1973).
- (82) R.B. Stinchcombe, *J. Phys.* C7, 179, (1974).
- (83) J. Bernasconi and H.J. Wisemann, *Phys. Rev.* B13, 1131, (1976).
- (84) J.A. Blackman, *J. Phys.* C9, 2049, (1976).
- (85) T. Odagaki, *Prog. Theor. Phys.* 54, 1067, (1975). See also *J. Phys. Soc. Japan* 39, 618, (1975).
- (86) A. Coniglio, *J. Phys.* A8, 1773, (1975).
- (87) J.M. Ziman, *J. Phys.* C1, 1532, (1968).
- (88) H. Scher and R. Zallen, *J. Chem. Phys.* 53, 3759, (1970).
- (89) R. Landauer, *J. Appl. Phys.* 23, 779, (1952).
- (90) A.I. Eatah, N.E. Cusack and J.G. Wright, *Phys. Lett.* 51A, 149, (1975).
- (91) K.F. Berggren and G. Lindell, *Solid State Commun.* 13, 1589, (1973).
- (92) D.J. Thouless, *Phys. Reports*, 13C (1974).
- (93) N.F. Mott, *Metal-Insulator Transitions*, Taylor and Francis (London, 1974).
- (94) A. Miller and E. Abrahams, *Phys. Rev.* 120, 745, (1960).
- (95) V. Ambegaokar, B.L. Halperin and J.S. Langer, *Phys. Rev.* B4, 2612, (1971).
- (96) B.B. Suprapto and P.N. Butcher, *J. Phys.* C8, L517, (1975).
- (97) M. Pollak, *J. Non-Cryst. Solids* 11, 1, (1972).
- (98) N.F. Mott and E.A. Davis, *Electron Processes in Non-Crystalline Materials*, Clarendon Press (Oxford, 1971).
- (99) F.G. Tricomi, *Integral Equations*, Interscience Publishers (New York, 1957).
- (100) J. Heinrichs and N. Kumar, *J. Phys.* C8, L510, (1975).

- (101) L. Hedin and B.I. Lundqvist, *J. Phys.* C4, 2064, (1971).
- (102) L.H. Thomas, *Proc. Camb. Phil. Soc.* 23, 542, (1926).
- (103) E. Fermi, *Z. Phys.* 48, 73, (1928).
- (104) R.R. Fessler, R. Kaplow and B.L. Averbach, *Phys. Rev.* 150, 34, (1966).
- (105) J.M. Ziman, Principles of the Theory of Solids, Cambridge University Press, (1972), p 153
- (106) P.M. Platzman and P. Eisenberger, *Phys. Rev. Lett.* 33, 152, (1974).  
P.M. Platzman, P. Eisenberger and P. Schmidt, *Phys. Rev. Lett.* 34, 18, (1975).
- (107) H.J. Höhberger, A. Otto and E. Petri, *Solid State Commun.* 16, 175, (1975).
- (108) G. Mukhopadhyay, R.K. Kalia and K.S. Singwi, *Phys. Rev. Lett.* 34, 950, (1975).
- (109) D. Pines and P. Nozieres, The Theory of Quantum Liquids, Benjamin (New York, 1966).
- (110) C.M. Care and N.H. March, *Adv. Phys.* 24, 101, (1975).
- (111) Figure 4.5 was kindly supplied to the author by Professor P.M. Platzman.
- (112) S. Cusack and N.H. March, *Int. J. Quantum Chem.* 9, 481, (1975).